Microbes and Environments

DIGEST

JAPANESE SOCIETY OF MICROBIAL ECOLOGY
JAPANESE SOCIETY OF SOIL MICROBIOLOGY
TAIWAN SOCIETY OF MICROBIAL ECOLOGY
JAPANESE SOCIETY OF PLANT MICROBE INTERACTIONS
JAPANESE SOCIETY FOR EXTREMOPHILES

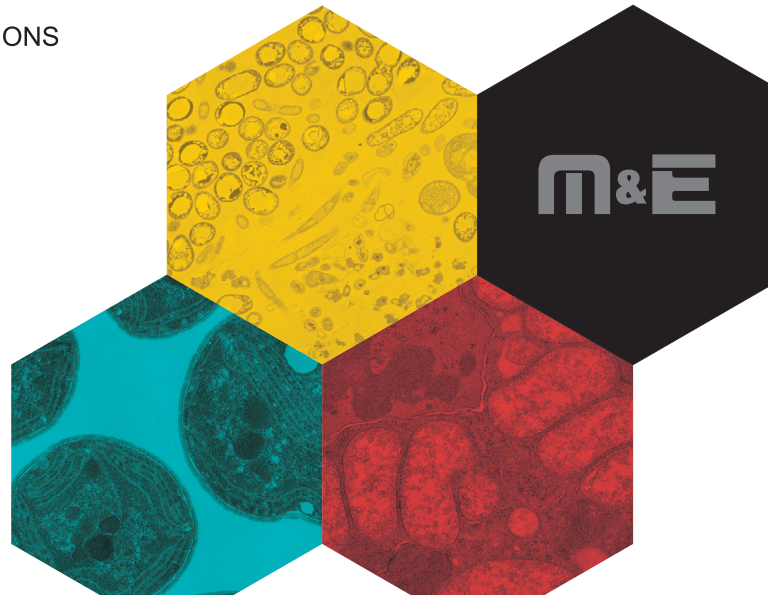

October 2023

Microbes and Environments
DIGEST 2023

CONTENTS

*Times cited at the end of 2022

About Microbes and Environments

Microbes and Environments (M&E) is an international, peer-reviewed, open access journal devoted to the publication of original and review articles regarding all aspects of research on microbial ecology and environmental microbiology. It is published quarterly in a printed and an electronic version by Japanese Society of Microbial Ecology (JSME), Japanese Society of Soil Microbiology (JSSM), Taiwan Society of Microbial Ecology (TSME), Japanese Society of Plant Microbe Interactions (JSPMI) and Japanese Society for Extremophiles (JSE).

Benefits for Authors

- Open access policy for electric publication in PubMed, PubMed Central, and J-Stage
- Included in Web of Science® by Clarivate Analytics
- Page charges: ¥60,000/article for JSME/JSSM/TSME/JSPMI/JSE members
  ¥140,000/article for non-members

Interest of the Journal

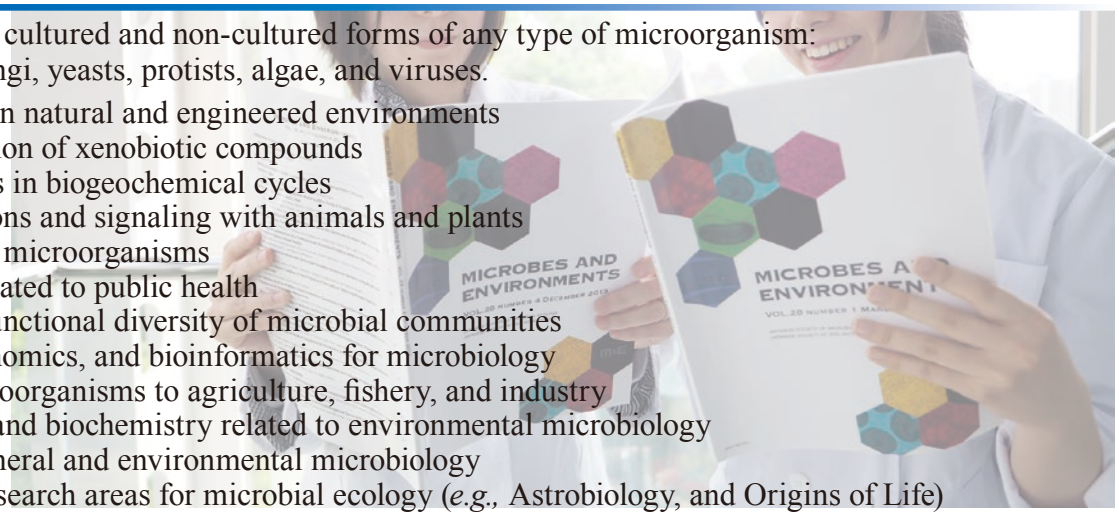

Articles can deal with cultured and non-cultured forms of any type of microorganism: Bacteria, Archaea, fungi, yeasts, protists, algae, and viruses.

· Microbial ecology in natural and engineered environments
· Microbial degradation of xenobiotic compounds
· Microbial processes in biogeochemical cycles
· Microbial interactions and signaling with animals and plants
· Interactions among microorganisms
· Microorganisms related to public health
· Phylogenetic and functional diversity of microbial communities
· Genomics, metagenomics, and bioinformatics for microbiology
· Application of microorganisms to agriculture, fishery, and industry
· Molecular biology and biochemistry related to environmental microbiology
· Methodology in general and environmental microbiology
· Interdisciplinary research areas for microbial ecology (*e.g.,* Astrobiology, and Origins of Life)
· Taxonomic description of novel microorganisms with ecological perspective
· Physiology and metabolisms of microorganisms
· Evolution of genes and microorganisms
· Genome report of microorganisms with ecological perspective
· Life in extreme environments

Message from Editor-in-Chief

Microbes and Environments is now becoming one of the important journals for microbial ecology. The journal is being edited by five academic societies, but the submission is open to all researchers including non-members. Microbes and Environments is an open access and freely available online journal. Manuscripts are rigorously reviewed by credible peer reviewers to ensure excellent scientific quality. Once a manuscript is accepted, it will be published immediately after proof corrections so that readers can see and read the paper in a timely fashion. Different from commercial journals, we are providing the publication opportunity with an affordable price. We are looking forward to receiving your high-quality manuscripts.

Shigeto Otsuka
The University of Tokyo, Japan

Submit Your Manuscript

http://www.microbes-and-environments.jp/

Microbes Environ. 37(1), 2022
https://www.jstage.jst.go.jp/browse/jsme2 doi:10.1264/jsme2.ME21094

MOST VALUABLE PAPER OF THE YEAR 2022

Phenolic Acids Induce Nod Factor Production in *Lotus japonicus–Mesorhizobium* Symbiosis

Masayuki Shimamura[1†], Takashi Kumaki[2†], Shun Hashimoto[2], Kazuhiko Saeki[3], Shin-ichi Ayabe[1], Atsushi Higashitani[2], Tomoyoshi Akashi[1*], Shusei Sato[2*], and Toshio Aoki[1]

[1]*Department of Applied Biological Sciences, Nihon University, Fujisawa, Kanagawa 252–0880, Japan;* [2]*Graduate School of Life Sciences, Tohoku University, Sendai, Miyagi 980–8577, Japan; and* [3]*Department of Biological Sciences and Kyousei Science Center for Life and Nature, Nara Women's University, Nara 630–8506, Japan*

(Received December 28, 2021—Accepted January 22, 2022—Published online March 12, 2022)

In legume–rhizobia symbiosis, partner recognition and the initiation of symbiosis processes require the mutual exchange of chemical signals. Chemicals, generally (iso)flavonoids, in the root exudates of the host plant induce the expression of *nod* genes in rhizobia, and, thus, are called *nod* gene inducers. The expression of *nod* genes leads to the production of lipochitooligosaccharides (LCOs) called Nod factors. Natural *nod* gene inducer(s) in *Lotus japonicus–Mesorhizobium* symbiosis remain unknown. Therefore, we developed an LCO detection method based on ultra-high-performance liquid chromatography–tandem-quadrupole mass spectrometry (UPLC-TQMS) to identify these inducers and used it herein to screen 40 phenolic compounds and aldonic acids for their ability to induce LCOs in *Mesorhizobium japonicum* MAFF303099. We identified five phenolic acids with LCO-inducing activities, including *p*-coumaric, caffeic, and ferulic acids. The induced LCOs caused root hair deformation, and nodule numbers in *L. japonicus* inoculated with *M. japonicum* were increased by these phenolic acids. The three phenolic acids listed above induced the expression of the *nodA*, *nodB*, and *ttsI* genes in a strain harboring a multicopy plasmid encoding NodD1, but not that encoding NodD2. The presence of *p*-coumaric and ferulic acids in the root exudates of *L. japonicus* was confirmed by UPLC-TQMS, and the induction of *ttsI*::*lacZ* in the strain harboring the *nodD1* plasmid was detected in the rhizosphere of *L. japonicus*. Based on these results, we propose that phenolic acids are a novel type of *nod* gene inducer in *L. japonicus–Mesorhizobium* symbiosis.

Key words: *nod* gene inducer, *Lotus japonicus–Mesorhizobium* symbiosis, phenolic acids, lipochitooligosaccharides, ultra-high-performance liquid chromatography–tandem-quadrupole mass spectrometry

Leguminous plants are characterized by their ability for symbiosis with a number of Gram-negative bacteria, collectively known as rhizobia. Rhizobia are free-living in soil, but change into bacteroids in the cells of specific host plants, in which they produce ammonium from atmospheric nitrogen and provide it to the host. Host–symbiont recognition and the initiation of symbiosis require the mutual exchange of chemical signals between leguminous plants and rhizobia. In host plants, the processes leading to root nodulation are triggered by rhizobial signal molecules called nod factors (NFs). NFs are lipochitooligosaccharides (LCOs) consisting of the oligomeric backbone of β-1,4-linked N-acetyl-D-glucosamine residues N-acylated at the non-reducing end. Chemical groups such as sulfate, fucose, and acetate, which vary according to the rhizobial strain, may substitute the oligosaccharide backbone (Liang *et al.*, 2014). The transmembrane receptor kinases of the host plant recognize specific NF structures and transmit a signal that triggers a series of symbiotic events, including root hair deformation, the formation and elongation of infection threads, and the induction of nodule primordia (Suzaki *et al.*, 2015). The induction of NF biosynthesis requires specific low-molecular-weight compounds exuded from the roots of the host plant, which are recognized by the rhizobial receptor NodD (Liu and Murray, 2016). When bound to the host-derived ligand, NodD serves as a transcription factor; it binds to *cis* elements called *nod* boxes and induces the transcription of a series of flanking genes, including *nod* genes, which encode enzymes involved in NF biosynthesis (Recourt *et al.*, 1989; Begume *et al.*, 2001; Liu and Murray, 2016). Therefore, these plant factors are called *nod* gene inducers. They include flavonoids and related compounds, such as flavanones, flavones, isoflavones, and chalcones, and function at very low concentrations of 10–100 μM (Peters *et al.*, 1986; Kosslak *et al.*, 1987; Hungria *et al.*, 1991). A *nod* box is also located upstream of the rhizobial type III secretion system (T3SS) cluster containing the *ttsI* gene (Okazaki *et al.*, 2010). T3SS secretes effector proteins that affect symbiosis in host plant cells (Okazaki *et al.*, 2013; Sugawara *et al.*, 2018; Kusakabe *et al.*, 2020).

Lotus japonicus, together with barrel medic (*Medicago truncatula*) and soybean (*Glycine max*), is a leguminous model system for molecular genetics and genomics

* Corresponding authors.
Tomoyoshi Akashi: E-mail: akashi.tomoyoshi@nihon-u.ac.jp;
Tel: +81–466–84–3353; Fax: +81–466–84–3353.
Shusei Sato: E-mail: shuseis@ige.tohoku.ac.jp;
Tel: +81–22–217–5688; Fax: +81–22–217–5691.
† These authors contributed equally to this work.
Toshio Aoki: deceased.

Citation: Shimamura, M., Kumaki, T., Hashimoto, S., Saeki, K., Ayabe, S., Higashitani, A., et al. (2022) Phenolic Acids Induce Nod Factor Production in *Lotus japonicus–Mesorhizobium* Symbiosis. *Microbes Environ* **37**: ME21094.
https://doi.org/10.1264/jsme2.ME21094

(Handberg and Stougaard, 1992; Udvardi *et al.*, 2005; Sato and Tabata, 2006). Data from whole-genome analyses of these species have provided insights into the origin and adaptive evolution of diverse leguminous plants (Cannon *et al.*, 2006; Hougaard *et al.*, 2008; Sato *et al.*, 2008; Young and Bharti, 2012; O'Rourke *et al.*, 2014). A more detailed understanding of symbiotic nitrogen fixation may be obtained by comparing the underlying molecular mechanisms among the three models. The reported *nod* gene inducers that act on *Mesorhizobium* strains, the symbionts of *L. japonicus*, are aldonic acids and related compounds, such as erythronic acid, tetronic acid, and succinic anhydride (Gagnon and Ibrahim, 1998). However, the induction of NF production in *Mesorhizobium* strains requires 10 mM tetronic acid or even higher concentrations of erythronic acid and succinic anhydride, more than a thousand-fold higher than those required for NF production in the symbionts of other legumes (Gagnon and Ibrahim, 1998). Furthermore, aldonic acids have not been detected in the root exudates or root tissues of *L. japonicus*. Therefore, the natural *nod* gene inducers of *L. japonicus–Mesorhizobium* symbiosis have not yet been identified.

Structural analyses using ultra-high-performance liquid chromatography coupled to quadrupole-time-of-flight (UPLC-QTOF) mass spectrometry (MS) and high-magnetic-field nuclear magnetic resonance spectroscopy revealed that *Mesorhizobium* NFs are a mixture of four major and four minor LCOs that vary in the fatty acid type, the number of carbamoyl groups at the non-reducing end, and the number of acetyl groups attached to fucose at the reducing end (Bek *et al.*, 2010). In the present study, we aimed to identify natural substances that are exuded from *L. japonicus* roots and act on *Mesorhizobium* strains as *nod* gene inducers by directly assaying NF production. We developed an assay method in which LCOs were extracted from small-scale cultures of *Mesorhizobium* strains in the presence of the candidate chemical compound and specifically detected by UPLC–tandem-quadrupole MS (TQMS). UPLC-TQMS is a convenient method for routine assays; however, its resolution is inferior to QTOF MS. We used this method to screen authentic samples of aldonic acids, flavonoids, and related phenolic compounds (instead of the fractionation of plant extracts or root exudates), and then examined the presence of the identified target compounds in the root exudates of *L. japonicus*. We identified five phenolic acids that induce NF production in *Mesorhizobium* strains.

NodD in *Rhizobium leguminosarum* is activated by naringenin, a *nod* gene inducer from *Medicago sativa* (Firmin *et al.*, 1986). When the heterologous *nodD* of *R. leguminosarum* was introduced into *Mesorhizobium japonicum* MAFF303099 (reclassified from *M. loti* based on genome sequence information; Martínez-Hidalgo *et al.*, 2016) via a multicopy plasmid, the application of naringenin induced NF production (López-Lara *et al.*, 1995; Niwa *et al.*, 2001; Bek *et al.*, 2010) and the expression of the *ttsI* gene, the regulator of T3SS (Okazaki *et al.*, 2010). Using a similar approach, namely, the introduction of endogenous *nodD* genes encoded by multicopy plasmids, we herein established which of the two NodD receptors, NodD1 or NodD2, of *M. japonicum* MAFF303099 interacted with the identified phenolic acids.

Materials and Methods

Chemicals

The following materials were purchased from the suppliers indicated in parentheses: chlorogenic acid (MP Biomedicals); gossypetin (Indofine Chemical Company); butein, eriodictyol, formononetin, herbacetin, isorhamnetin, kaempferol, myricetin, and quercetin (Extrasynthèse); daidzein and genistein (LC Laboratories); vestitol (Plantech); apigenin, biochanin A, coniferyl alcohol, *o*-coumaric acid, *m*-coumaric acid, coumestrol, 5-hydroxyferulic acid, luteolin, naringenin, phloretic acid, sinapic acid, and umbelliferone (Merck); *p*-coumaric acid, erythronic acid, isoferulic acid, and succinic anhydride (TCI); caffeic acid, *trans*-cinnamic acid, 3,4-dimethoxycinnamic acid, ferulic acid, *p*-methoxycinnamic acid, phenylalanine, tetronic acid, and L-tyrosine (FUJIFILM Wako Pure Chemical). Umbellic acid was prepared from umbelliferone by a treatment with 1 M NaOH at 90°C for 1 h. Isoliquiritigenin was obtained from our laboratory stock (Shimamura *et al.*, 2007).

NFs (LCOs) and Mesorhizobium *strains*

The plasmid pMP2112 encoding *R. leguminosarum* bv. *trifolii* nodD (López-Lara *et al.*, 1995) and a sample of the NF derived from *M. japonicum* MAFF303099 harboring pMP2112 were provided by H. Kouchi of the International Christian University, Japan. pMP2112 was transferred into *M. japonicum* MAFF303099 (Kaneko *et al.*, 2000; Saeki and Kouchi, 2000).

The bacterial strains and plasmids used in the present study are summarized in Supplementary Table S1. The *nodD1* and *nodD2* deletion (Δ*nodD1-nodD2*) variant of *M. japonicum* MAFF303099 was generated by homologous recombination as described by Hattori *et al.* (2002). The cosmid c243 was digested with *Bam*HI and ligated with a 1.9-kbp *Bam*HI fragment of the kanamycin resistance gene *neo* from pUCKM1 (Saeki *et al.*, 1991). In the resultant knockout plasmid pEMA49, the *nodD1* (*mll6179*)–*nolL* (*mlr8757*)–*nodD2* (*mlr6182*)–*mll6183–mlr6185* region was replaced with the *neo* gene. The generated allele was homogenotized with the endogenous genomic locus in *M. japonicum* to produce the Δ*nodD* variant. The construct was verified by Southern hybridization using c243 as a probe.

The *nodA* deletion (Δ*nodA*) variant was constructed essentially as described above, but with the precise in-frame deletion of the NodA coding region. An allele in which *nodA* was replaced with the spectinomycin resistance gene *aadA* was constructed by PCR amplification from pKST001R (Hanyu *et al.*, 2009) with primers to add overhangs (wan_mlr8755_upper and wan_mlr8755_lower). The amplified allele was then exchanged in *Escherichia coli* with the endogenous *mlr8755* allele in the cosmid c242.1 (Hattori *et al.*, 2002) in the presence of the phage lambda Red recombinase (Datsenko and Wanner, 2000) to generate the knockout plasmid pML8755DA. The correct construction of the Δ*nodA* variant was verified by PCR with the primers KS_nodSJ_F01S and KSnodC_Rev01 as well as by Southern hybridization using the wild-type PCR product as a probe.

In the functional analysis of *nodD*, the *nodD1* and *nodD2* genes were introduced separately into *M. japonicum* MAFF303099 and ML033 (Okazaki *et al.*, 2010) as follows. The 1,272-bp fragment containing the coding and promoter regions of *nodD1* (*mlr6182*) and the 1,365-bp fragment containing those of *nodD2* (*mll6179*) were amplified by PCR with the primer pairs pBBR1_nodD1_Fw and pBBR1_nodD1_Rv, and pBBR1_nodD2_Fw and pBBR1_nodD2_Rv, respectively (Supplementary Table S2). PCR products were cloned into pBBR1MCS-2 (Kovach *et al.*, 1995) by In-Fusion HD cloning (Clontech). The plasmids obtained (p*Mj*-NodD1 and p*Mj*-NodD2, respectively) were introduced separately into *E. coli* DH5α and mobilized into *M. japonicum* MAFF303099 using the previously described bacterial conjugation system (Kusakabe *et al.*, 2020). One day after

conjugation, transformants containing p*Mj*-NodD1 or p*Mj*-NodD2 were selected on tryptone–yeast-extract plates containing 100 μg mL^{-1} phosphomycin and 50 μg mL^{-1} kanamycin. Plasmid transfer was confirmed by PCR.

Culture conditions for M. japonicum *MAFF303099 and extraction of LCOs*

M. japonicum MAFF303099 was pre-cultured in TY medium at 28°C overnight. An aliquot of the culture was diluted with fresh TY medium (10 mL, OD_{660}=0.001) and supplemented with the antibiotics and phenolics shown in Table 1. Regarding *M. japonicum* MAFF303099 carrying pMP2112, antibiotics and naringenin (final concentration, 1 μM) were added to the culture medium. Diluted cultures were grown at 28°C for 24 h, centrifuged (8,000×*g*, room temperature, 2 min), and LCOs were then extracted from the supernatants with *n*-butanol.

Extraction of root exudates from legume seedlings

The seeds of alfalfa (*M. sativa*), red clover (*Trifolium pratense*), and *L. japonicus* B-129 Gifu were sterilized with solution containing 2% (v/v) sodium hypochlorite and 0.02% (v/v) Tween-20 for 10 min, rinsed five times with sterilized distilled water, and immersed in sterilized distilled water at room temperature overnight. They were then sown in a plastic container containing B&D liquid medium (pH 6.8) and cultivated at 25°C (16 h light/8 h dark) for 7 days. Media containing seedling exudates were collected and loaded onto Oasis HLB cartridges (Waters), and exudate components were eluted with ethanol.

UPLC-TQMS analysis

The butanol extracts of bacterial cultures and the ethanol extracts of root exudates were concentrated by evaporation, dissolved in 50% acetonitrile, and filtered through polytetrafluoroethylene membrane filters (Merck). UPLC analyses were conducted on Quattro Premier XE (Waters). Separation was performed on an Acquity UPLC BEH C18 column (2.1×100 mm, Waters) at 40°C and a flow rate of 0.38 mL min^{-1}. Gradient elution was performed with 0.1% formic acid in water (A) and 0.1% formic acid in acetonitrile (B) as follows. LCOs: 44% B (0–4 min), 44–85% B (4–7 min), 85–99.5% B (7–7.1 min), 99.5% B (7.1–7.2 min); root exudates: 5–15% B (0–7 min), 15–99% B (7–10 min).

Table 1. NF (LCO)-inducing activities of compounds tested in the present study.

Class	Compound	PubChem CID	Activity*
Phenylpropanoids	L-Phenylalanine (**1**)	6140	–
	L-Tyrosine (**2**)	6057	–
	trans-Cinnamic acid (**3**)	444539	–
	p-Coumaric acid (**4**)	637542	+
	Caffeic acid (**5**)	689043	+
	Ferulic acid (**6**)	445858	++
	5-Hydroxyferulic acid (**7**)	446834	+
	Sinapic acid (**8**)	637775	–
	Coniferyl alcohol (**9**)	1549095	–
	Umbellic acid (**10**)	446611	–
	Umbelliferone (**11**)	5281426	–
	Chlorogenic acid (**12**)	1794427	–
	Phloretic acid (**13**)	10394	+
	o-Coumaric acid (**14**)	637540	–
	m-Coumaric acid (**15**)	637541	–
	3,4-Dimethoxycinnamic acid (**16**)	717531	–
	Isoferulic acid (**17**)	736186	–
	p-Methoxycinnamic acid (**18**)	699414	–
Chalcones	Butein	5281222	–
	Isoliquiritigenin	638278	–
Flavanones	(*2S*)-Eriodictyol	440735	–
	(*2S*)-Naringenin	439246	–
Flavones	Apigenin	5280443	–
	Luteolin	5280445	–
Flavonols	Gossypetin	5280647	–
	Herbacetin	5280544	–
	Isorhamnetin	5281654	–
	Kaempferol	5280863	–
	Myricetin	5281672	–
	Quercetin	5280343	–
Isoflavones	Biochanin A	5280373	–
	Daidzein	5281708	–
	Formononetin	5280378	–
	Genistein	5280961	–
	Pseudobaptigenin	5281805	–
Isoflavans	(*3R*)-Vestitol	182259	–
Coumestans	Coumestrol	5281707	–
Aldonic acids	Erythronic acid (lactonized)	5325915	–
	Succinic anhydride	7922	–
	Tetronic acid (lactonized)	521261	–

*: ++ and + indicate LCO-inducing activity at 0.3 mg L^{-1} (++) and 15 mg L^{-1} (+); – no activity.

MS spectra were acquired with Quattro Premier v. 4.1 software (Waters) under the following conditions. Qualitative analyses: the selected ion recording (SIR) mode, electrospray ionization (ESI) positive mode, capillary voltage 3.0 kV, cone voltage 30 V, desolvation gas flow rate 800 L h^{-1} at 400°C, cone gas flow rate 50 L h^{-1}, and source temperature 120°C. Quantitative analyses: the selected reaction monitoring (SRM) mode; conditions described above except that the capillary voltage was 3.5 kV and the cone voltage was 50 V. SRM conditions for phenolic acids in root exudates are shown in Supplementary Table S3.

Isolation of rhizobia from root nodules of L. japonicus

Mature *L. japonicus* plants collected near the coast of Kanagawa, Japan, were dubbed "Bishamon" (34°54'10.3"N 139°53'15.7"E) and "Nojimazaki" (35°08'26.5"N 139°39'36.0"E). Nodules were harvested, and their surfaces were sterilized with solution containing 2% (v/v) sodium hypochlorite and 0.02% (v/v) Tween-20 for 10 min and then rinsed five times with sterilized distilled water. Nodules were crushed individually with a pestle in the presence of 40% glycerol, and the homogenates were spread on TY agar medium at 28°C for 10–14 days. A rhizobial colony was isolated from each nodule and named Bishamon1-c2 or Nojimazaki1-a1. Nodule formation by the isolated rhizobia in *L. japonicus* B-129 Gifu was examined according to Aoki *et al.* (2021). The procedure for LCO extraction from rhizobia, namely, Bishamon1-c2, Nojimazaki1-a1, and Tono (Kawaguchi *et al.*, 2002), was the same as that for *M. japonicum* MAFF303099 described above.

Root hair deformation assay

The root hair deformation assay was performed with the *n*-butanol extract of *M. japonicum* MAFF303099 according to previously described methods, except that B&D liquid and agar media adjusted to pH 6.8 (Broughton and Dilworth, 1971) were used instead of half-strength nitrogen-free HM nutrients (Imaizumi-Anraku *et al.*, 1997). LCOs were extracted with *n*-butanol from cultures of *M. japonicum* MAFF303099 treated with caffeic acid and purified on a solid-phase extraction column. An *n*-butanol extract prepared from mock-treated *M. japonicum* was used as a control. Purified LCOs and the control sample were used to treat 7-day-old *L. japonicus* B-129 Gifu for 24 h, and the roots were stained with toluidine blue and observed by light microscopy.

Expression analysis of ttsI*,* nodA*, and* nodB *genes*

To analyze the transcriptional regulation of the *ttsI* gene by phenolic acids, we used a chromosomally integrated translational *lacZ* fusion with the ML033 *ttsI* promoter (ML033) as previously described (Okazaki *et al.*, 2010). In the β-galactosidase assay, approximately 50 µL of pre-cultured (stationary phase) *Mesorhizobium* strains were inoculated into 5 mL of TY liquid medium (OD_{660} 0.01) in 50-mL tubes and grown for 21 h with or without phenolic acids at a final concentration of 10 µM.

β-Galactosidase activity was assessed in a microplate assay as previously described (Griffith and Wolf, 2002). The expression of the *nodA* and *nodB* genes was analyzed by qRT-PCR. Pre-cultured (mid-log phase) *Mesorhizobium* strains (1.5 mL) were inoculated into 1.5 mL of TY liquid medium in 15-mL tubes with or without phenolic acids at a final concentration of 10 µM and grown for 4 h. Bacterial RNA was stabilized by adding RNAprotect Bacteria Reagent (Qiagen) and extracted with an RNeasy Mini kit (Qiagen), and purified total RNA was then treated with Recombinant DNase I (Takara Bio). cDNA was synthesized from total RNA using an ExScript RT Reagent Kit (Takara Bio). The primer pairs used in the qRT-PCR analysis are listed in Supplementary Table S2. All qRT-PCR measurements were performed in a C1000 Thermal Cycler (Bio-Rad) with a Kapa SYBR Fast qPCR Kit (Kapa Biosystems). The relative expression of the selected genes was calculated as $2^{-\Delta\Delta Ct}$ using the *16S rRNA* gene as a reference. All experiments were performed for three technical and three biological replicates. The primers used to assess the expression levels of the various target genes are listed in Supplementary Table S2.

Root X-Gal staining assay

L. japonicus MG-20 plants were grown for 10 days on 1/2 MS medium agar plates, and ML033, ML033/p*Mj*-nodD1, or ML033/p*Mj*-nodD2 suspensions containing approximately 10^8 cells were inoculated onto the root surface with low melting point agar containing 0.02% X-Gal. Low melting point agar containing 0.02% X-Gal without rhizobia cells was used as a mock control. Blue staining was observed after a 2-days incubation at 25°C.

Results

Screening of compounds for LCO-inducing activity in rhizobia based on direct LCO detection by UPLC-TQMS

To detect NF production with high sensitivity and reproducibility, we established an analytical method to detect LCOs in rhizobial culture media using UPLC-TQMS. When an authentic LCO sample was analyzed in the SIR mode by UPLC-TQMS, a major peak appeared with a retention time of 5–5.5 min and a minor peak appeared after 6 min (Fig. 1a). To monitor an authentic LCO, we set the *m*/*z* value to 1502.7 based on the consecutive mass spectra of the major peak (Fig. 1b), which we presumed to correspond to previously reported NodMl-V (C18:1, Me, Cb, AcFuc) (López-Lara *et al.*, 1995; Niwa *et al.*, 2001; Bek *et al.*, 2010). The analysis of LCOs extracted from the culture medium of *M. japonicum* MAFF303099 carrying the pMP2112 plasmid, which harbored *nodD* from *R. leguminosarum*, in the presence of 1 µM naringenin also revealed a major peak at 5–5.5 min (Fig. 1a).

The established analytical method was used to test the LCO-inducing activities of 40 phenolic compounds, including phenylpropanoids, chalcones, flavanones, flavones, flavonols, isoflavones, an isoflavan, and a coumestan, as well as aldonic acids that were previously reported to exhibit *nod* gene-inducing activity (Table 1). LCO induction was analyzed by culturing *M. japonicum* MAFF303099 with 0.3 or 15 mg L^{-1} of the tested compounds, followed by *n*-butanol extraction of the culture medium and UPLC-TQMS analyses using the SIR mode at *m*/*z* 1502.7 (Fig. 1b). LCO was produced in the presence of five phenolic acids at 15 mg L^{-1}: *p*-coumaric acid (**4**), caffeic acid (**5**), ferulic acid (**6**), 5-hydroxyferulic acid (**7**), and phloretic acid (**13**) (Fig. 1c and Table 1). Only ferulic acid (**6**) promoted LCO production at 0.3 mg L^{-1} (Table 1). Among the 40 compounds tested, the remaining 35 compounds, including cinnamic acid, produced few or no LCOs (Table 1). We evaluated the reproducibility of LCO-inducing activities at various concentrations of these five phenolic acids employing the SRM mode of UPLC-TQMS and found that their activity increased in different concentration-dependent manners up to 100 µM (Fig. 1d). At 1 µM, only ferulic acid (**6**) was active, and its activity was the highest among the five inducers at 10 µM. In contrast, caffeic acid (**5**) showed weak activity up to 10 µM, but was the most active inducer at 100 µM. *p*-Coumaric acid (**4**), 5-hydroxyferulic acid (**7**), and phloretic acid (**13**) were only active at 100 µM (Fig. 1d).

Using the deletion variants of *M. japonicum* MAFF303099, we confirmed that the LCO-inducing activi-

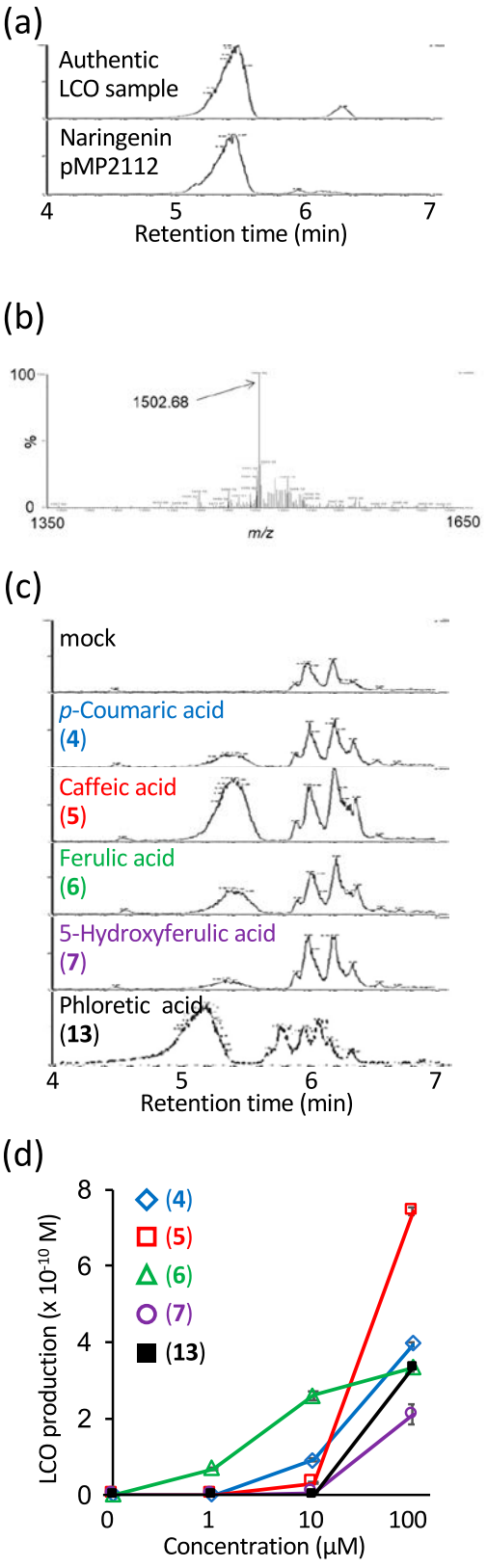

Fig. 1. Phenolic acids induce the production of NFs (LCOs) in *Mesorhizobium japonicum* MAFF303099. UPLC-TQMS analysis of an authentic LCO sample and naringenin-induced LCOs in *M. japonicum* harboring pMP2112. Chromatograms recorded by the SIR mode at m/z 1502.7 (a) and the mass spectrum at a retention time of 5.41 min (b). (c) UPLC-TQMS analysis of LCOs produced in *M. japonicum* MAFF303099 after the application of the indicated compounds at 15 mg L^{-1}. (d) LCO production induced by different concentrations of phenolic acids listed in (c). Error bars show S.E. (n=4).

ties of *p*-coumaric acid (**4**), caffeic acid (**5**), and ferulic acid (**6**) depended on the *nodA* and *nodD* genes (Supplementary Fig. S1).

Phenolic acids induce LCO production in native Mesorhizobium *strains*

To investigate whether the phenolic acids identified by screening using *M. japonicum* MAFF303099 generally induce LCOs in native *L. japonicus* rhizobia, we tested three additional *Mesorhizobium* strains isolated from native *L. japonicus*: Tono (Kawaguchi *et al.*, 2002), Nojimazaki 1-a1, and Bishamon 1-c2 (the present study). The phenolic acids tested, namely, *p*-coumaric acid (**4**), caffeic acid (**5**), ferulic acid (**6**), and 5-hydroxyferulic acid (**7**), produced LCOs with good reproducibility and at levels that were significantly higher (25- to 60-fold) in all native *Mesorhizobium* strains than in *M. japonicum* MAFF303099 (Fig. 2a). No adverse effects of these phenolic acids on the growth of rhizobia were observed at the concentrations used (Fig. 2b).

Biological activities of phenolic acids toward the host plant L. japonicus

To examine the abilities of the LCOs produced to function as NFs for *L. japonicus*, we assessed their root hair deformation activities. The root hairs of *L. japonicus* treated with 1 nM LCOs, which were induced by 100 μM caffeic acid, showed bending deformation, and some root hair tips were curled (Supplementary Fig. S2a, b, and c). The control sample had no effect on root hairs (Supplementary Fig. S2d).

Exogenous *nod* gene inducers have been shown to increase the nodule number in pea and soybean (Novák *et al.*, 2002; Pan *et al.*, 2008); therefore, we tested the effects of phenolic acids on *L. japonicus* inoculated with *M. japonicum*. The number of mature nodules significantly increased after 4 weeks in the presence of 10 μM ferulic acid (Fig. 3a and b) or 10 μM caffeic acid (Fig. 3c).

NodD1 acts as a receptor for phenolic acids

Rhizobia perceive *nod* gene inducers, such as flavonoids, through their binding to the transcriptional activator NodD, which up-regulates the expression of *nod* genes and the *ttsI* gene, a regulator of T3SS (Firmin *et al.*, 1986; Okazaki *et al.*, 2010). To examine transcriptional responses to the identified phenolic acids, we used *M. japonicum* ML033, in which the translational fusion of *lacZ* with *ttsI* was integrated into the chromosome of *M. japonicum* MAFF303099 (Okazaki *et al.*, 2010). No significant increases in β-galactosidase activity were detected in the presence of 1 μM *p*-coumaric acid (**4**), caffeic acid (**5**), or ferulic acid (**6**) (Fig. 4a). We then introduced one of the endogenous *nodD* genes via a multicopy plasmid, followed by an analysis using pMP2112 harboring *nodD* from *R. leguminosarum*. We constructed separate multicopy plasmids harboring *nodD1* (p*Mj*-NodD1) or *nodD2* (p*Mj*-NodD2), and transferred them into *M. japonicum* ML033.

After a 21-h culture with 1 μM *p*-coumaric acid (**4**), caffeic acid (**5**), or ferulic acid (**6**), β-galactosidase activity significantly increased in ML033/p*Mj*-NodD1, but not in ML033/p*Mj*-NodD2 (Fig. 4a). Induction levels were similar

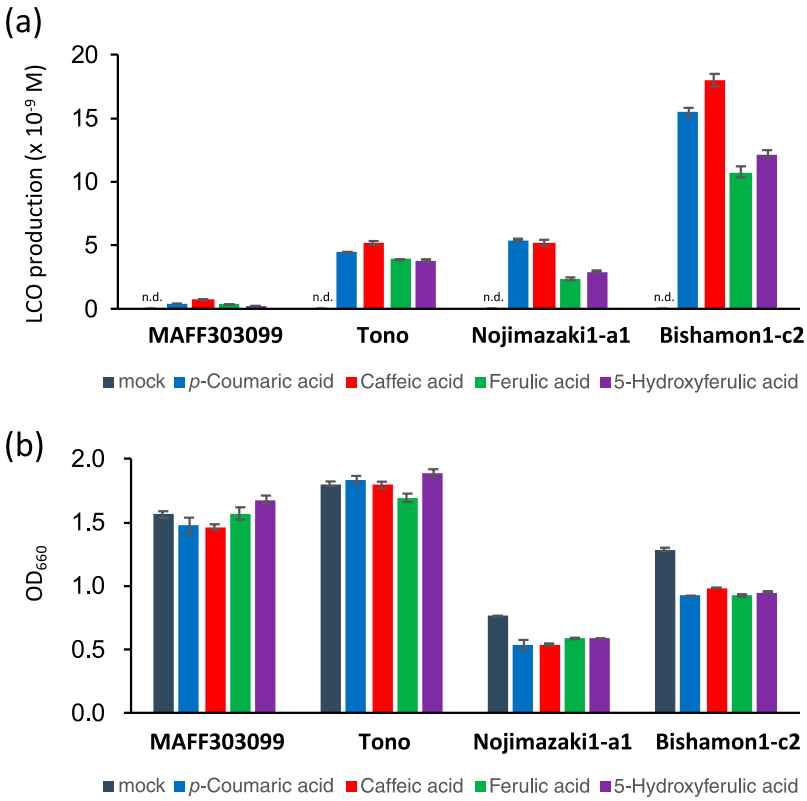

Fig. 2. Production of LCOs and growth of *Mesorhizobium* strains isolated from different locations in the presence of phenolic acids. (a) LCO production in *M. japonicum* MAFF303099, Tono, Nojimazaki 1-a1, and Bishamon 1-c2. (b) Growth of the strains tested in panel (a). Error bars show S.E. (n=3 or 4).

to that with 1 μM naringenin in ML033/pMP2112 (Fig. 4a), which carries *nodD* from *R. leguminosarum* (López-Lara *et al.*, 1995). In contrast, cinnamic acid (**3**), which did not induce LCO production in the screening described above, did not induce β-galactosidase activity in any of the strains (Fig. 4a).

The concentration dependence of β-galactosidase activity in ML033/p*Mj*-NodD1 induced by each phenolic acid (10 nM to 10 μM) is shown in Fig. 4b. *p*-Coumaric acid (**4**) and ferulic acid (**6**) both significantly induced activity at the lowest concentration tested (10 nM), whereas caffeic acid (**5**) only induced it at 1 and 100 μM. This concentration dependence was similar to that observed in the direct detection of LCO production (Fig. 1).

We then conducted qRT-PCR to investigate whether phenolic acids induce the transcriptional activation of the NF biosynthesis genes *nodA* and *nodB* using the ML033/pMj-NodD1 strain. The *nodA* gene was significantly induced by 1 μM ferulic acid (**6**) and caffeic acid (**5**), while the *nodB* gene was significantly induced at both 1 and 10 μM, similar to the *ttsI* gene (Fig. 5). Caffeic acid (**5**) exerted similar effects to ferulic acid (**6**) (Fig. 5). As in the β-galactosidase assay, cinnamic acid (**3**) did not induce *nodA*, *nodB*, or *ttsI* expression (data not shown). The above results revealed that the *M. japonicum* NodD1 receptor recognizes phenolic acids, such as ferulic and caffeic acids, and activates the transcription of the *nod* genes.

Phenolic acids exuded from legume roots

To elucidate whether phenolic compounds were exuded from the roots of *L. japonicus*, we used the SRM mode of UPLC-TQMS to analyze the components of culture media 7 days after hydroponic cultures of *L. japonicus*, red clover, and alfalfa. The levels of five phenolic acids that induce the production of NFs (*p*-coumaric acid [**4**], caffeic acid [**5**], ferulic acid [**6**], 5-hydroxyferulic acid [**7**], and phloretic acid [**13**]) and those of phenolic acids that do not (cinnamic acid [**3**] and sinapic acid [**8**]) were quantified. *p*-Coumaric acid (**4**) and ferulic acid (**6**) were detected in hydroponic media from all three plant species, with the levels of *p*-coumaric acid (**4**) being higher in exudates from *L. japonicus* (Table 2). Cinnamic acid (**3**) was only secreted by *L. japonicus* (Table 2). Trace levels (0.2 nmol g^{-1} FW plants or 0.6 nmol mg^{-1} root exudate) of caffeic acid (**5**), sinapic acid (**8**), and phloretic acid (**13**) were detected, whereas 5-hydroxyferulic acid (**7**) was undetectable (less than 0.2 nmol g^{-1} FW plant or 0.6 nmol mg^{-1} root exudate) in either legume.

To monitor the induction of the *ttsI*::*lacZ* fusion in ML033 series strains in the rhizosphere of *L. japonicus*, approximately 10^8 rhizobial cells were spread on the roots of 10-day-old seedlings grown on agar medium with X-Gal. The inoculation with the ML033/p*Mj*-NodD1 strain resulted in X-gal blue staining on and around the root surface (Supplementary Fig. S3). The inoculation of the ML033/p*Mj*-NodD2 strain resulted in X-gal staining only on the root surface. These results strongly suggest that phenolic acid(s) activating NodD1 were exuded not only on the root surface, but also into the rhizosphere of *L. japonicus*.

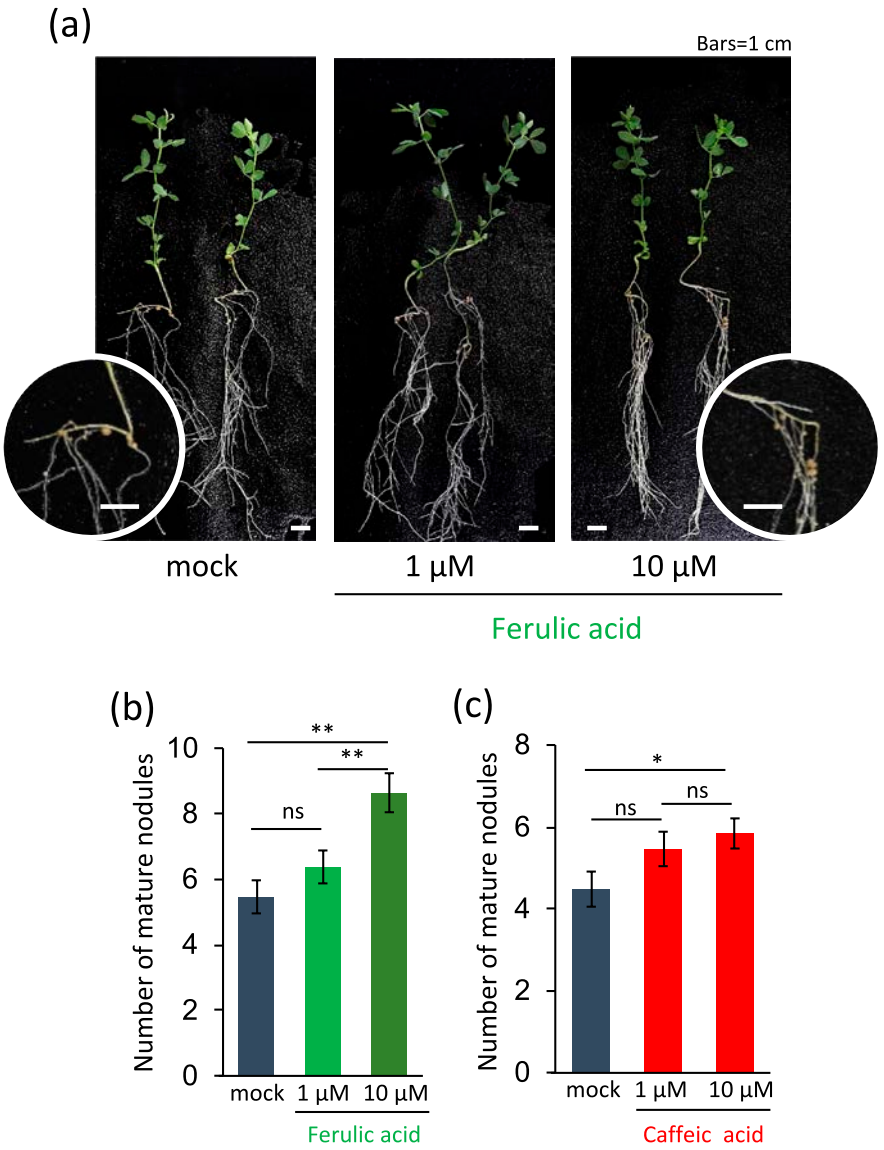

Fig. 3. Promotion of nodulation by phenolic acids. (a) Typical images of 4-week-old *Lotus japonicus* MG-20 inoculated with *Mesorhizobium japonicum* MAFF303099 in the absence or presence of ferulic acid. Scale bars: 1 cm. (b, c) Number of mature nodules in the absence or presence of (b) ferulic acid or (c) caffeic acid. Error bars show S.E. (n=22–27). Significant differences between the absence (mock) and presence of phenolic acids were assessed by the Student's t-test (** P<0.01, * P<0.05, *ns*, not significant).

Discussion

The *nod* gene inducer in *L. japonicus–Mesorhizobium* symbiosis has not been identified despite decades of research. Therefore, we developed a highly sensitive method to analyze LCOs using UPLC-TQMS. MS was previously applied to the study of LCOs, mainly for a structural analysis (Niwa *et al.*, 2001; Bek *et al.*, 2010). To use MS for screening, we simplified purification and reduced the required culture volume, which allowed us to evaluate 40 phenolic compounds. Among them, we identified five phenolic acids that had the potential to induce LCO production in *M. japonicum* MAFF303099. The production of LCOs was enhanced by increases in the concentrations of each of these phenolic acids. LCOs produced by *M. japonicum* MAFF303099 in the presence of caffeic acid (**5**) induced root hair deformation, and nodule numbers in *L. japonicus* inoculated with *M. japonicum* were increased by the addition of ferulic acid (**6**) and caffeic acid (**5**). These results clearly identified phenolic compounds, but not flavonoids, as *nod* gene inducers. Phenolic acids are produced via shikimic acid through the phenylpropanoid pathway, and also as intermediates of the monolignol pathway in vascular plants. A previous study reported that rhizobia utilized phenolic acids as carbon sources (Blum *et al.*, 2000). A number of *nod* gene inducers have been identified in legumes, and most of them are (iso)flavonoids (Liu and Murray, 2016); to the best of our knowledge, this is the first study to demonstrate that phenolic acids function as *nod* gene inducers.

The identified candidate *nod* gene inducers of *L. japonicus* are phenylpropanoids with a carboxylic acid group, in contrast to coniferyl alcohol (**9**) and chlorogenic acid (**12**) (Fig. 6). A comparison with phenolic acids that did not induce LCOs (Table 2), *i.e.* L-phenylalanine (**1**),

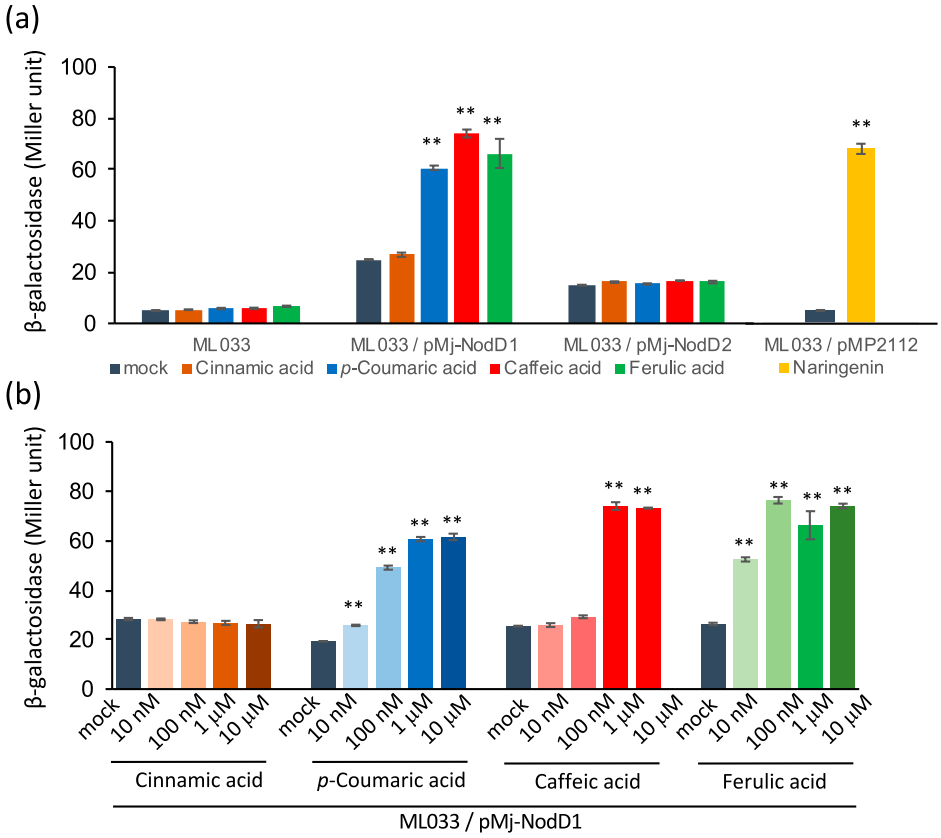

Fig. 4. Effects of phenolic acids on the expression of *lacZ*-fused *ttsI*. (a) Effects of harboring p*Mj*-NodD1, the p*Mj*-NodD2 plasmid, or pMP2112 on β-galactosidase induction by the indicated phenolic acids (1 μM). (b) β-Galactosidase activity in *Mesorhizobium japonicum* MAFF303099 harboring p*Mj*-NodD1 in the presence of different concentrations of the phenolic acids tested in the panel (a). Error bars show S.E. (n=3 or 4). Significant differences between the absence (mock) and presence of phenolic acids were assessed by the Student's t-test (** P<0.01).

trans-cinnamic acid (**3**), umbellic acid (**10**), *o*-coumaric acid (**14**), *m*-coumaric acid (**15**), 3,4-dimethoxycinnamic acid (**16**), isoferulic acid (**17**), and *p*-methoxycinnamic acid (**18**), suggested that a hydroxyl at C-4 and a hydrogen at C-2 or C-6 are important for the ability to induce NFs in *M. japonicum* (Fig. 6). A single methoxy group did not preclude LCO-inducing activity, whereas two methoxy groups, as in sinapic acid (**8**), did. A double bond between α and β carbons appears to be important for the induction of LCO production, but is not essential because weak induction was detected with phloretic acid (**13**). Therefore, the basic structure of a *nod* gene inducer appears to be that of *p*-coumaric acid (**4**) with at most a single methoxy group at C-3 or C-5 and hydrogens at C-2 and C-6. We suggest that the carboxylic acid group and the C-3, C-4, and C-5 positions of the phenyl ring were recognized by NodD.

Aldonic acids have been shown to promote LCO biosynthesis in *Mesorhizobium* strains (Gagnon and Ibrahim, 1998). In our experiments, none of the three aldonic acid compounds tested induced LCO production at the concentrations at which the five phenolic acids induced it. Gagnon and Ibrahim (1998) identified aldonic acids in the root exudates of *Lupinus albus* by screening based on measurements of the β-galactosidase activities of *Rhizobium lupini* strains harboring *nodC*::*lacZ* fusions, and 10 mM tetronic acid was required to induce detectable LCO production in *M. japonicum* R7A. We only tested concentrations up to 100 μM, which may explain why the aldonic acids tested did not induce LCOs. Since tetronic acid was not detected in the root exudates or seed metabolites of *L. japonicus* (Hashiguchi *et al.*, 2018), aldonic acids cannot be endogenous *nod* gene inducers of *L. japonicus*.

In contrast to aldonic acids, the presence of *p*-coumaric acid (**4**), ferulic acid (**6**), and *trans*-cinnamic acid (**3**) was confirmed in the root exudates of *L japonicus* (Table 2). In addition, *p*-coumaric acid (**4**) and ferulic acid (**6**) are listed as metabolites in the seeds of experimental and wild accessions of *L. japonicus* in LegumeBase, the resource database of National BioResource Project *Lotus*/*Glycine* (Hashiguchi *et al.*, 2018). Phenolic acids have also been reported in the root exudates of other legume and non-legume plants (Mandal *et al.*, 2010). We identified *p*-coumaric acid (**4**) and ferulic acid (**6**) in the root exudates of *T. pratense* and *M. sativa* (Table 2), and, thus, these phenolic acids do not appear to contribute to host specificity. Since phenolic acids are generally present in the rhizosphere, the responses of *Mesorhizobium* strains to them may contribute to their associations with a broad range of plants, including non-host plants. *M. japonicum* MAFF303099 associates with non-host plants, such as *Arabidopsis thaliana* (Poitout *et al.*, 2017), as a root epiphyte. T3SS may play a role in this relationship, as reported in *Bradyrhizobium* strains (Piromyou *et al.*, 2015). In the present study, the expression of *ttsI*, a regulator of the T3SS gene cluster, was induced by phenolic

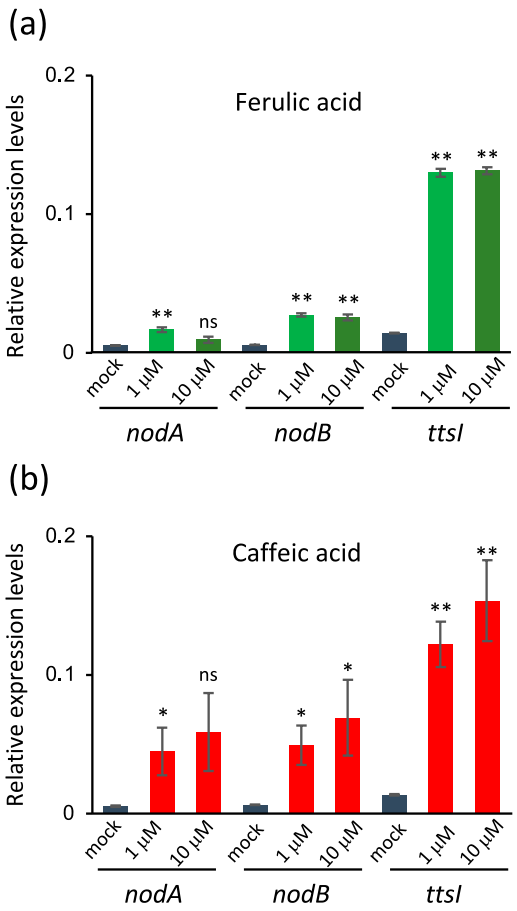

Fig. 5. qRT-PCR analysis of the expression of *nodA*, *nodB*, and *ttsI* genes in *Mesorhizobium japonicum* MAFF303099 harboring p*Mj*-NodD1 in the absence or presence of (a) ferulic acid or (b) caffeic acid. Error bars show S.E. (n=3 or 4). Significant differences between the absence (mock) and presence of phenolic acids were assessed by the Student's t-test (** P<0.01, * P<0.05, *ns*, not significant).

acids at higher levels than that of *nodA* in *M. japonicum* MAFF303099 carrying p*Mj*-NodD1 (Fig. 5). Therefore, phenolic acid recognition by *Mesorhizobium* strains may have a function against non-host plants by inducing T3SS. Regarding host specificity, differences in the concentrations of phenolic acids in root exudates may affect host specificity in *L. japonicus–Mesorhizobium* symbiosis because the concentration of *p*-coumaric acid (**4**) in the root exudates of *L. japonicus* was more than ten-fold higher than those in the root exudates of red clover and alfalfa (Table 2). The NF receptors of host plants are important for recognition that affects the host range in plant–rhizobia symbiotic interactions (Radutoiu *et al.*, 2007; Bek *et al.*, 2010). We confirmed the function of LCOs induced by caffeic acid (**5**) as endogenous NFs for *L. japonicus* by demonstrating their ability to induce root hair deformation (Supplementary Fig. S2). The number of mature nodules was increased by the addition of phenolic acid-type *nod* gene inducers together with an inoculation with *M. japonicum* (Fig. 3), as previously reported in pea and soybean (Novák *et al.*, 2002; Pan *et al.*, 2008). Therefore, the recognition of phenolic acids by *Mesorhizobium* strains may function in two ways: the production of T3SS may contribute to associations with a wide range of plants, and, at the same time, the production of LCOs may function in host recognition in symbiotic interactions.

Although we confirmed LCO production after treatments with five phenolic acids, we failed to detect the induction of *nod* genes by RT-PCR or *ttsI* expression using its promoter fused to *lacZ* in the genome (Fig. 4a). The transcript levels of genes regulated by NodD may be below the detection level of normal RT-PCR and a single copy of *lacZ* in the genome of *M. japonicum* MAFF303099; this may explain our failure to identify *nod* gene inducers in *L. japonicus–Mesorhizobium* symbiosis, even though it has been widely used as a model of symbiosis in legume plants (Liu and Murray, 2016). The *nodA* promoter fused to *lacZ* in a multicopy plasmid (pMP220) has been used to detect *lacZ* expression in *M. japonicum* MAFF303099 (Kojima *et al.*, 2012). We adopted this approach and attempted to increase the copy number of *nodD* genes by introducing *nodD1* or *nodD2* into a multicopy plasmid. This analysis revealed that NodD1 was more sensitive to phenolic acids than NodD2, indicating a functional differentiation between NodD1 and NodD2 with regards to the perception of phenolic acid signals. In *M. japonicum* R7A, NodD1 and NodD2 are functionally redundant for nodulation, with *nodD1* mutants exhibiting only a slight delay in nodulation (Rodpothong *et al.*, 2009). Kelly *et al.* (2018) showed the preferential activation of NodD1 and NodD2 by different compounds produced at defined stages of symbiotic infection. NodD1 is primarily involved in the induction of downstream genes within root hair infection threads. Since phenolic acids are intermediates in the biosynthesis of a number of phenolic compounds, such as flavonoids and monolignols, it is reasonable that they act as *nod* gene inducers in root hair infection threads. However, we detected *p*-coumaric acid (**4**) and ferulic acid (**6**) in the root exudates of *L. japonicus* (Table 2) and *lacZ* gene induction in the rhizosphere using an *M. japonicum* strain with the *nodD1* plasmid (Supplementary Fig. S3). Therefore, the *nod* gene–inducing activities of phenolic acids are not restricted to root hair infection threads,

Table 2. Characteristics of hydroponic cultures and phenolic acid contents in root exudates of three leguminous plants. Values are mean total contents±S.E. (n=4).

	Seed germinated (g DW)	Plant FW (g)	Root exudates (mg)	Contents (nmol g^{-1} FW plant)			Contents (nmol mg^{-1} root exudate)		
				3	**4**	**6**	**3**	**4**	**6**
Lotus japonicus	0.82	1.44	2.7	4.0±0.1	11.9±0.3	2.0±0.0	21.1±0.6	63.2±1.3	10.5±0.1
red clover	0.69	3.38	2.7	n.d.	0.3±0.0	1.7±0.0	n.d.	4.0±0.0	21.6±0.1
alfalfa	2.07	10.21	8.2	n.d.	0.4±0.0	0.6±0.0	n.d.	5.0±0.0	8.0±0.1

FW, fresh weight. **3**, *trans*-cinnamic acid; **4**, *p*-coumaric acid; **6**, ferulic acid; n.d., not detected.

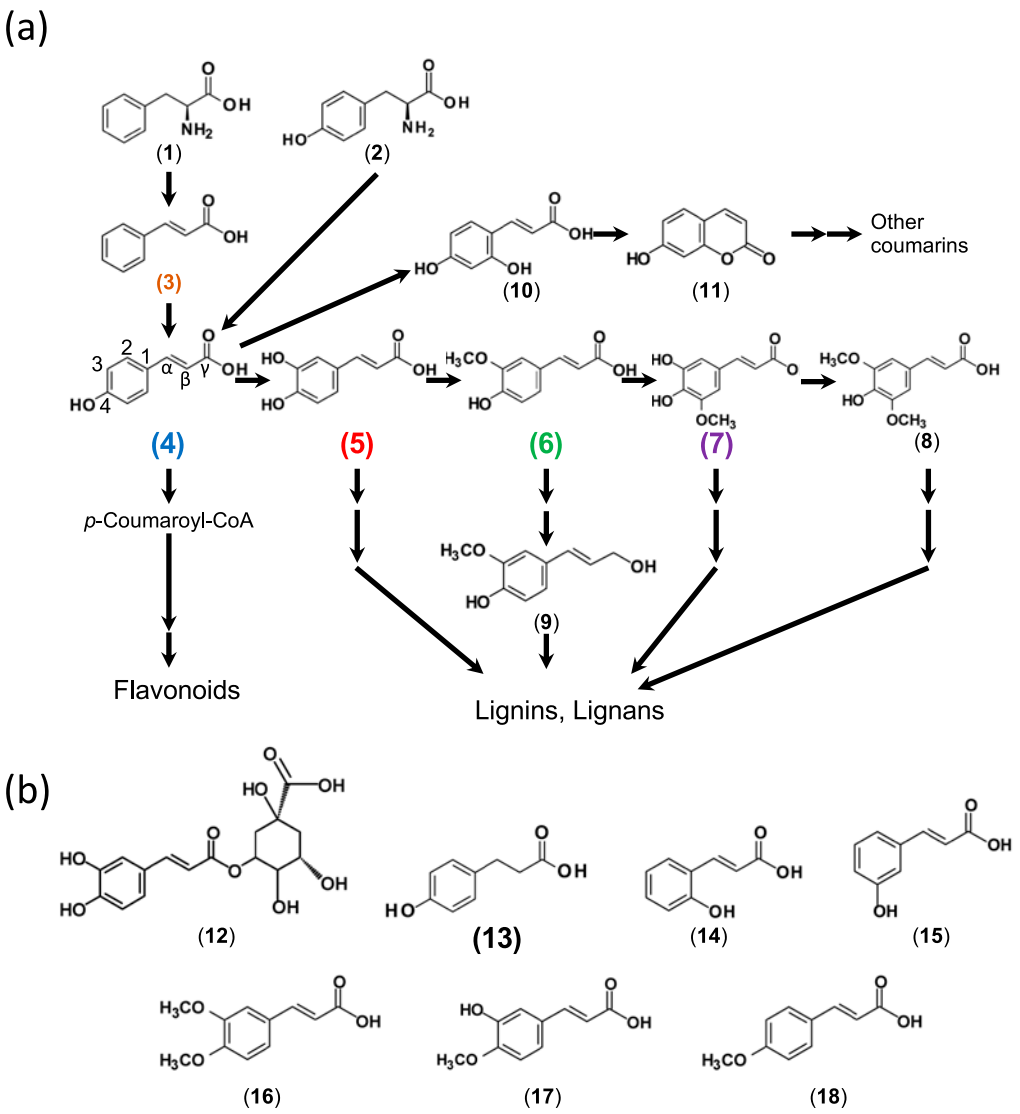

Fig. 6. Chemical structures of phenolic acids used in the present study. (a) Phenolic acids in the major phenylpropanoid pathway towards coumarins, lignins, and lignans. (b) Other phenolic acids. See Table 1 for compound names.

they may also be involved in a wide range of associations in the rhizosphere.

In the present study, we used the direct detection of LCOs to screen for *nod* gene inducers in *L. japonicus–Mesorhizobium* symbiosis. We identified five candidate compounds in the group of phenolic acids, and detected two in the root exudates of *L. japonicus*. By increasing the copy number of one of the two *nodD* genes in *M. japonicum*, we revealed that phenolic acids as *nod* gene inducers were mainly recognized by NodD1. Overall, we propose that phenolic acids are a novel type of *nod* gene inducer in the *L. japonicus–Mesorhizobium* symbiosis system. Therefore, substances that act as mutual symbiotic signals from both sides, *L. japonicus* and *M. japonicum*, are now revealed. The present results will accelerate the elucidation of the regulatory mechanisms in this symbiotic system.

Acknowledgements

We dedicate this report to the memory of the late Professor Toshio Aoki (1961–2019), the last author and principle investigator of this work. The late Professor Aoki designed and conducted the central part of this research, including the establishment of the LCO detection system using UPLC-TQMS, the screening of phenolic compounds, the confirmation of the NF activity of LCO induced by phenolic acids, and the detection of phenolic acids in root exudates.

This work was supported by JSPS KAKENHI Grant Number JP20250915, JST-Mirai Program Grant Number JPMJMI20E4, and JST CREST Grant Number JPMJCR16O1 Japan. We would like to thank Ms. Chikako Mistuoka for her excellent technical assistance. We would also like to express our gratitude to Prof. Hiroshi Kouchi for NF from *M. japonicum* and the plasmid pMP2112, Prof. Hisayuki Mitsui for the plasmid pBBR1MCS-2, and Prof. Shin Okazaki for the *M. japonicum* ML033 strain. The accessions of the *L. japonicus* and *Mesorhizobium* strains were provided by the National BioResource Project '*Lotus*/*Glycine*'.

References

Aoki, T., Kawaguchi, M., Imaizumi-Anraku, H., Akao, S., Ayabe, S., and Akashi, T. (2021) Mutants of *Lotus japonicus* deficient in flavonoid biosynthesis. *J Plant Res* **134**: 341–352.

Begume, A.A., Leibovitch, S., Migner, P., and Zhang, F. (2001) Specific flavonoids induced *nod* gene expression and pre-activated *nod* genes of *Rhizobium leguminosarum* increased pea (*Pisum sativum* L.) and lentil (*Lens culinaris* L.) nodulation in controlled growth chamber environments. *J Exp Bot* **52**: 1537–1543.

Bek, A.S., Sauer, J., Thygesen, M.B., Duus, J.Ø., Petersen, B.O., Thirup, S., *et al.* (2010) Improved characterization of nod factors and genetically based variation in LysM receptor domains identify amino acids expendable for nod factor recognition in *Lotus* spp. *Mol Plant-Microbe Interact* **23**: 58–66.

Blum, U., Staman, K.L., Flint, L.J., and Shafer, S.R. (2000) Induction and/or selection of phenolic acid-utilizing bulk-soil and rhizosphere bacteria and their influence on phenolic acid phytotoxicity. *J Chem Ecol* **26**: 2059–2078.

Broughton, W.J., and Dilworth, M.J. (1971) Control of leghaemoglobin synthesis in snake beans. *Biochem J* **125**: 1075–1080.

Cannon, S.B., Sterck, L., Rombauts, S., Sato, S., Cheung, F., Gouzy, J., *et al.* (2006) Legume genome evolution viewed through the *Medicago truncatula* and *Lotus japonicus* genomes. *Proc Natl Acad Sci U S A* **103**: 14959–14964.

Datsenko, K.A., and Wanner, B.L. (2000) One-step inactivation of chromosomal genes in *Escherichia coli* K-12 using PCR products. *Proc Natl Acad Sci U S A* **97**: 6640–6645.

Firmin, J.L., Wilson, K.E., Rossen, L., and Johnston, W.B. (1986) Flavonoid activation of nodulation genes in Rhizobium reversed by other compounds present in plants. *Nature* **324**: 90–92.

Gagnon, H., and Ibrahim, R.K. (1998) Aldonic acids: A novel family of *nod* gene inducers of *Mesorhizobium loti*, *Rhizobium lupini*, and *Sinorhizobium meliloti*. *Mol Plant-Microbe Interact* **11**: 988–998.

Griffith, K.L., and Wolf, R.E. (2002) Measuring β-galactosidase activity in bacteria: Cell growth, permeabilization, and enzyme assays in 96-well arrays. *Biochem Biophys Res Commun* **290**: 397–402.

Handberg, K., and Stougaard, J. (1992) *Lotus japonicus*, an autogamous, diploid legume species for classical and molecular genetics. *Plant J* **2**: 487–496.

Hanyu, M., Fujimoto, H., Tejima, K., and Saeki, K. (2009) Functional differences of two distinct catalases in *Mesorhizobium loti* MAFF303099 under free-living and symbiotic conditions. *J Bacteriol* **191**: 1463–1471.

Hashiguchi, M., Tanaka, H., Muguerza, M., Akashi, R., Sandal, N.N., Andersen, S.U., *et al.* (2018) *Lotus japonicus* genetic, mutant, and germplasm resources. *Curr Protoc Plant Biol* **3**: e20070.

Hattori, Y., Omori, H., Hanyu, M., Kaseda, N., Mishima, E., Kaneko, T., *et al.* (2002) Ordered cosmid library of the *Mesorhizobium loti* MAFF303099 genome for systematic gene disruption and complementation analysis. *Plant Cell Physiol* **43**: 1542–1557.

Hougaard, B.K., Madsen, L.H., Sandal, N., Moretzsohn, M.C. Fredslund, J., Schauser, L., *et al.* (2008) Legume anchor markers link syntenic regions between *Phaseolus vulgaris*, *Lotus japonicus*, *Medicago truncatula* and Arachis. *Genetics* **179**: 2299–2312.

Hungria, M., Joseph, C.M., and Phillips, D.A. (1991) Anthocyanidins and flavanols, major *nod* gene inducers from seeds of black-seeded common bean (*Phaseolus vulgaris* L.). *Plant Physiol* **97**: 751–775.

Imaizumi-Anraku, H., Kawaguchi, M., Koiwa, H., Akao, S., and Syōno, K. (1997) Two ineffective-nodulating mutants of *Lotus japonicus*—Different phenotypes caused by the blockage of endocytotic bacterial release and nodule maturation. *Plant Cell Physiol* **38**: 871–881.

Kaneko, T., Nakamura, Y., Sato, S., Asamizu, E., Kato, T., Sasamoto, S., *et al.* (2000) Complete genome structure of the nitrogen-fixing symbiotic bacterium *Mesorhizobium loti*. *DNA Res* **7**: 331–338.

Kawaguchi, M., Imaizumi-Anraku, H., Koiwa, H., Niwa, S., Ikuta, A., Syono, K., and Akao, S. (2002) Root, root hair, and symbiotic mutants of the model legume *Lotus japonicus*. *Mol Plant-Microbe Interact* **15**: 17–26.

Kelly, S., Sullivan, T.J.S., Kawaharada, Y., Radutoiu, S., Ronson, W.C., and Stougaard, J. (2018) Regulation of Nod factor biosynthesis by alternative NodD proteins at distinct stages of symbiosis provides additional compatibility scrutiny. *Environ Microbiol* **20**: 97–110.

Kojima, K., Yokoyama, T., Ohkama-Ohtsu, N., Saengkerdsub, S., Itakura, M., Mitsui, H., *et al.*, (2012) Exploration of natural nod gene inducers for Mesorhizobium loti in seed and root exudates of *Lotus corniculatus*. *Soil Microorganisms* **66**: 12–21.

Kosslak, R.M., Bookland, R., Barkei, J., Paaren, H.E., and Appelbaum, E.R. (1987) Induction of *Bradyrhizobium japonicum* common *nod* genes by isoflavones isolated from *Glycine max*. *Proc Natl Acad Sci U S A* **84**: 7428–7432.

Kovach, M.E., Elzer, P.E., Hill D.S., Robertson G.T., Farris, M.A., Roop II, R.M., *et al.* (1995) Four new derivatives of the broad-host-range cloning vector pBBR1MCS, carrying different antibiotic-resistance cassettes. *Gene* **166**: 175–176.

Kusakabe, S., Higasitani, N., Kaneko, T., Yasuda, M., Miwa, H., Okazaki, S., *et al.* (2020) *Lotus* accessions possess multiple checkpoints triggered by different type III secretion system effectors of the wide-host-range symbiont *Bradyrhizobium elkanii* USDA61. *Microbes Environ* **35**: ME19141.

Liang, Y., Tóth, K., Cao, Y., Tanaka, K., Espinoza, C., and Stacey, G. (2014) Lipochitooligosaccharide recognition: an ancient story. *New Phytol* **204**: 289–296.

Liu, C.W., and Murray, J.D. (2016) The role of flavonoids in nodulation host-range specificity: An update. *Plants* **5**: 33.

López-Lara, I.M., van den Berg, J.D.J., Thomas-Oates, J.E., Glushka, J., Lugtenberg, B.J.J., and Spaink, H.P. (1995) Structural identification of the lipo-chitin oligosaccharide nodulation signals of *Rhizobium loti*. *Mol Microbiol* **15**: 627–638.

Mandal, S.M., Chakraborty, D., and Dey, S. (2010) Phenolic acids act as signaling molecules in plant-microbe symbioses. *Plant Signal Behav* **5**: 359–368.

Martínez-Hidalgo, P., Ramírez-Bahena, M.H., Flores-Félix, J.D., Igual, J.M., Sanjuán J., León-Barrios, M., *et al.* (2016) Reclassification of strains MAFF 303099^{T} and R7A into *Mesorhizobium japonicum* sp. nov. *Int J Syst Bacteriol* **66**: 4936–4941.

Niwa, S., Kawaguchi, M., Imaizumi-Anraku, H., Chechetka, S.A., Ishizaka, M., Ikuta, A., *et al.* (2001) Responses of a model legume *Lotus japonicus* to lipochitin oligosaccharide nodulation factors purified from *Mesorhizobium loti* JRL501. *Mol Plant-Microbe Interact* **14**: 848–856.

Novák, K., Chovanec, P., Škrdleta, V., Kropáčová, M., Lisá, L., and Němcová, M. (2002) Effect of exogenous flavonoids on nodulation of pea (*Pisum sativum* L.). *J Exp Bot* **53**: 1735–1745.

Okazaki, S., Okabe, S., Higashi, M., Shimoda, Y., Sato, S., Tabata, S., *et al.* (2010) Identification and functional analysis of type 3 effector proteins in *Mesorhizobium loti*. *Mol Plant-Microbe Interact* **23**: 223–234.

Okazaki, S., Kaneko, T., Sato, S., and Saeki, K. (2013) Hijacking of leguminous nodulation signaling by the rhizobial type III secretion system. *Proc Natl Acad Sci U S A* **110**: 17131–17136.

O'Rourke, J.A., Bolon, Y.T., Bucciarelli, B., and Vance, C.P. (2014) Legume genomics: understanding biology through DNA and RNA sequencing. *Ann Bot* **113**: 1107–1120.

Pan, B., Zhang, F., and Smith, D.L. (2008) Genistein addition to the rooting medium of soybean at the onset of nitrogen fixation increases nodulation. *J Plant Nutr* **21**: 1631–1639.

Peters, N.K., Frost, J.W., and Long, S.R. (1986) A plant flavone, luteolin, induces expression of *Rhizobium meliloti* nodulation genes. *Science* **233**: 977–980.

Piromyou, P., Songwattana, P., Greetatorn, T., Okubo, T., Chiba-Kakizaki, K., Prakamhang, J., *et al.* (2015) The Type III Secretion System (T3SS) is a determinant for rice-endophyte colonization by non-photosynthetic *Bradyrhizobium*. *Microbes Environ* **30**: 291–300.

Poitout, A., Martinière, A., Kucharczyk, B., Queruel, N., Silva-Andia, J., Mashkoor, S., *et al.* (2017) Local signalling pathways regulate the *Arabidopsis* root developmental response to *Mesorhizobium loti* inoculation. *J Exp Bot* **68**: 1199–1211.

Radutoiu, S., Madsen, L.H., Madsen, E.B., Jurkiewicz, A., Fukai, E., Quistgaard, E.M.H., *et al.* (2007) LysM domains mediate lipochitin–oligosaccharide recognition and *Nfr* genes extend the symbiotic host range. *EMBO J* **26**: 3923–3935.

Recourt, K., Brussel, A.A.N., Driessen, A.J.M., and Lugtenberg, B.J.J. (1989) Accumulation of a *nod* gene inducer, the flavonoid naringenin, in the cytoplasmic membrane of *Rhizobium leguminosarum* biovar *viciae* is caused by the pH-dependent hydrophobicity of naringenin. *J Bacteriol* **171**: 4370–4377.

Rodpothong, P., Sullivan, J.T., Songsrirote, K., Sumpton, D., Cheung, K.W., Thomas-Oates, J., *et al.* (2009) Nodulation gene mutants of *Mesorhizobium loti* R7A-nodZ and nolL mutants have host-specific phenotypes on *Lotus* spp. *Mol Plant-Microbe Interact* **22**: 1546–1554.

Saeki, K., Suetsugu, Y., Tokuda, K., Miyatake, Y., Young, D.A., Marrs, B.L., *et al.* (1991) Genetic analysis of functional differences among distinct ferredoxins in *Rhodobacter capsulatus*. *J Biol Chem* **266**: 12889–12895.

Saeki, K., and Kouchi, H. (2000) The *Lotus* symbiont, *Mesorhizobium loti*: molecular genetic techniques and application. *J Plant Res* **113**: 457–465.

Sato, S., and Tabata, S. (2006) *Lotus japonicus* as a platform for legume research. *Curr Opin Plant Biol* **9**: 128–132.

Sato, S., Nakamura, Y., Kaneko, T., Asamizu, E., Kato, T., Nakao, M., *et al*. (2008) Genome structure of the legume, *Lotus japonicus*. *DNA Res* **15**: 227–239.

Shimamura, M., Akashi, T., Sakurai, N., Suzuki, H., Saito, K., Shibata, D., *et al.* (2007) 2-Hydroxyisoflavanone dehydratase is a critical determinant of isoflavone productivity in hairy root cultures of *Lotus japonicus*. *Plant Cell Physiol* **48**: 1652–1657.

Sugawara, M., Takahashi, S., Umehara, Y., Iwano, H., Tsurumaru, H., Odake, H., *et al.* (2018) Variation in bradyrhizobial NopP effector determines symbiotic incompatibility with Rj2-soybeans via effector-triggered immunity. *Nat Commun* **9**: 3139.

Suzaki, T., Yoro, E., and Kawaguchi, M. (2015) Leguminous plants: inventors of root nodules to accommodate symbiotic bacteria. *Int Rev Cell Mol Biol* **316**: 111–158.

Udvardi, M.K., Tabata, S., Parniske, M., and Stougaard, J. (2005) *Lotus japonicus*: legume research in the fast lane. *Trends Plant Sci* **10**: 222–228.

Young, N.D., and Bharti, A.K. (2012) Genome-enabled insights into legume biology. *Annu Rev Plant Biol* **63**: 283–305.

Microbes Environ. 36(2), 2021
https://www.jstage.jst.go.jp/browse/jsme2 doi:10.1264/jsme2.ME21007

MOST VALUABLE PAPER OF THE YEAR 2021

Bioelectrical Methane Production with an Ammonium Oxidative Reaction under the No Organic Substance Condition

Ha T.T Dinh[1,2], Hiromi Kambara[1], Yoshiki Harada[1], Shuji Matsushita[1,3], Yoshiteru Aoi[4], Tomonori Kindaichi[1], Noriatsu Ozaki[1], and Akiyoshi Ohashi[1]*

[1]*Department of Civil and Environmental Engineering, Graduate School of Advanced Science and Engineering, Hiroshima University, 1–4–1, Kagamiyama, Higashi-Hiroshima, Hiroshima 739–8527, Japan;* [2]*Faculty of Environment, Ho Chi Minh City University of Natural Resources and Environment, 236 Le Van Sy, 1 Ward, Tan Binh District, Ho Chi Minh City, Vietnam;* [3]*Agricultural Technology Research Center, Hiroshima Prefectural Technology Research Institute, 6869, Hara, Hachihonmatsu, Higashi-Hiroshima, Hiroshima 739–0151, Japan; and* [4]*Program of Biotechnology, Graduate School of Integrated Sciences for Life, Hiroshima University, 1–3–1, Kagamiyama, Higashi-Hiroshima, Hiroshima 739–8530, Japan*

(Received January 25, 2021—Accepted May 1, 2021—Published online June 17, 2021)

The present study investigated bioelectrical methane production from CO_2 without organic substances. Even though microbial methane production has been reported at relatively high electric voltages, the amount of voltage required and the organisms contributing to the process currently remain unknown. Methane production using a biocathode was investigated in a microbial electrolysis cell coupled with an NH_4^+ oxidative reaction at an anode coated with platinum powder under a wide range of applied voltages and anaerobic conditions. A microbial community analysis revealed that methane production simultaneously occurred with biological denitrification at the biocathode. During denitrification, NO_3^- was produced by chemical NH_4^+ oxidation at the anode and was provided to the biocathode chamber. H_2 was produced at the biocathode by the hydrogen-producing bacteria *Petrimonas* through the acceptance of electrons and protons. The H_2 produced was biologically consumed by hydrogenotrophic methanogens of *Methanobacterium* and *Methanobrevibacter* with CO_2 uptake and by hydrogenotrophic denitrifiers of *Azonexus*. This microbial community suggests that methane is indirectly produced without the use of electrons by methanogens. Furthermore, bioelectrical methane production occurred under experimental conditions even at a very low voltage of 0.05 V coupled with NH_4^+ oxidation, which was thermodynamically feasible.

Key words: ammonia oxidation, bio-electricity, denitrification, methane production, microbial community

Methane is the prime component of natural gas and is widely utilized as an energy source worldwide. It is mainly produced by biological and physical actions that collectively contribute to 20–80% of natural gas reserves (Rice and Claypool, 1981). Methane is physically produced through the thermal decomposition of organic matter in association with the formation of coal, gas, and oil (Schoell, 1988). Conversely, biological methane formation is primarily performed by methanogenic microbes (methanogens) in anaerobic environments (Whiticar *et al.*, 1986; Whiticar, 1999). Only methanogenic archaea are known to act as methanogens and use substrates produced from organic matter during fermentation, such as acetate, formate, and hydrogen gas. This methane fermentation occurs in nature, but has also been applied as an eco-friendly wastewater treatment technology (Onodera, 2013; Townsend-Small *et al.*, 2016). Artificially produced biogas may be utilized as an energy source after purification.

It is possible to generate electricity from organic substances. Microbial fuel cell (MFC) technology and its application to wastewater treatment have been extensively examined (Logan *et al.*, 2006; Sarmin *et al.*, 2019; Wang *et al.*, 2020). Conversely, in microbial electrosynthesis systems (MESs), methane is produced by providing electricity (Rabaey and Rozendal, 2010; Eerten-Jansen *et al.*, 2012). High methane production is expected when MESs are applied to wastewater treatment because of the combination of methane fermentation using organic substances and the conversion of CO_2 to methane by microbes through electricity (Clauwaert *et al.*, 2008; Clauwaert and Verstraete, 2009; Zhao *et al.*, 2016; Park *et al.*, 2018; Peng *et al.*, 2019). Ding *et al.* (2016) identified 0.8 V as the optimal applied voltage for appropriate wastewater treatment and maximum methane production using an MES.

In the MES, bioelectrical methane production is performed without organic substrates (Cheng *et al.*, 2009; Villano *et al.*, 2010; Zhen *et al.*, 2015). Cheng *et al.* (2009) reported that carbon dioxide was reduced to methane at a biocathode potential of <–0.7 V (vs. Ag/AgCl). At –1.0 V (vs. Ag/AgCl), the electron capture efficiency of methane production was 96%. Two mechanisms have been proposed for biological methane production using a biocathode. At high applied voltages, methane may be produced by hydrogenotrophic methanogens using abiotic H_2 formed in water oxidation (Wagner *et al.*, 2009; Eerten-Jansen *et al.*, 2012). In this case, H_2 is an important intermediate for methane production. The second mechanism is direct electrotrophic methane production. Cheng *et al.* (2009) reported that some

* Corresponding author. E-mail: ecoakiyo@hiroshima-u.ac.jp;
Tel: +81–82–424–7823; Fax: +81–82–424–7823.

Citation: Dinh, T. T H., Kambara, H., Harada, Y., Matsushita, S., Aoi, Y., Kindaichi, T., et al. (2021) Bioelectrical Methane Production with an Ammonium Oxidative Reaction under the No Organic Substance Condition. *Microbes Environ* **36**: ME21007.
https://doi.org/10.1264/jsme2.ME21007

methanogens must use electrons with CO_2 to directly produce methane, without hydrogen as an intermediary. Previous studies on extracellular electron transfer demonstrated that applied voltage may not be effective at promoting methane production, suggesting a pathway without H_2 (Rotaru *et al.*, 2013; Lohner *et al.*, 2014; Holmes *et al.*, 2017; Lee *et al.*, 2017). However, there are insufficient experimental data to prove direct electrotrophic methane production. It currently remains unclear whether bioelectrical methane production occurs via direct and/or indirect reaction(s) in MESs.

The CO_2 reduction potential to methane $E^{0'}_{cat}$ at the biocathode is –0.24 V (vs. SHE) under the standard condition at pH=7. When coupled with H_2O oxidation ($E^{0'}_{an}$=0.81 V vs SHE) at the anode, methane production in an MES occurs thermodynamically by applying more than 1.05 V under the standard condition. If the oxidation of inorganic compounds with a lower potential (such as NH_4^+ oxidation to NO_3^- and N_2: $E^{0'}_{an}$=0.36 V and –0.29 V vs. SHE, respectively) occurs instead of H_2O oxidation, methane may be produced at a lower applied voltage. However, MES studies have not provided sufficient information on the oxidation reaction at the anode, with experiments being conducted at relatively high voltages.

In the present study, we designed an MES experiment in which an organic substrate was not supplied, and NH_4^+ was added to the anode chamber to investigate whether methane production is possible even at very low applied voltages. Although the reaction of electrotrophic methane production with NH_4^+ oxidation to N_2 thermodynamically proceeded even without a supply of electricity, this is the first study to report coupling to the NH_4^+ oxidative reaction. In addition, the microbial community was analyzed to identify the organisms involved in bioelectrical methane production.

Materials and Methods

MES set-up

The MES used in the present study consisted of two glass chambers, each with an effective volume of 70 mL, which were connected by a 10-cm salt bridge containing 2% (w/w) agar (KF-30; Fujirika) and 20% (w/w) KCl (Fig. S1). The top of each chamber was connected to a 10-mL loss-of-resistance glass syringe to release the pressure generated in the chamber by the gas produced and also facilitate gas collection. A 9-cm^2 electrode of carbon cloth (Toyobo) was installed in both chambers. The biocathode and anode electrodes were connected to a DC power supply (Array 3600 Series; T&C Technology) using a platinum wire. A 100-Ω resistor was inserted between the power supply and biocathode electrode to estimate the electric current by measuring voltage using a digital multimeter (FlePow; Levin Japan). Even if the external resister was inserted, the effect on the actual applied voltage was negligible when the internal resistance of the MES was high. A small amount of anaerobic sludge taken from a laboratory-scale upflow anaerobic sludge blanket (UASB) reactor was inoculated on the surface of the cathode electrode. Platinum powder (10% by weight of platinum on carbon powder; E-TEK, C-1 10% Pt on Vulcan XC-72) was coated on the surface of the anode, as described in previous studies (Müller and Spitzer, 1905; Nutt and Kapur, 1968; De Vooys *et al.*, 2001; Bunce and Bejan, 2011; Li *et al.*, 2017).

MES operation

The MES was operated in the batch-processing mode at 30°C in a thermostatic chamber. The anodic and biocathodic chambers were filled with the same medium without organic substances and deoxidized through a nitrogen purge. The medium was composed of $NaHCO_3$ (200 mg L^{-1}), NH_4Cl (190 mg L^{-1}), NaH_2PO_4 (17 mg L^{-1}), and Na_2HPO_4 (124 mg L^{-1}), as well as trace elements, including $FeSO_4{\cdot}7H_2O$ (7 mg L^{-1}), $CoCl_2{\cdot}6H_2O$ (1.7 mg L^{-1}), $ZnSO_4{\cdot}7H_2O$ (1.5 mg L^{-1}), HBO_3 (0.6 mg L^{-1}), $MnCl_2{\cdot}4H_2O$ (4.2 mg·L^{-1}), $NiCl_2{\cdot}4H_2O$ (0.4 mg L^{-1}), $CuCl_2{\cdot}2H_2O$ (0.27 mg L^{-1}), and $Na_2MoO_2{\cdot}2H_2O$ (0.25 mg L^{-1}), at a pH of 7.5. The medium was completely replaced at intervals of 3, 5, 6, and 13 d, with the batch experiment being repeated 20 times over 110 d of operation. Each batch duration time was determined according to gas production for gas sampling. Each batch experiment was performed at a constant applied voltage in the range of 0.05–3.0 V to investigate whether methane production is possible even at low voltages. After setting up the MES, a voltage was immediately supplied to enhance microbial activity at the biocathode, and the anode was unsterilized.

Sampling and analyses

The volume of gas production in the respective chambers was measured using an airtight syringe. CH_4, N_2, CO_2, and H_2 concentrations were then measured using a gas chromatograph equipped with a thermal conductivity detector (GC-TCD; Shimadzu GC-8A). NH_4^+, NO_3^-, and NO_2^- concentrations in the medium were measured by ion chromatography (Shimadzu HPLC-20A) at the start and end of each batch operation. Dissolved CH_4 and N_2 concentrations were estimated using Henry's law.

Microbial community

The sludge sample at the biocathode was collected on day 110 of the last MES operation and washed with phosphate buffer. DNA was extracted using the FastDNA® SPIN Kit for Soil (MP Biomedicals), according to the manufacturer's instructions. PCR amplification of the 16S rRNA gene was performed using the primer sets 341'F (5′-CCTAHGGGRBGCAGCAG-3′) and 805R (5′-GACTACHVGGGTATCTAATCC-3′) with KAFA HiFi Hotstart ReadyMix (Kapa Biosystems). PCR conditions were as follows: the initial denaturation of DNA at 95°C for 3 min, followed by 25 cycles at 95°C for 30 s, at 55°C for 30 s, and at 72°C for 30 s, with a final extension at 72°C for 5 min. The PCR product was purified and sequenced by the emulsion method using Illumina/Miseq (Illumina) at Hokkaido System Science. The sequences obtained were analyzed using QIIME (v1.8.0) (Caporaso *et al.*, 2010). Operational taxonomic units (OTUs) were grouped based on a threshold value of 97% identity for DNA using the UCLUST algorithm (Edgar, 2010). These OTUs were classified using the Greengenes database (McDonald *et al.*, 2012; Werner *et al.*, 2012).

Sequence data were deposited in the DDBJ database under DDBJ/EMBL/GenBank accession number DRA011341.

Results

Performance of batch experiments

In MES batch operations, we initially attempted to apply a relatively high voltage of 2.0 V over 3 d. Once a higher current of approximately 0.18 mA was observed, it immediately decreased to 0.09 mA and gradually declined over time, as shown in Fig. 1. However, no gas bubbles were visible in either the biocathode or anode chambers, despite the sludge inoculation being expected to enable methane production activity. The 3-d batch experiment was then

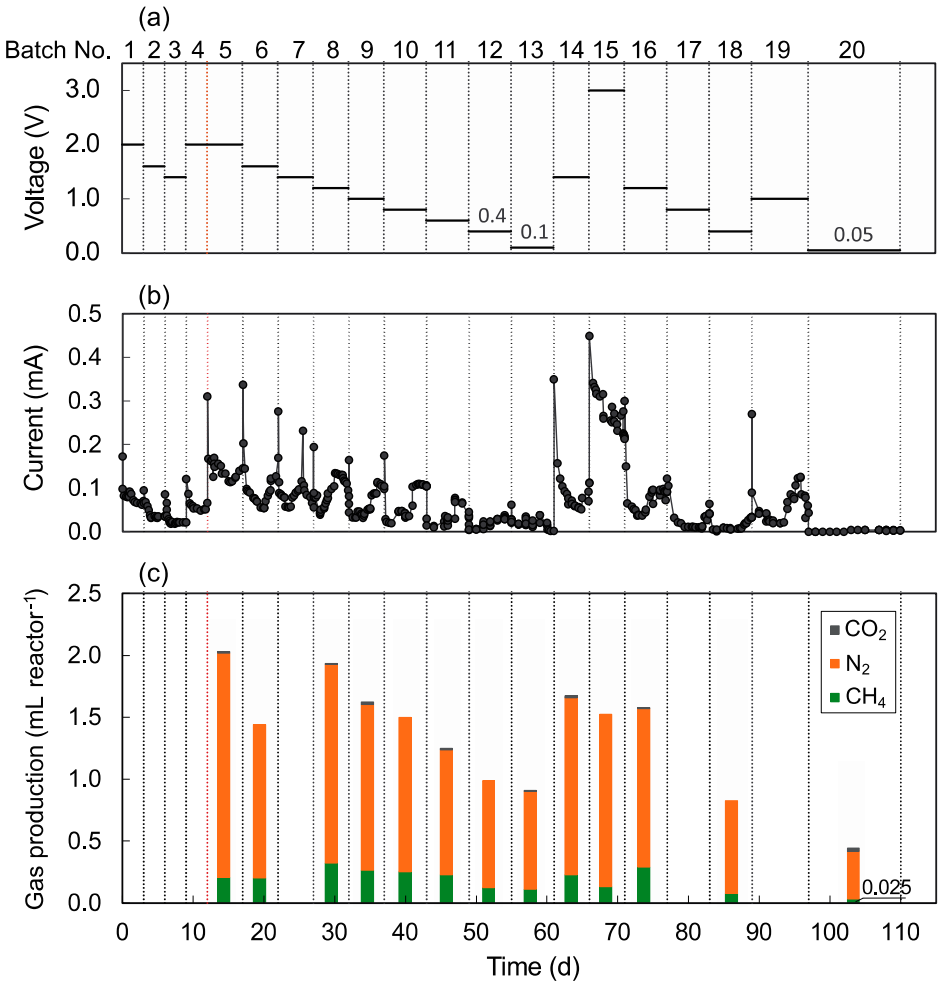

Fig. 1. Time courses of applied voltage (a), current (b), and gases (CH_4, N_2, and CO_2) produced (c) in batch experiments.

repeated with changes in bulk liquid, but at lower voltages of 1.6 V and 1.4 V, resulting in current behaviors that were the same as those at 2.0 V. Under these conditions, very few bubbles were observed in the biocathode chamber. In the next batch operation, bubbles were observed where the applied voltage was returned to 2.0 V. However, it was not possible to sample the gas produced because of its low volume.

Therefore, we changed the batch interval time from 3 to 5 d from day 12 onwards, except for some special batches. More bubbles were produced in the biocathode chamber and collected as a gas in the fifth batch operation at 2.0 V. The gas produced was approximately 2.0 mL on days 12–17 (Fig. 1). As expected, methane was detected, but its concentration was only 10.0%. The main component of the gas was N_2, with a very low concentration of CO_2. The current was markedly higher than that in the previous batch experiment at the same voltage. The current also decreased for approximately 3 d, but increased thereafter. A significant difference was observed in current behavior between the small and large gas production chambers. In control batch experiments without the inoculation, methane was not detected in the range of 1.0–2.0 V; however, hydrogen production was observed at an applied voltage higher than 1.2 V in the cathode chamber. Methane production is expected to be derived from inorganic carbon in the presence of microbes on the carbon cloth, the biological activity of which may be enhanced after 17 d of operation; however, no bubbles were observed in the anode chamber under any of the conditions used.

To investigate the effects of voltage on methane production, experiments were continuously performed while decreasing the applied voltage step-by-step down to 0.1 V until day 61 (Fig. 1). The current slightly decreased with voltage reductions; however, its pattern of behavior was similar in each batch period. Gas containing CH_4 and N_2 was produced at any voltage, except during days 22–27 when gas sampling failed.

Since high N_2 concentrations of approximately 75 to 90% were detected, we reconducted batch experiments under almost identical conditions over a range of 0.05–3.0 V on days 55–110 to reveal the source of N_2 yield by measuring ammonium, nitrate, and nitrite. In the last batch operation, we also attempted methane production at a very low voltage of 0.05 V. A small amount of gas containing 6.09% CH_4 was collected, even at the lowest voltage, particularly over a prolonged period of 13 d. NH_4^+ and NO_3^- concentrations decreased in both the biocathode and anode chambers (Fig. S2). Total nitrogen ions in the two chambers decreased in all batches, suggesting that the yield of N_2 was derived from

inorganic nitrogen ions. Regarding the nitrogen balance, a strong relationship was observed between the amount of consumed NH_4^+ plus NO_3^- and produced N_2 (Fig. S3). Cecconet *et al.* (2019) reported the accumulation of NO_2^- and N_2O in a biocathodic denitrification process for groundwater bioremediation. However, these intermediates in denitrification were not detected in this MES experiment. The lack of accumulation of intermediates may have been caused by the slow reaction.

Effects of voltage on gas production

Although a 100-Ω external resistor was inserted, the voltage supplied was nearly equal to the actual applied voltage between the biocathode and anode because the current versus supplied voltage was small throughout the experiment, as shown in Fig. 1. The gas production rate was significantly dependent on the applied voltage, as shown in Fig. 2. CH_4 production slightly increased in proportion to the voltage with 0.306 mL at 1.2 V, after which it decreased to 0.128 mL at 3.0 V. These results suggest that a very high voltage does not always enhance methane production and may have a negative effect on microbes. The N_2 production rate was similar to that of CH_4 with respect to the effects of voltage; however, large fluctuations were observed. This suggests that microbes also play a role in N_2 production. The retained microbes were expected to grow and increase with the operational time. However, they were slightly detached when bulk liquid was replaced as a result of changes in batch conditions. Therefore, the number of microbes was unstable, possibly contributing to fluctuations in gas production.

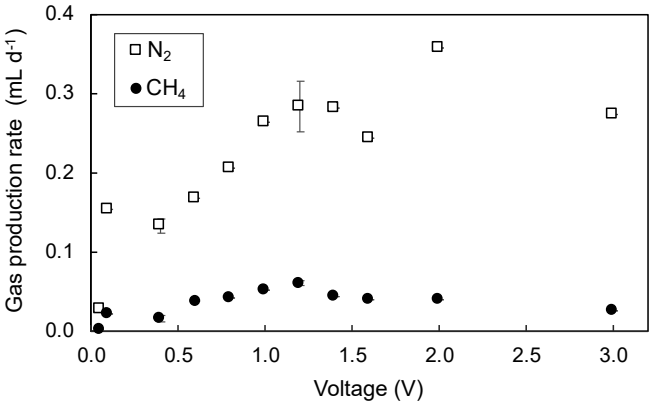

Fig. 2. Gas production rates at different applied voltages.

Microbial community

In the 16S rRNA gene sequencing of the biomass sample on day 110, more than 100,000 reads, including domain bacteria and archaea, were obtained, and the number of OTUs exceeded 1,200. Sequencing results revealed the presence of bacterial and archaeal communities (Fig. 3). Archaea comprised only 3.9% of the total reads.

The major families of bacteria were *Porphyromonadaceae*, *Rhodocyclaceae*, and *Geobacterceae*, accounting for 26.8, 11.4, and 10.7%, respectively. The three families made up approximately 45% of all microbes. Of the most dominant family *Porphyromonadaceae*, approximately 50% was the obligately anaerobic genus of *Petrimonas*, while 29.8% uncultured genera were detected (Fig. 3). *Petrimonas* consists of hydrogen-producing bacteria (Lu *et al.*, 2012; Sun *et al.*, 2015; Liu *et al.*, 2016), suggesting that hydrogen is pro-

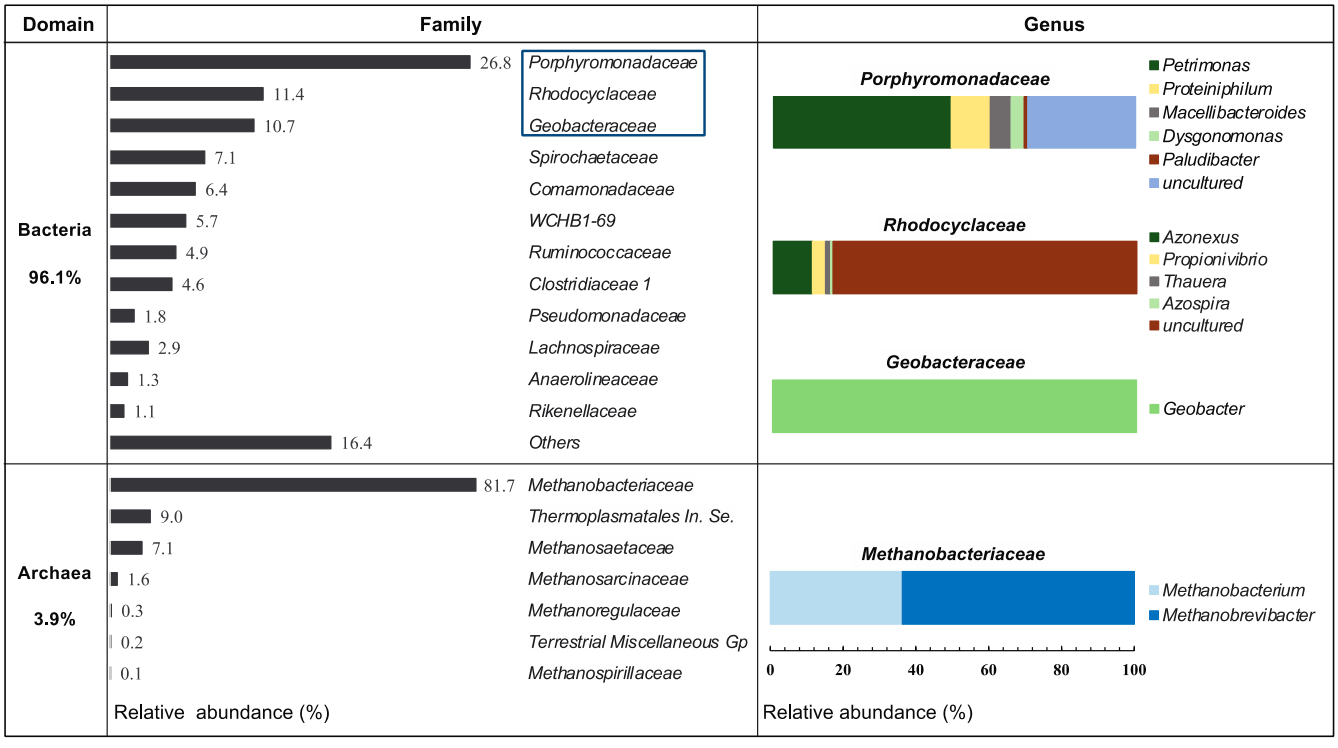

Fig. 3. Microbial community of a biomass sample on day 110, based on the 16S rRNA gene.

duced in the biocathode chamber. Most bacteria belonging to *Rhodocyclaceae* exhibit denitrification activity (Zhao *et al.*, 2013; Wang *et al.*, 2017). The predominant *Azonexus* genus detected, which may grow on molecular hydrogen as an electron donor (Zhao *et al.*, 2011; Liang *et al.*, 2021), plays an important role in the denitrification process to produce nitrogen gas. Only *Geobacter* was detected within the *Geobacterceae* family. The presence of electrically conductive pili or flagella on *Geobacter* species is reportedly linked to electron transfer in the MFC (Cabezas *et al.*, 2015; Yan *et al.*, 2020). In the present study, *Geobacter* appeared to be responsible for electron transfer to yield biogas.

Regarding archaea, all OTUs were *Euryarchaeota*. The majority of *Euryarchaeota* detected were methanogens, with the dominant family (81.7%) being *Methanobacteriaceae*, a hydrogen-utilizing methanogen (Fig. 3). Two genera, *Methanobrevibacter* and *Methanobacterium*, were detected at concentrations of 63.8 and 36.3%, respectively (Fig. 3). They played a major role in CH_4 production in the biocathode chamber. In addition, *Methanosaetaceae*, an obligate acetoclastic methanogen, was detected, albeit at a low concentration (7.1%); therefore, acetate may be produced and converted to CH_4. However, its contribution appears to have been insignificant.

The biological contributors to denitrification and methane production were identified; the produced gas containing CH_4 and N_2 may be explained by the presence of these microbes. Therefore, we demonstrated the biological production of CH_4 through the provision of electricity, even at very low voltages, and in the absence of organic substances in the MES.

Discussion

NH_4^+ oxidation was observed in the anode chamber, although at insignificant amounts, indicating that NH_4^+ was oxidized by donating electrons to the biocathode. Platinum is commonly accepted as the most promising catalyst in the electrochemical oxidation of ammonia (*e.g.*, De Vooys *et al.*, 2001; Li *et al.*, 2017). Müller and Spitzer (1905) reported that the anodic products of electrolyzing ammonia at a platinum anode were mainly NO_3^- and N_2 (25%–35%). With over-oxidation, NO_2^- and NO_3^- products were observed at applied voltages of higher than +0.6 V (vs Ag/AgCl) (Endo *et al.*, 2005; Bunce and Bejan, 2011). NO_3^- was also reportedly formed from NH_4^+ by catalytic oxidation with PtO_x (Fóti and Comninellis, 2004; Panizza and Cerisola, 2009). Since platinum powder was coated on the surface of the anode with a carbon cloth electrode in the present study, similar reactions to the electrolysis of water occurred; however, neither N_2 nor NO_2^- production was observed.

The oxidation of NH_4^+ at the anode may be represented as follows:

$$1/8\ NH_4^+ + 3/8\ H_2O \rightarrow 1/8\ NO_3^- + 5/4\ H^+ + e^- \quad (1)$$

The NO_3^- produced was transferred to the biocathode chamber through the salt bridge by diffusion, resulting in a decrease in the concentration of NO_3^- in the anode chamber (Fig. S3) because of N_2 production in the biocathode chamber.

CH_4 and N_2 production in the biocathode chamber suggest that the reduction reactions of NO_3^- and CO_2, respectively, are represented as follows:

$$1/8\ CO_2 + H^+ + e^- \rightarrow 1/8\ CH_4 + 1/4\ H_2O \quad (2)$$
$$1/5\ NO_3^- + 6/5\ H^+ + e^- \rightarrow 1/10\ N_2 + 3/5\ H_2O \quad (3)$$

Based on Faraday's laws of electrolysis, the number of donated electrons, *Ne* [mol], may be calculated from the measured current using the following equation:

$$Ne = \frac{\int I dt}{F} \quad (4)$$

where I is current (A), t is time (s), and F is Faraday's constant (C mol^{-1}).

Assuming that all yield electrons *Ne*, calculated as per Eq. (4), are used for the reduction of only CO_2 or NO_3^-, the amounts of CH_4 and N_2 produced versus the electron yield were calculated using Eqs. (2) and (3), respectively. Measured CH_4 production was markedly less than the calculated value, while measured N_2 production was also smaller than the theoretical value under this assumption (Fig. S4). Therefore, the two reductions were simultaneously performed, and *Ne* was distributed in both reductions. The required electrons for measured CH_4 production from CO_2 reduction were estimated using Eq. (2), with the ratio of required electrons to total measured electrons *Ne* shown in Fig. 4. The electron ratio slightly decreased with the applied voltage, rather than remaining constant. At very low voltages of 0.05 and 0.1 V, approximately 40% of the current was used for CO_2 reduction to CH_4, while only approximately 5% was utilized at 3 V. Assuming that the current to electron ratio was used for CO_2 reduction and that the remaining electrons were used for NO_3^- reduction to N_2, as per Eq. (3), it is possible to estimate CH_4 and N_2 production from *Ne*. Fig. 5 compares measured and estimated CH_4 and N_2 production, with the curve showing the relationship between the electron ratio and voltage in Fig. 4 used in the calculation. A good agreement was observed for both CH_4 and N_2 production, meaning that the electron balance was almost maintained in this experiment, and the production of CH_4 and N_2

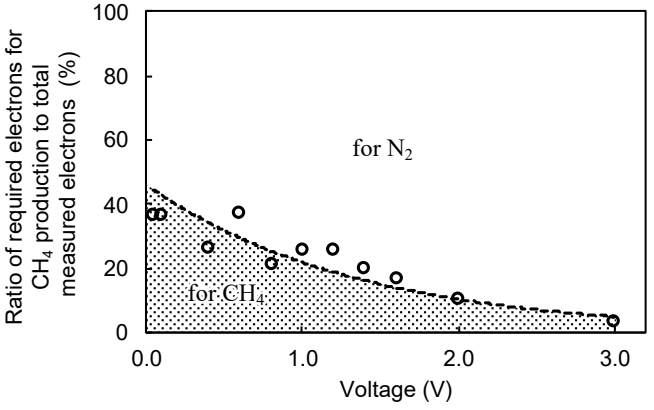

Fig. 4. Relationship between the ratio of required electrons for CH_4 production to total measured electrons *Ne* and applied voltage.

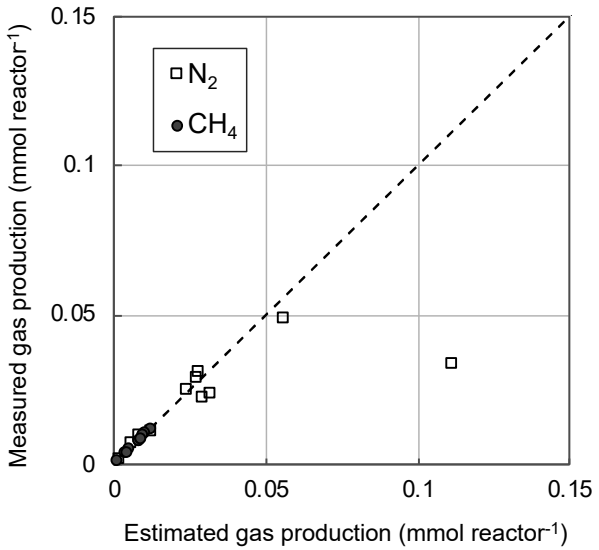

Fig. 5. Comparison between measured and estimated gas production. An estimation of produced CH_4 and N_2 was performed assuming that all electrons *Ne* were used for the reduction of both CO_2 and NO_3^-, while electrons from the ratio in Fig. 4 were used for CH_4 production.

may theoretically be performed in the biocathode chamber according to the reduction reactions of Eqs. (2) and (3). However, at a high voltage of 3.0 V, the calculated value of produced N_2 was markedly greater than the measured value (Fig. 5), indicating that some electrons were used for other reductions by chemical and/or microbial reactions. If NO_3^- reduction to NH_4^+ instead of N_2, which is the reverse reaction at the anode, is performed at the biocathode at high voltages, the reversible reactions will lead to a waste of electrons yielded in the MES. A previous study reported that a high imposing voltage exerted a negative effect on methanogens (Ding *et al.*, 2016) and nitrate-reducing bacteria (Li *et al.*, 2001; Ding *et al.*, 2016), and excessive voltage not only inhibited microbial activity, but also induced chemical reactions.

Hydrogen was not detected. However, hydrogen was expected to be produced in the biocathode chamber because of the presence of hydrogenotrophic methanogens, such as *Methanobacterium* and *Methanobrevibacter*, and the hydrogenotrophic denitrifiers of *Rhodocyclaceae (Azonexus)*. Furthermore, the hydrogen-producing bacteria *Petrimonas* were present. Previous studies on MESs also detected hydrogenotrophic methanogens, such as *Methanobrevibacter*, *Methanocorpusculum*, and *Methanoculleus sp.* (Sasaki *et al.*, 2011; Van Eerten-Jansen *et al.*, 2013; Jiang *et al.*, 2014; Siegert *et al.*, 2015). Cheng *et al.* (2019) reported that *Methanobacterium palustre* methanogens directly use electrons to produce methane without organic substances. However, this study did not provide sufficient evidence of electron utilization. Although *Geobacter* species are well-known to have the ability to transfer electrons, it was surprising that the dominant genus identified in this study was *Petrimonas* due to the lack of available information on the electron transfer ability of this genus. However, *Petrimonas* may accept electrons to produce hydrogen, which may be provided to the detected hydrogenotrophic methanogens and denitrifiers in the absence of an organic substrate in the reactor. During the bio-electrochemical production of hydrogen, it is reasonable to assume that a very small amount of hydrogen is electrochemically formed and biologically consumed. However, this electrochemical pathway may only negligibly contribute to production because hydrogen-producing *Petrimonas* was dominant in the microbial community.

Hydrogenotrophic methanogens and denitrifiers compete for the shared substrate of H_2 produced at the biocathode. Denitrifiers are dominant in wastewater treatments under anoxic conditions in the presence of nitrate; this phenomenon may be explained by Gibbs free energy. The energy obtained in the denitrification reaction of Eq. (3) is markedly larger than that in the methane production reaction of Eq. (2). However, under hydrogenotrophic conditions, methanogens and denitrifiers were both enriched even though denitrification dominated throughout the experiment. At the lowest applied voltage of 0.05 V, approximately 40% of the H_2 produced was utilized for methane production by the methanogens. However, with an increase in the applied voltage, the utilization ratio decreased (Fig. 4), indicating that the applied voltage affected the utilization of H_2 by methanogens and denitrifiers. H_2 production and concentrations are expected to increase at higher voltages. Microbes with a high affinity for substrates generally consume substrates faster than those with low affinity. The Monod constant K_m for H_2 uptake was reportedly 1 and 2 μM for *Methanobacterium ruminatium* (Lovley and Goodwin, 1988) and *Methanobrevibacter formicium* (Schauer and Ferry, 1980), respectively. In contrast, Smith *et al.* (1994) reported that the K_m of hydrogenotrophic denitrifiers ranged between 0.3 and 3.32 μM. If methanogens had lower K_m than the denitrifiers at the biocathode, indicating a higher affinity for H_2 and lower maximum H_2 uptake rate, the phenomenon of a decreasing current ratio in methane production with an increasing applied voltage, as shown in Fig. 4, may be explained by this difference in K_m between methanogens and denitrifiers.

Based on the experimental results obtained, Fig. 6 proposes a scheme for the process of electronic methane production used in the present study, without organic substances in the MES. Ammonium is oxidized to nitrate by a Pt catalyst at the anode with electron release. The nitrate formed is transferred into the biocathode chamber through the salt bridge. At the biocathode, the hydrogen-producing bacteria *Petrimonas* biochemically produce H_2 by accepting electrons and protons. The H_2 produced is biologically consumed by hydrogenotrophic methanogens of *Methanobacterium* and *Methanobrevibacter* coupled with CO_2 uptake, and by the hydrogenotrophic denitrifiers of *Rhodocyclaceae (Azonexus)*, with transferred nitrate reduction resulting in the production of methane and N_2, respectively. Consequently, the overall reaction at the anode and biocathode in the MES is as follows:

$$1/8\ CO_2+1/3\ NH_4^+ \rightarrow 1/8\ CH_4+1/6\ N_2+1/3\ H^++1/4\ H_2O$$
$$\Delta G^{0\prime}=-3.134\ \text{kJ mol}^{-1}\ e^- \quad (5)$$

Thermodynamically, this reaction proceeds under the standard condition even without the provision of external

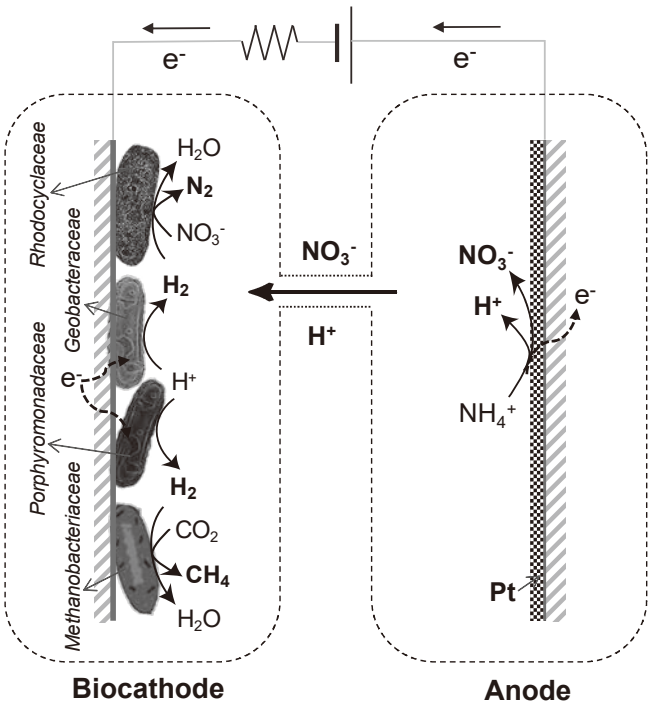

Fig. 6. Scheme of electronic methane and nitrogen production in MES without organic substances.

energy, such as electricity, because of the negative Gibbs free energy $\Delta G^{0'}$ value. The actual condition, for example, at an applied voltage of 0.1 V was as follows: p_{CH4}=0.36 atm, p_{N2}=0.65 atm, p_{CO2}=0.03 atm, $[H^+]=15.1\times10^{-5}$ M, and $[NH_4^+]=5.38\times10^{-3}$ M. In this case, the actual Gibbs free energy ΔG ($=\Delta G^{0'}+RT\ \ln[K]$) was estimated to have a value of –5.18 kJ mol^{-1} e$^-$, suggesting that the production of methane and N_2 is expected. Therefore, the present study revealed that even in an inorganic environment, biological methane production coupled with denitrification is possible in combination with catalytic ammonium oxidation, even at very low applied voltages <0.1 V, through the three key players of hydrogenotrophic methanogens, denitrifiers, and hydrogen-producing bacteria.

Acknowledgements

This research was supported by the Japan Society for the Promotion of Science (JSPS) as a Grant-in-Aid for scientific research (grant numbers 17H01300). We would like to thank Editage (www.editage.jp) for English language editing.

References

Bunce, N.J., and Bejan, D. (2011) Mechanism of electrochemical oxidation of ammonia. *Electrochim Acta* **56**: 8085–8093.

Cabezas, A., Pommerenke, B., Boon, N., and Friedrich, M.W. (2015) *Geobacter*, *Anaeromyxobacter* and *Anaerolineae* populations are enriched on anodes of root exudate-driven microbial fuel cells in rice field soil. *Environ Microbiol Rep* **7**: 489–497.

Caporaso, J.G., Kuczynski, J., Stombaugh, J., Bittinger, K., Bushman, F.D., Costello, E.K., *et al.* (2010) QIIME allows analysis of high-throughput community sequencing data. *Nat Methods* **7**: 335–336.

Cecconet, D., Bolognesi, S., Callegari, A., and Capodaglio, A.G. (2019) Controlled sequential biocathodic denitrification for contaminated groundwater bioremediation. *Sci Total Environ* **651**: 3107–3116.

Cheng, S., Xing, D., Call, D.F., and Logan, B.E. (2009) Direct biological conversion of electrical current into methane by electromethanogenesis. *Environ Sci Technol* **43**: 3953–3958.

Clauwaert, P., Tolêdo, R., van der Ha, D., Crab, R., Verstraete, W., Hu, H., *et al.* (2008) Combining biocatalyzed electrolysis with anaerobic digestion. *Water Sci Technol* **57**: 575–579.

Clauwaert, P., and Verstraete, W. (2009) Methanogenesis in membraneless microbial electrolysis cells. *Appl Microbiol Biotechnol* **82**: 829–836.

De Vooys, A.C.A., Koper, M.T.M., Van Santen, R.A., and Van Veen, J.A.R. (2001) The role of adsorbates in the electrochemical oxidation of ammonia on noble and transition metal electrodes. *J Electroanal Chem* **506**: 127–137.

Ding, A., Yang, Y., Sun, G., and Wu, D. (2016) Impact of applied voltage on methane generation and microbial activities in an anaerobic microbial electrolysis cell (MEC). *Chem Eng J (Amsterdam, Neth)* **283**: 260–265.

Edgar, R.C. (2010) Search and clustering orders of magnitude faster than BLAST. *Bioinformatics* **26**: 2460–2461.

Eerten-Jansen, M.C.A.A.V., Heijne, A.T., Buisman, C.J.N., and Hamelers, H.V.M. (2012) Microbial electrolysis cells for production of methane from CO_2: long-term performance and perspectives. *Int J Energy Res* **36**: 809–819.

Endo, K., Katayama, Y., and Miura, T. (2005) A rotating disk electrode study on the ammonia oxidation. *Electrochim Acta* **50**: 2181–2185.

Fóti, G., and Comninellis, C. (2004) Electrochemical oxidation of organics on iridium oxide and synthetic diamond based electrodes. In *Mod Aspects Electrochem*. White, R.E., Conway, B.E., Vayenas, C.G., and Gamboa-Adelco, M.E. (eds). Boston, MA: Springer, pp. 87–130.

Holmes, D.E., Shrestha, P.M., Walker, D.J.F., Dang, Y., Nevin, K.P., Woodard, T.L., and Lovley, D.R. (2017) Metatranscriptomic evidence for direct interspecies electron transfer between *Geobacter* and *Methanothrix* species in methanogenic rice paddy soils. *Appl Environ Microbiol* **83**: e00223–17.

Jiang, Y., Su, M., and Li, D. (2014) Removal of sulfide and production of methane from carbon dioxide in Microbial Fuel Cells–Microbial Electrolysis Cell (MFCs–MEC) coupled system. *Appl Biochem Biotechnol* **172**: 2720–2731.

Lee, J.-Y., Park, J.-H., and Park, H.-D. (2017) Effects of an applied voltage on direct interspecies electron transfer via conductive materials for methane production. *Waste Manage (Oxford, U K)* **68**: 165–172.

Li, X.-G., Cao, H.-B., Wu, J.-C., and Yu, K.-T. (2001) Inhibition of the metabolism of nitrifying bacteria by direct electric current. *Biotechnol Lett* **23**: 705–709.

Li, Z.-F., Wang, Y., and Botte, G.G. (2017) Revisiting the electrochemical oxidation of ammonia on carbon-supported metal nanoparticle catalysts. *Electrochim Acta* **228**: 351–360.

Liang, D., He, W., Li, C., Wang, F., Crittenden, J.C., and Feng, Y. (2021) Remediation of nitrate contamination by membrane hydrogenotrophic denitrifying biofilm integrated in microbial electrolysis cell. *Water Res* **188**: 116498.

Liu, Q., Ren, Z.J., Huang, C., Liu, B., Ren, N., and Xing, D. (2016) Multiple syntrophic interactions drive biohythane production from waste sludge in microbial electrolysis cells. *Biotechnol Biofuels* **9**: 162.

Logan, B.E., Hamelers, B., Rozendal, R., Schröder, U., Keller, J., Freguia, S., *et al.* (2006) Microbial fuel cells: Methodology and technology. *Environ Sci Technol* **40**: 5181–5192.

Lohner, S.T., Deutzmann, J.S., Logan, B.E., Leigh, J., and Spormann, A.M. (2014) Hydrogenase-independent uptake and metabolism of electrons by the archaeon *Methanococcus maripaludis*. *ISME J* **8**: 1673–1681.

Lovley, D.R., and Goodwin, S. (1988) Hydrogen concentrations as an indicator of the predominant terminal electron-accepting reactions in aquatic sediments. *Geochim Cosmochim Acta* **52**: 2993–3003.

Lu, L., Xing, D., and Ren, N. (2012) Pyrosequencing reveals highly diverse microbial communities in microbial electrolysis cells involved in enhanced H_2 production from waste activated sludge. *Water Res* **46**: 2425–2434.

McDonald, D., Price, M.N., Goodrich, J., Nawrocki, E.P., DeSantis, T.Z., Probst, A., *et al.* (2012) An improved Greengenes taxonomy with explicit ranks for ecological and evolutionary analyses of bacteria and archaea. *ISME J* **6**: 610–618.

Müller, E., and Spitzer, F. (1905) Über die Elektrolytische Oxydation des Ammoniaks und Ihre Abhängigkeit vom Anodenmaterial. *Z Elektrochem Angew Physik Chem* **11**: 917–931 (in German).

Nutt, C.W., and Kapur, S. (1968) Mechanism of oxidation of ammonia on platinum. *Nature* **220**: 697–698.

Onodera, I. (2013) Development of methane fermentation technology for wastewater treatment. *Tappi J* **67**: 82–85.

Panizza, M., and Cerisola, G. (2009) Direct and mediated anodic oxidation of organic pollutants. *Chem Rev* **109**: 6541–6569.

Park, J., Lee, B., Tian, D., and Jun, H. (2018) Bioelectrochemical enhancement of methane production from highly concentrated food waste in a combined anaerobic digester and microbial electrolysis cell. *Bioresour Technol* **247**: 226–233.

Peng, H., Zhao, Z., Xiao, H., Yang, Y., Zhao, H., and Zhang, Y. (2019) A strategy for enhancing anaerobic digestion of waste activated sludge: Driving anodic oxidation by adding nitrate into microbial electrolysis cell. *J Environ Sci (Beijing, China)* **81**: 34–42.

Rabaey, K., and Rozendal, R. (2010) Microbial electrosynthesis—Revisiting the electrical route for microbial production. *Nat Rev Microbiol* **8**: 706–716.

Rice, D.D., and Claypool, G.E. (1981) Generation, accumulation, and resource potential of biogenic gas. *AAPG Bull* **65**: 5–25.

Rotaru, A.-E., Shrestha, P.M., Liu, F., Shrestha, M., Shrestha, D., Embree, M., *et al.* (2013) A new model for electron flow during anaerobic digestion: direct interspecies electron transfer to *Methanosaeta* for the reduction of carbon dioxide to methane. *Energy Environ Sci* **7**: 408–415.

Sarmin, S., Ethiraj, B., Islam, M.A., Ideris, A., Yee, C.S., and Khan, M.M.R. (2019) Bio-electrochemical power generation in petrochemical wastewater fed microbial fuel cell. *Sci Total Environ* **695**: 133820.

Sasaki, K., Morita, M., Sasaki, D., Hirano, S., Matsumoto, N., Ohmura, N., and Igarashi, Y. (2011) Methanogenic communities on the electrodes of bioelectrochemical reactors without membranes. *J Biosci Bioeng* **111**: 47–49.

Schauer, N.L., and Ferry, J.G. (1980) Metabolism of formate in *Methanobacterium formicicum*. *J Bacteriol* **142**: 800–807.

Schoell, M. (1988) Multiple origins of methane in the Earth. *Chem Geol* **71**: 1–10.

Siegert, M., Li, X.-F., Yates, M.D., and Logan, B.E. (2015) The presence of hydrogenotrophic methanogens in the inoculum improves methane gas production in microbial electrolysis cells. *Front Microbiol* **5**: 778.

Smith, R.L., Ceazan, M.L., and Brooks, M.H. (1994) Autotrophic, hydrogen-oxidizing, denitrifying bacteria in groundwater, potential agents for bioremediation of nitrate contamination. *Appl Environ Microbiol* **60**: 1949–1955.

Sun, R., Zhou, A., Jia, J., Liang, Q., Liu, Q., Xing, D., and Ren, N. (2015) Characterization of methane production and microbial community shifts during waste activated sludge degradation in microbial electrolysis cells. *Bioresour Technol* **175**: 68–74.

Townsend-Small, A., Disbennett, D., Fernandez, J.M., Ransohoff, R.W., Mackay, R., and Bourbonniere, R.A. (2016) Quantifying emissions of methane derived from anaerobic organic matter respiration and natural gas extraction in Lake Erie. *Limnol Oceanogr* **61**: S356–S366.

Van Eerten-Jansen, M.C.A.A., Veldhoen, A.B., Plugge, C.M., Stams, A.J.M., Buisman, C.J.N., and Ter Heijne, A. (2013) Microbial community analysis of a methane-producing biocathode in a bioelectrochemical system. *Archaea* **2013**: 481784.

Villano, M., Aulenta, F., Ciucci, C., Ferri, T., Giuliano, A., and Majone, M. (2010) Bioelectrochemical reduction of CO_2 to CH_4 via direct and indirect extracellular electron transfer by a hydrogenophilic methanogenic culture. *Bioresour Technol* **101**: 3085–3090.

Wagner, R.C., Regan, J.M., Oh, S.-E., Zuo, Y., and Logan, B.E. (2009) Hydrogen and methane production from swine wastewater using microbial electrolysis cells. *Water Res* **43**: 1480–1488.

Wang, W., Zhang, Y., Li, M., Wei, X., Wang, Y., Liu, L., *et al.* (2020) Operation mechanism of constructed wetland-microbial fuel cells for wastewater treatment and electricity generation: A review. *Bioresour Technol* **314**: 123808.

Wang, Y., Tian, H., Huang, F., Long, W., Zhang, Q., Wang, J., *et al.* (2017) Time-resolved analysis of a denitrifying bacterial community revealed a core microbiome responsible for the anaerobic degradation of quinoline. *Sci Rep* **7**: 14778.

Werner, J.J., Koren, O., Hugenholtz, P., DeSantis, T.Z., Walters, W.A., Caporaso, J.G., *et al.* (2012) Impact of training sets on classification of high-throughput bacterial 16s rRNA gene surveys. *ISME J* **6**: 94–103.

Whiticar, M.J., Faber, E., and Schoell, M. (1986) Biogenic methane formation in marine and freshwater environments: CO_2 reduction vs. acetate fermentation—Isotope evidence. *Geochim Cosmochim Acta* **50**: 693–709.

Whiticar, M.J. (1999) Carbon and hydrogen isotope systematics of bacterial formation and oxidation of methane. *Chem Geol* **161**: 291–314.

Yan, Y., Li, T., Zhou, L., Tian, L., Yan, X., Liao, C., *et al.* (2020) Spatially heterogeneous propionate conversion towards electricity in bioelectrochemical systems. *J Power Sources* **449**: 227557.

Zhao, H.-P., Van Ginkel, S., Tang, Y., Kang, D.-W., Rittmann, B., and Krajmalnik-Brown, R. (2011) Interactions between perchlorate and nitrate reductions in the biofilm of a hydrogen-based membrane biofilm reactor. *Environ Sci Technol* **45**: 10155–10162.

Zhao, H.-P., Ontiveros-Valencia, A., Tang, Y., Kim, B., Ilhan, Z.E., Krajmalnik-Brown, R., and Rittmann, B. (2013) Using a two-stage hydrogen-based membrane biofilm reactor (MBfR) to achieve complete perchlorate reduction in the presence of nitrate and sulfate. *Environ Sci Technol* **47**: 1565–1572.

Zhao, Z., Zhang, Y., Yu, Q., Ma, W., Sun, J., and Quan, X. (2016) Enhanced decomposition of waste activated sludge via anodic oxidation for methane production and bioenergy recovery. *Int Biodeterior Biodegrad* **106**: 161–169.

Zhen, G., Kobayashi, T., Lu, X., and Xu, K. (2015) Understanding methane bioelectrosynthesis from carbon dioxide in a two-chamber microbial electrolysis cells (MECs) containing a carbon biocathode. *Bioresour Technol* **186**: 141–148.

Microbes Environ. Vol. 35, No. 1, 2020
https://www.jstage.jst.go.jp/browse/jsme2 doi:10.1264/jsme2.ME19086

Enzymatic Degradation of *p*-Nitrophenyl Esters, Polyethylene Terephthalate, Cutin, and Suberin by Sub1, a Suberinase Encoded by the Plant Pathogen *Streptomyces scabies*

Raoudha Jabloune[1], Mario Khalil[1], Issam E. Ben Moussa[1], Anne-Marie Simao-Beaunoir[1], Sylvain Lerat[1], Ryszard Brzezinski[1], and Carole Beaulieu[1]*

[1]*Département de Biologie, Université de Sherbrooke, Sherbrooke (QC), J1K 2R1, Canada*

(Received June 27, 2019—Accepted December 15, 2019—Published online February 27, 2020)

The genome of *Streptomyces scabies*, the predominant causal agent of potato common scab, encodes a potential cutinase, the protein Sub1, which was previously shown to be specifically induced in the presence of suberin. The *sub1* gene was expressed in *Escherichia coli* and the recombinant protein Sub1 was purified and characterized. The enzyme was shown to be versatile because it hydrolyzes a number of natural and synthetic substrates. Sub1 hydrolyzed *p*-nitrophenyl esters, with the hydrolysis of those harboring short carbon chains being the most effective. The V_{max} and K_m values of Sub1 for *p*-nitrophenyl butyrate were 2.36 mol g^{-1} min^{-1} and 5.7 10^{-4} M, respectively. Sub1 hydrolyzed the recalcitrant polymers cutin and suberin because the release of fatty acids from these substrates was observed following the incubation of the enzyme with these polymers. Furthermore, the hydrolyzing activity of the esterase Sub1 on the synthetic polymer polyethylene terephthalate (PET) was demonstrated by the release of terephthalic acid (TA). Sub1 activity on PET was markedly enhanced by the addition of Triton and was shown to be stable at 37°C for at least 20 d.

Key words: actinobacteria, common scab, cutinase, esterase, potato

Streptomycetes are Gram-positive bacteria that are known for their ability to produce a wide range of secondary metabolites and for the complexity of their morphological development. Although most streptomycetes species are saprophytic soil inhabitants, some are plant pathogens. Among them, *Streptomyces scabies* is the predominant causal agent of potato common scab and causes important economic losses in Canada (Hill and Lazarovits, 2005), as well as in most potato growing areas. Common scab is characterized by corky lesions on the surface of potato tubers. Similar to other soil-inhabiting streptomycetes, *S. scabies* produces a large variety of extracellular enzymes, including various glycosyl hydrolases and esterases (Komeil *et al.*, 2013; Beaulieu *et al.*, 2016). These enzymes may participate in pathogenesis because the penetration of *S. scabies* into host plants is considered to be facilitated by the secretion of extracellular cell wall-degrading enzymes (Beauséjour *et al.*, 1999).

The potato tuber is covered by a periderm that is composed of three types of tissues: phellem, phellogen, and phelloderm (Tyner *et al.*, 1997). The wall of phellem cells impregnated with suberin, a plant polymer recalcitrant to bio-degradation, is composed of a polyaromatic domain covalently linked to a polyaliphatic moiety (Bernards, 2002). The polyaromatic domain, a lignin-like structure, consists of a hydroxycinnamic acid-derived polymeric matrix (Bernards and Lewis, 1998). The polyaliphatic domain shares structural and chemical similarities with cutin, another polyester component of plant cuticles. Cutin and suberin both act as physical barriers against plant pathogens (Khatri *et al.*, 2011). Cutin and suberin are polymers of fatty acid derivatives linked by ester bonds. Cutin is mostly composed of C16 and C18 ω-hydroxyacids, polyhydroxyacids, epoxyacids, and α,ω-dicarboxylic acids. Suberin may be distinguished from cutin by higher contents of hydroxycinnamic acids, fatty alcohols, and saturated aliphatics with long chains (Beisson *et al.*, 2012).

Cutinases hydrolyze the plant leaf cuticle by cleaving the ester bounds of cutin (Dutta *et al.*, 2009). Therefore, cutinases belong to the esterase group, and more specifically to a class of serine esterases that contain the catalytic triad (serine, histidine and aspartate) with the active serine in the consensus sequence Gly-His/Tyr-Ser-X-Gly (Martinez *et al.*, 1994). Some fungal cutinases, such as the cutinase CcCUT1 of the fungus *Coprinopsis cinerea*, also exhibit the ability to degrade suberin (Kontkanen *et al.*, 2009). As lipolytic enzymes, cutinases have interesting properties for applications in various industrial processes (Carvalho *et al.*, 1999). For example, some cutinases exhibit the ability to degrade synthetic polyesters, such as polycaprolactone (Murphy *et al.*, 1996) and polyethylene terephthalate (PET) (Vertommen *et al.*, 2005; Eberl *et al.*, 2009; Ribitsch *et al.*, 2015).

Previous studies suggested that the bacterium *S. scabies* possesses the ability to degrade suberin. This pathogenic bacterium exhibits strong esterase activity in the presence of suberized tissues (Beauséjour *et al.*, 1999). Furthermore, a secretome analysis of *S. scabies* cultures grown in the presence of suberin revealed the presence of esterases, which are predicted to play a role in lipid metabolism (Komeil *et al.*, 2014; Beaulieu *et al.*, 2016). Among them, the Sub1 protein exhibits 33% identity with the cutinase CcCUT1 of the fungus *C. cinerea* (Komeil *et al.*, 2013). Interestingly, *sub1*

* Corresponding author. E-mail: Carole.Beaulieu@USherbrooke.ca; Tel: +1–819–821–7011; Fax: +1–819–821–7921.

gene expression was previously reported to be specifically induced in the presence of suberin (Komeil *et al.*, 2013). The cutinase from *Aspergillus oryzae* (PDB ID: 3GBS) is hallmarked by a central β-sheet of five parallel strands surrounded by ten α-helices (Liu *et al.*, 2009), as found for the predicted three-dimensional structure of the protein Sub1 (Supplemental Fig. S1). The model of the Sub1 protein also predicts the formation of two disulfide bonds (Cys31–Cys103; Cys178–Cys185) and a catalytic triad including residues Ser 114, Asp 182, and His 195 (Komeil *et al.*, 2013).

The main objectives of the present study were to produce the Sub1 protein, purify and characterize its enzymatic properties, and demonstrate that it functions as a polyesterase with the ability to degrade biopolymers, such as cutin and suberin, as well as the synthetic polyester PET.

Materials and Methods

Bacterial strains and culture conditions

An inoculum of *S. scabies* EF-35 (HER1481) was prepared in tryptic soy broth (10^8 spores in 25 mL), as described previously (Komeil *et al.*, 2013). Cultures of *S. scabies* EF-35 were incubated with shaking (250 rpm) at 30°C. *Escherichia coli* strains DH5α (Invitrogen) and SHuffle T7 (New England Biolabs) were grown in LB medium supplemented where necessary with kanamycin (30 μg mL^{-1}) and were then incubated with shaking (250 rpm) at 37°C.

Suberin and cutin preparation

A suberin-enriched potato periderm was obtained as previously described (Kolattukudy and Agrawal, 1974). The extracted material was dried under a hood, ground using a coffee mill, and stored at room temperature. To further remove residual polysaccharides in the potato periderm, this material was exposed to microbial degradation in the presence of *S. scabies* EF-35, as described by Beaulieu *et al.* (2016). The *S. scabies* inoculum (1 mL) was added to 50 mL of minimal medium consisting of a mineral solution (0.5 g L^{-1} $[NH_4]_2SO_4$, 0.5 g L^{-1} K_2HPO_4, 0.2 g L^{-1} $MgSO_4$-$7H_2O$, and 10 mg L^{-1} $FeSO_4$-$7H_2O$) and 1 g L^{-1} of the suberin-enriched potato periderm. After a 30-d incubation, 10 mL of fresh mineral solution and 200 μL of the *S. scabies* inoculum were both added to the culture and the incubation was extended for an additional 30 d. The culture was centrifuged at 3,450×*g* for 20 min, and the pellet was resuspended in 100 mL of sterile water and then autoclaved for 15 min. The suspension was washed with sterile water to remove bacterial cell debris. The resulting material (purified potato suberin) was dried at 50°C for 24 h. Cutin was isolated from apples following the protocol of Walton and Kolattukudy (1972).

DNA extraction

Genomic DNA was isolated from 48-h bacterial cultures of *S. scabies* EF-35 using the GenElute Bacterial Genomic DNA Kit (Sigma-Aldrich) according to the manufacturer's instructions. Plasmid DNA was isolated from 12-h *E. coli* cultures using the GenElute™ Plasmid Miniprep Kit (Sigma-Aldrich) following the manufacturer's instructions.

Cloning of sub1 in E. coli

The *sub1* coding sequence, deprived of its signal peptide (GenBank accession number MK689853), was amplified by PCR from the genomic DNA of *S. scabies* EF-35 using the primers F-pET (5′-ATATCCATGGCCGCCTGCACGGACATCG-3′) and R-pET (5′-ATATCTCGAGTTAGATCTTGGTCGCGGCGAAGG-3′). The PCR mix contained 20 ng of DNA, 2.5 μL of *Taq* polymerase buffer, 0.5 μL of dNTPs (10 mM), 0.5 μL (each) of forward and reverse primers (10 μM), and 0.125 μL of DNA *Taq* polymerase (New England Biolabs), in a total volume of 25 μL. PCR conditions consisted of 2 min at 95°C followed by 30 cycles at 95°C for 30 s, at 64°C for 1 min, and at 68°C for 1 min, with a final extension at 68°C for 5 min. PCR was performed using the thermocycler T100 (Bio-Rad). Amplification products were migrated on a 1% agarose gel (Sambrook and Russell, 2001), purified from gels using the MinElute Gel Extraction Kit (Qiagen), and cloned into the pET-30a(+) vector (Novagen). The amplification product and cloning vector pET-30a(+) were both digested using the restriction enzymes *Nco*I and *Xho*I. Enzyme T4 DNA ligase (New England Biolabs) was used to ligate plasmid ends to amplicons following the manufacturer's instructions. Ligation products were heat shock-transformed into competent cells of *E. coli* DH5α as per the manufacturer's instructions (New England Biolabs). Bacteria were then incubated overnight on LB agar medium supplemented with kanamycin (30 μg mL^{-1}). The plasmid insert was sequenced at a sequencing and genome genotyping platform (CHUL, University Laval, Quebec City, Canada). The plasmid pET-30a(+), with or without the *sub1* insert, was transformed into the expression host *E. coli* SHuffle T7, as previously described.

Protein extraction

Cultures of *E. coli* SHuffle T7 carrying pET without or with the *sub1* gene insert (*E. coli* SHuffle T7-pET and *E. coli* SHuffle T7-pET-*sub1*) were incubated on LB agar medium supplemented with kanamycin. When OD_{600} reached 0.6–0.8, isopropyl β-D-1-thiogalactopyranoside (IPTG) was added to the culture (0 to 1.0 mM, final concentration) and bacteria were incubated at 25°C for an additional 24 h. Cells were harvested by centrifugation (3,450×*g*) for 10 min, pellets were washed twice with saline (NaCl 0.9%) and then resuspended in a buffer solution (50 mM NaH_2PO_4 and 300 mM NaCl, pH 8.0) supplemented with EDTA (2.5 mM). The suspensions were sonicated on ice four times for 10 s and centrifuged (3,450×*g*) at 4°C for 30 min to remove cell debris. The supernatant was collected and successively passed through filters with pore sizes of 0.45 and 0.2 μm. The resulting protein solution was stored at 4°C.

Purification of the protein Sub1

An affinity column Ni-NT cOmplete His-Tag purification column (Roche) was used to purify the protein Sub1 from the cytoplasmic fraction of *E. coli* SHuffle T7-pET-*sub1*, following the manufacturer's instructions. Elution buffer A (50 mM NaH_2PO_4, 300 mM NaCl, pH 8.0), supplemented with different concentrations of imidazole (5 to 250 mM), was used for column washing and His6-tagged protein elution. Protein fractions were subjected to sodium dodecyl sulfate-polyacrylamide gel electrophoresis (SDS-PAGE) migration along with the marker PageRuler™ Prestained Protein Ladder (Thermo Scientific), as described by Komeil *et al.* (2014). Proteins were stained with Coomassie brilliant blue R-250 (Bio-Rad; Lauzier *et al.*, 2008) and fractions containing purified Sub1 were pooled. This mixture was dialyzed in phosphate-buffered solution (PBS) to remove imidazole. Protein concentrations were measured according to Bradford (Bradford, 1976).

Esterase activity of Sub1 on p*-nitrophenyl esters*

Esterase activity was assessed by spectrophotometrically measuring the absorbance of *p*-nitrophenol using the substrates *p*-nitrophenyl butyrate (C4), *p*-nitrophenyl octanoate (C8), *p*-nitrophenyl decanoate (C10), and *p*-nitrophenyl dodecanoate (C12) (Sigma-Aldrich). The molar extinction coefficient of *p*-nitrophenol in Tris-HCl (20 mM, pH 7.5) at room temperature is 12,000 M^{-1} cm^{-1} at 420 nm. This enzymatic assay was performed as described previously (Komeil *et al.*, 2013) with slight modifications. In a 1.5-mL plastic cuvette, 20 μL of 100×-diluted Sub1 (60 ng) was added to 970 μL of Tris-HCl (20 mM, pH 7.5), with or without Triton X-100 (0.5%), and 10 μL of a 20 mM *p*-nitrophenyl ester substrate (0.2 mM final concentration). The absorbance at

420 nm of this reaction mix was measured at room temperature every 10 s for 1 min. The increase in absorbance of each sample was read against a blank without purified protein. One unit (U) was the amount of enzyme liberating 1 µmol of *p*-nitrophenol min^{-1} under the assay conditions. The V_{max} and K_m values of the enzyme Sub1 were assessed using the software GraphPad Prism7, according to the Michaelis-Menten equation, with different concentrations of the C4 substrate.

Esterase activity of Sub1 on natural and synthetic polymers

Suberin and cutin were exposed to the enzyme Sub1 as follows. Suberin or cutin (10 mg) was added to 350 µL of Tris-HCl (20 mM, pH 7.5) supplemented with 50 µL of the purified enzyme Sub1 (15 µg). Control assays (blanks) were made of suberin and cutin without the addition of the enzyme Sub1. The mixture was incubated at room temperature for 20 d. Colorimetric assays of free fatty acids released from the biopolymer were performed every 5 d using a Free Fatty Acid Quantification Colorimetric/Fluorometric Kit (BioVision) according to the manufacturer's instructions. A standard curve was prepared with palmitic acid to convert absorbance at 570 nm into fatty acid concentrations.

The hydrolyzing activity of Sub1 was also estimated on polyethylene terephthalate (PET) by measuring the amount of terephthalic acid (TA) released from PET according to Nimchua *et al.* (2008) with slight modifications. Assays were conducted in 2-mL tubes containing 10 mg of PET (ground granules, Sigma-Aldrich), 1 mL of Tris-HCl (20 mM, pH 7.5), and 3 µg of the enzyme Sub1. In the first experiment, the effects of Triton on Sub1 performance were tested. Tubes, with or without Triton X-100 (0.5%), were incubated at 37°C and the concentrations of TA released in the incubation media were recorded after 10 and 15 d. Blank assays, in which the enzyme Sub1 was omitted, were used as controls. Tubes were then centrifuged (1 min) and 50 µL of the collected supernatant was added to 350 µL of Tris-HCl (20 mM, pH 7.5) into quartz cuvettes. Absorbance at 240 nm was measured to assess TA concentrations (using a standard curve). In another experiment, the stability of Sub1, using PET as a substrate, was assessed at 37 and 50°C over a 20-d period. The incubation medium contained Triton X-100 (0.5%) and the concentration of TA released in the reaction mix was measured every 5 d, as described above.

Results

Heterologous production of Sub1

The *S. scabies sub1* gene was cloned into a pET expression vector (data not shown) and expressed in *E. coli* strain SHuffle T7. The cytoplasmic extract of *E. coli* SHuffle T7-pET-*sub1* was characterized by a thick and dense band of approximatively 25 kDa, which was absent from the protein profile of *E. coli* SHuffle T7-pET (Fig. 1). In *E. coli* SHuffle T7-pET-*sub1*, Sub1 was produced even in the absence of IPTG, while thicker protein bands were observed when *sub1* gene expression was induced by this compound (Fig. 1).

The cytoplasmic fraction from cultures of *E. coli* Shuffle T7-pET-*sub1* showed, in the absence of the induction with IPTG, that esterase activity on the C4 substrate (58.8 µmol mL^{-1}) was significantly higher than that in control *E. coli* SHuffle T7-pET (1.6 µmol mL^{-1}) after 30 min of the incubation (Fig. 2). The esterase activity of *E. coli* SHuffle T7-pET-*sub1* was inducible with IPTG and was quickly observable in the reaction mix. After 5 min of the incubation, the highest activity reached 32.2 µmol mL^{-1} when

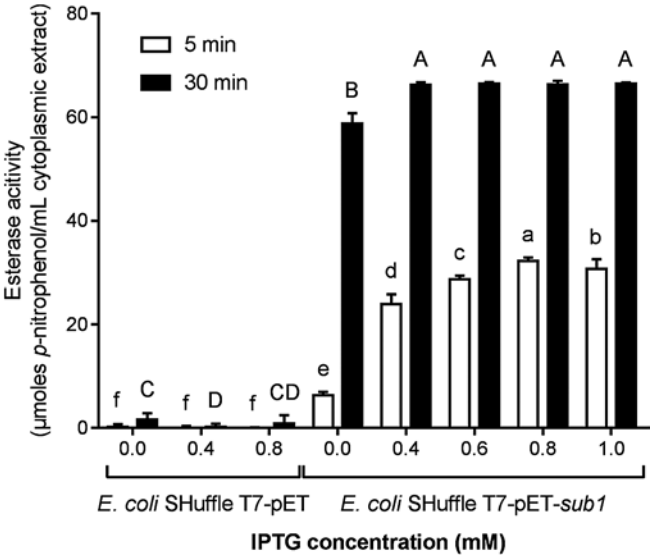

Fig. 2. Esterase activity of cytoplasmic extracts from *Escherichia coli* SHuffle T7 transformed with plasmid pET without (*E. coli* SHuffle T7-pET) or with (*E. coli* SHuffle T7-pET-sub1) the *sub1* insert and exposed to various concentrations of IPTG. Activity is expressed as the concentration of *p*-nitrophenol released from *p*-nitrophenyl butyrate substrate in 5- and 30-min reactions. These results are the means of five replicates±SD. Bar values accompanied by the same lower case letter or upper case letter were not significantly different.

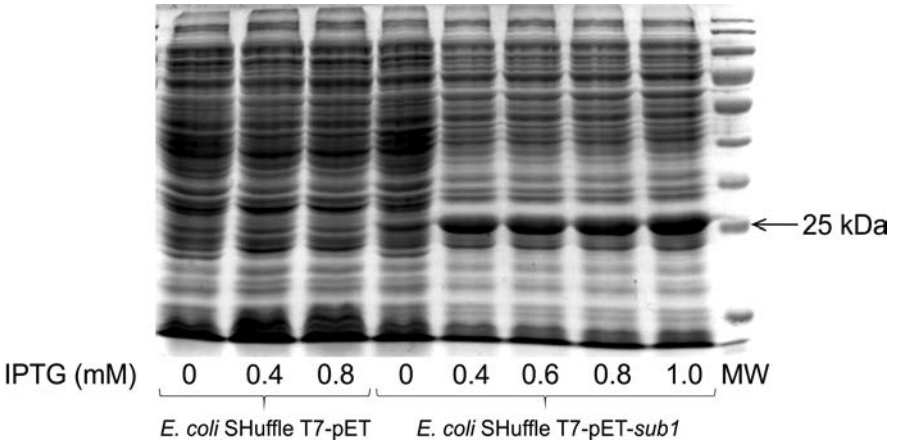

Fig. 1. SDS-PAGE gel of the cytoplasmic extract obtained from pET-transformed *Escherichia coli* strain SHuffle T7, without (*E. coli* SHuffle T7-pET) or with (*E. coli* SHuffle T7-pET-*sub1*) the insert of the *sub1* gene, after induction with different concentrations of IPTG.

0.8 mM IPTG was added to the culture, while activity was 6.3 µmol mL^{-1} in the absence of IPTG (Fig. 2).

Purification of the recombinant protein His-Sub1

An affinity column Ni-NT (cOmplete His-Tag) was used to purify the recombinant protein Sub1 from the cytoplasmic fraction of *E. coli* SHuffle T7-pET-*sub1*. By comparing the migration profile of the cytoplasmic fraction and the flow-through (Fig. 3, lanes 2 and 3, respectively), the band corresponding to the recombinant protein His-Sub1 (25 kDa) was present in the cytoplasmic fraction, while no band was present in the flow-through fraction, indicating that the Sub1 protein bound the column. The presence of imidazole in the elution buffer allows the elution of His-tag proteins from the column. At imidazole concentrations ranging between 4 and 10 mM, the elution buffer released the majority of the contaminant proteins, while a low quantity of Sub1 was released with 10 mM imidazole (lane 7, Fig. 3). A detectable quantity of Sub1 was eluted with no contaminant proteins when 50 mM imidazole buffer was used (lane 8, Fig. 3). However, at 200 mM imidazole, no recombinant protein was detected (lane 9, Fig. 3). A mass spectrometry analysis confirmed that the purified protein was Sub1 (data not shown). Purification efficacy was estimated by comparing the esterase activities (with 0.4 mM *p*-nitrophenol butyrate as the substrate) of the cytoplasmic fraction and the purified protein. The esterase activity of Sub1 was 52-fold higher in the purified extract (23.0 U mL^{-1}) than in the cytoplasmic crude extract (0.4 U mL^{-1}).

Esterase activity of the Sub1 protein on p-*nitrophenyl esters*

The esterase activity of Sub1 on the *p*-nitrophenyl esters of varying carbon chain lengths was assessed in the presence and absence of Triton X-100. Independent of the presence of Triton X-100, Sub1 was more active on *p*-nitrophenyl butyrate (C4) and *p*-nitrophenyl octanoate (C8) than on *p*-nitrophenyl esters with longer carbon chains (C10 and C12, Fig. 4). The presence of Triton X-100 increased the esterase activity of the enzyme on all of these substrates (Fig. 4). The highest esterase activity (14.6 U $nmol^{-1}$ or 616 U mg^{-1} Sub1) was obtained on the C4 substrate in the presence of Triton X-100. Thus, V_{max} and K_m values for esterase Sub1 were calculated using the latter substrate. As shown in Fig. 5, the initial velocity (V_0) of the hydrolysis reaction increased when higher concentrations of the substrate *p*-nitrophenol butyrate (*p*-NPB) were used. According to the Michaelis-Menten equation, V_{max} was 55.8±2.0 U $nmol^{-1}$ Sub1 (2,361±84.5 U mg^{-1} Sub1) and K_m was 0.57±0.04 mM *p*-NPB.

Effects of the Sub1 esterase on polymers

Sub1 was shown to hydrolyze suberin and cutin, releasing 1.22±0.06 and 2.65±0.18 nmol of fatty acids (palmitic acid equivalent) μg^{-1} Sub1 from these polymers, respectively, after 20 d of the incubation. The ability of Sub1 to degrade cutin and suberin appeared to be stable over the experimental time course at room temperature because the amounts of fatty acids released in the incubation medium correlated with time (P<0.0001; Fig. 6).

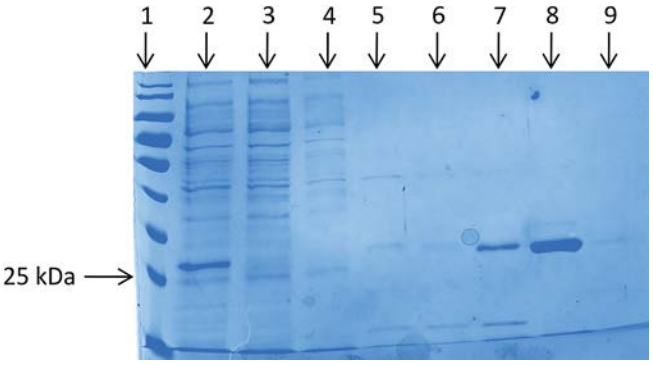

Fig. 3. SDS–PAGE gel of cytoplasmic soluble proteins obtained from *Escherichia coli* transformed with SHuffle T7-pET-*sub1*, after fractionation on the affinity column (IMAC). Lane 1, molecular weight marker; lane 2, cytoplasmic extract; lane 3, flow-through; lane 4, proteins released after washing with buffer A; lanes 5 to 9, proteins released after washing with buffer A supplemented with 4, 5, 10, 50, or 200 mM imidazole, respectively.

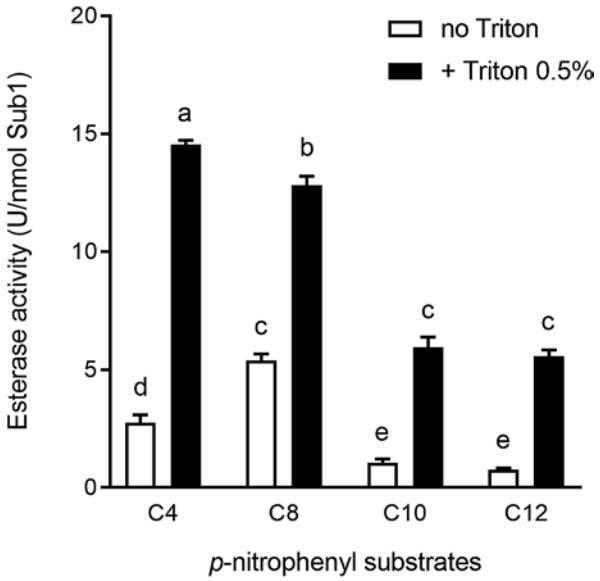

Fig. 4. Esterase activity of the purified Sub1 enzyme using *p*-nitrophenyl substrates of different carbon chain sizes (C4, C8, C10, and C12) in the absence or presence of Triton X-100 (0.5%). Data shown are the mean±SD of three replicates. Bar values accompanied by the same letter are not significantly different.

On the other hand, the release of TA showed that the Sub1 esterase also had the ability to hydrolyze the synthetic substrate PET. The addition of Triton X-100 to the reaction mix enhanced the hydrolysis of PET by *ca.* 2.6-fold (P<0.0001, *t*-test; Fig. 7A) after 10 and 15 d of the incubation. The esterase activity of Sub1 on PET, in the presence of Triton X-100, increased over the incubation time because the amount of TA released during the degradation of PET correlated with the incubation time (P<0.0001; Fig. 7B). The enzyme Sub1 showed high stability at 37°C over the test period (20 d) because the concentration of TA released in the incubation medium linearly correlated with time (r^2=0.9874). However, the stability of Sub1 at 50°C fit a non-linear curve (r^2=0.9667).

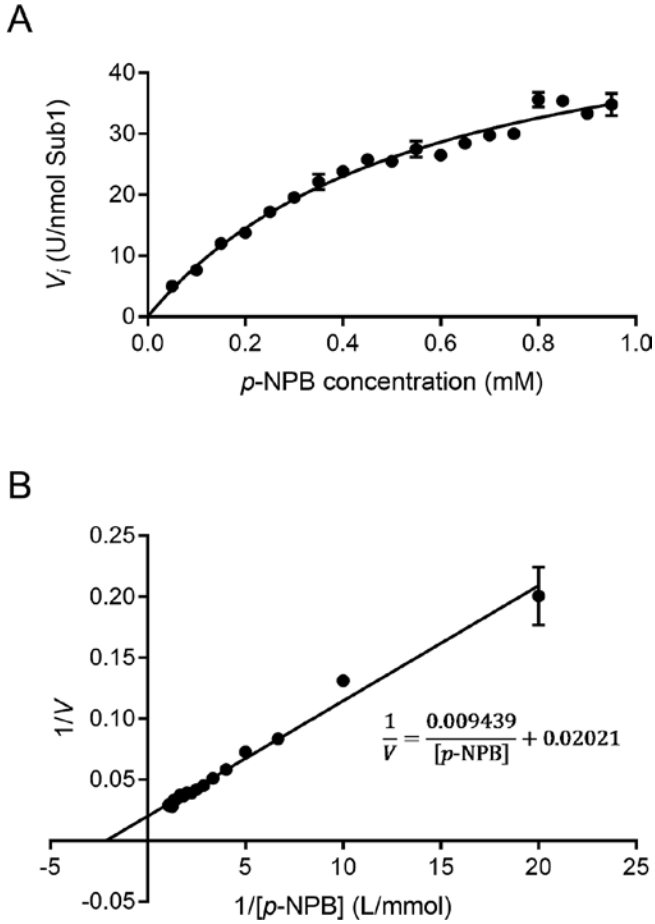

Fig. 5. Effects of substrate (*p*-NPB) concentrations on the initial speed (V_0) of the hydrolysis reaction of the esterase Sub1. (A) Michaelis-Menten kinetic and (B) Lineweaver-Burk plot. Data are the means±SD of three replicates.

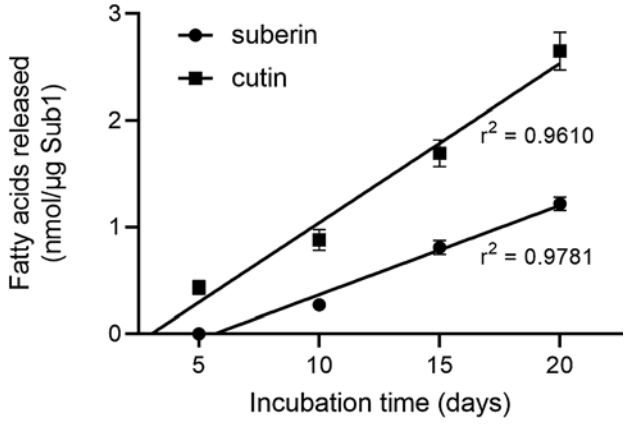

Fig. 6. Degradation of cutin and suberin by enzyme Sub1 at room temperature over a 20-d period, as expressed by the release of fatty acids in the incubation medium. Data are the means±SD of four replicates.

Discussion

S. scabies may colonize potato tuber surfaces and is able to directly penetrate potato cells (Loria *et al.*, 2003). Previous studies proposed that its entry into potato tuber tissues may be facilitated by the production of esterases that degrade suberin present in the potato periderm (McQueen and Schottel, 1987; Beauséjour *et al.*, 1999; Komeil *et al.*, 2013). Although suberin degradation has not yet been examined in detail, some fungal cutinases exhibit activity towards suberin (Kontkanen *et al.*, 2009). The protein Sub1 is part of the *S. scabies* secretome when this bacterium is grown in the presence of suberin (Beaulieu *et al.*, 2016) and the *sub1* gene is induced in the presence of suberin (Komeil *et al.*, 2013). This study predicted that Sub1 was a cutinase due to its high sequence homology with other cutinases of fungal origin. The present results confirm this prediction because Sub1 exhibited the ability to hydrolyze both cutin and suberin.

In the present study, the heterologous production of the *S. scabies* Sub1 protein was successfully achieved in *E. coli*. Other studies also reported the heterologous expression of bacterial esterases in *E. coli* (Chen *et al.*, 2008; Su *et al.*, 2013; Ribitsch *et al.*, 2015). The molecular weight of His-tagged Sub1 was estimated herein to be 25 kDa, which is consistent with the predicted molecular weight of mature Sub1 (18.7 kDa) plus the His-tag (4.9 kDa). Therefore, the molecular weight of Sub1 appears to be less than that of most bacterial cutinases, such as Tfu-0882 and Tfu-0883

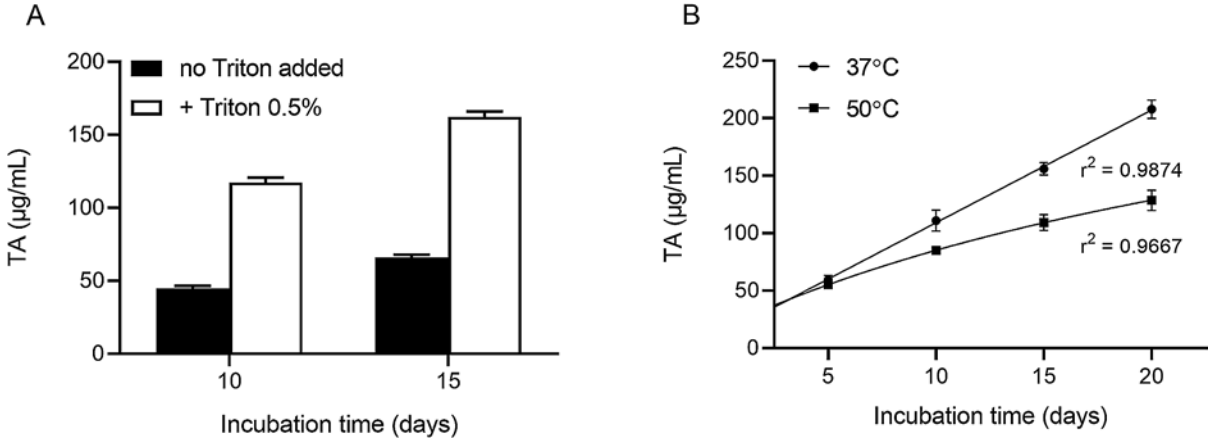

Fig. 7. Concentrations of terephthalic acid (TA) released following the hydrolysis of ground particles of polyethylene terephthalate by 3 µg of the Sub1 enzyme. (A) Effects of the presence of Triton X-100 (0.5%) on Sub1 performance after 10 and 15 d of incubation (at 37°C). (B) Sub1 enzymatic stability (in the presence of 0.5% Triton X-100) during 20 d of incubation at 37 and 50°C. TA concentrations were measured every 5 d. Data are the means±SD of four replicates.

from *Thermobifida fusca* (29 kDa; Chen *et al.*, 2008), but is closer to those of fungal plant pathogen cutinases, such as CcCUT1 from *C. cinerea* (18.8 kDa; Kontkanen *et al.*, 2009) and CutA from *Botrytis cinerea* (18 kDa; van der Vlugt-Bergmans *et al.*, 1997).

As reported with other cutinases, purified Sub1 also has the ability to hydrolyze *p*-nitrophenyl esters. Sub1 was more active on *p*-nitrophenyl esters with short carbon chains, *i.e.* *p*-nitrophenyl butyrate (*p*-NPB, C4) and *p*-nitrophenyl octanoate (C8), than on those with longer carbon chains (C10 and C12). Other microbial cutinases have also been reported to be more active on *p*-nitrophenyl esters harboring short fatty acid chains (Purdy and Kolattukudy, 1973; Kontkanen *et al.*, 2009). Using *p*-nitrophenyl butyrate as a substrate, the activity of Sub1 followed a typical Michaelis-Menten curve. The Sub1 enzyme showed affinity towards this substrate (K_m=5.7 10^{-4} M), similar to two cutinases of *Fusarium solani* pv. *pisi* with K_m of 3.5 10^{-4} M and of 7.5 10^{-4} M, respectively (Kolattukudy *et al.*, 1981). Although streptomycetes such as *S. scabies* and filamentous fungi belong to different kingdoms, they exhibit similar lifestyles and often share the same ecological niches (Wösten and Willey, 2000). Their mycelia colonize various organic polymers and produce large amounts of extracellular enzymes to retrieve nutrients from these substrates. Therefore, similarities between Sub1 and fungal cutinases may reflect an adaptation to a similar lifestyle. Other *Streptomyces* extracellular enzymes, *e.g.* chitosanases from the GH75 family, are encoded by genes that are also mainly represented in fungal and actinobacterial genomes (Lacombe-Harvey *et al.*, 2018).

Sub1 has high similarity, at the amino acid level, to the cutinase CUT1 from *F. solani*, which is able to degrade suberin. Similar to CUT1, the present results indicated that Sub1 exhibits hydrolysis activity on suberin. However, Sub1 and CUT1 showed higher activity on cutin than on suberin, even though *S. scabies* and *F. solani* both infect and colonize potato tubers and are, thus, frequently in contact with potato suberin (Fiers *et al.*, 2012). This finding indicates that the presence of aromatic compounds in suberin also contributes to its recalcitrant nature (Faber, 1979). However, difficulties are associated with comparing the efficacy of Sub1 with fungal cutinases because the methods used to monitor cutinase activity differ between studies (van der Vlugt-Bergmans *et al.*, 1997; Kontkanen *et al.*, 2009; Chen *et al.*, 2013; the present results). To the best of our knowledge, Sub1 represents the first bacterial cutinase for which activity towards suberin has been demonstrated. Based on the ecological niche of this pathogen, in which potato tubers, but not the aerial part of the plant, are infected, suberin most likely represents an important substrate for Sub1 in the environment and, consequently, Sub1 may be designated as a suberinase. While the ability to degrade cutin has been shown to be important for the pathogenicity of various fungal plant pathogens (Feng *et al.*, 2011; Wang *et al.*, 2017), there is no evidence to show that the ability to degrade suberin represents an asset in the infection process of plant pathogens. The Sub1 protein does not appear to be an essential pathogenicity factor for *S. scabies* because the *sub1* gene has not been detected in other common scab-inducing *Streptomyces* species, such as *S. acidiscabies* (Komeil *et al.*, 2013), and its primary benefit may involve the degradation of refractory polymers. However, Sub1 may confer an advantage to *S. scabies* over other common scab-inducing species by facilitating direct penetration, tuber colonization, and persistence in potato tuber debris.

While Sub1 is conserved in only a few streptomycetes, it presents high homology not only with some fungal cutinases, but also with cutinase-like enzymes from animal pathogenic mycobacteria (Komeil *et al.*, 2013). These bacteria do not encounter cutin or suberin in their environment; however, cutinases were identified as multifunctional enzymes that act on phospholipids, polysorbates, triacylglycerols, and triolein (Schué *et al.*, 2010; Monu and Meena, 2016). As multifunctional enzymes, cutinases have a number of applications in industry (Carvalho *et al.*, 1998). In the present study, the effects of Sub1 on PET, a synthetic polyester that is widely used in the production of textiles, were tested. Sub1 was shown to degrade PET because the quantity of terephthalic acid released from the synthetic polymer depended on the enzyme concentration and increased over the incubation time. The enzyme Sub1 maintained its activity at 37°C for at least 20 d, showing that it is stable, as has been demonstrated for other cutinases (Dutta *et al.*, 2009). Due to their functional properties, cutinases are considered to be a link between esterases and lipases (Chahinian *et al.*, 2002). The addition of a non-ionic surfactant, such as Triton, into a reaction mix generally promotes the activity of lipases, but does not affect the activity of most cutinases. For example, the presence of Triton in the reaction mix increased the hydrolysis of polyester bis-(benzoyloxyethyl) terephthalate (3PET) by a lipase secreted by *Thermomyces lanuginosus*, whereas it did not exert any effect when the same substrate was exposed to cutinases secreted by *T. fusca* and *F. solani* (Eberl *et al.*, 2009). Triton increases the activity of lipases by promoting the opening of a peptide lid located over the active site of the enzyme; such a lid is not present in cutinases (Eberl *et al.*, 2009). As observed with most cutinases, the addition of Triton X-100 did not affect cutin hydrolysis by Sub1 (data not shown). Nevertheless, the hydrolysis of *p*-nitrophenyl esters and of PET by Sub1 was enhanced in the presence of Triton.

The present study established that the *sub1* gene of *S. scabies* encodes a protein acting as a suberinase. The versatility of Sub1 may also be considered for adoption in industrial applications. A cutinase-like enzyme has recently attracted global public attention. This enzyme, originally characterized in the bacterium *Ideonella sakaiensis* 201-F6, is able to degrade PET and has been reclassified as a PETase (Yoshida *et al.*, 2016). Thereafter, Austin *et al.* (2018) introduced modifications to the binding cleft of this enzyme and produced an engineered PETase with better plastic-degrading properties than the native enzyme. The current need for enzymes with the ability to degrade refractory polymers of anthropic origin makes further studies on the capabilities of Sub1 very relevant.

Acknowledgements

The authors thank Peter Moffett for the critical review of the manuscript. This work was funded by the Natural Sciences and Engineering Research Council of Canada (grant number 018602).

References

Austin, H.P., Allen, M.D., Donohoe, B.S., Rorrer, N.A., Kearns, F.L., Silveira, R.L., *et al.* (2018) Characterization and engineering of a plastic-degrading aromatic polyesterase. *Proc Natl Acad Sci U S A* **115**: E4350–E4357.

Beaulieu, C., Sidibé, A., Jabloune, R., Simao-Beaunoir, A.-M., Lerat, S., Monga, E., and Bernards, M.A. (2016) Physical, chemical and proteomic evidence of potato suberin degradation by the plant pathogenic bacterium *Streptomyces scabiei*. *Microbes Environ* **31**: 427–434.

Beauséjour, J., Goyer, C., Vachon, J., and Beaulieu, C. (1999) Production of thaxtomin A by *Streptomyces scabies* strains in plant extract containing media. *Can J Microbiol* **45**: 764–768.

Beisson, F., Li-Beisson, Y., and Pollard, M. (2012) Solving the puzzles of cutin and suberin polymer biosynthesis. *Curr Opin Plant Biol* **15**: 329–337.

Bernards, M.A., and Lewis, N.G. (1998) The macromolecular aromatic domain in suberized tissue: a changing paradigm. *Phytochemistry* **47**: 915–933.

Bernards, M.A. (2002) Demystifying suberin. *Can J Bot* **80**: 227–240.

Bradford, M.M. (1976) A rapid and sensitive method for the quantitation of microgram quantities of protein utilizing the principle of protein-dye binding. *Anal Biochem* **72**: 248–254.

Carvalho, C.M.L., Aires-Barros, M.R., and Cabral, J.M.S. (1998) Cutinase structure, function and biocatalytic applications. *Electron J Biotechnol* **1**: 160–173.

Carvalho, C.M.L., Aires-Barros, M.R., and Cabral, J.M.S. (1999) Cutinase: from molecular level to bioprocess development. *Biotechnol Bioeng* **66**: 17–34.

Chahinian, H., Nini, L., Boitard, E., Dubès, J.-P., Comeau, L.-C., and Sarda, L. (2002) Distinction between esterases and lipases: a kinetic study with vinyl esters and TAG. *Lipids* **37**: 653–662.

Chen, S., Tong, X., Woodard, R.W., Du, G., Wu, J., and Chen, J. (2008) Identification and characterization of bacterial cutinase. *J Biol Chem* **283**: 25854–25862.

Chen, S., Su, L., Chen, J., and Wu, J. (2013) Cutinase: characteristics, preparation, and application. *Biotechnol Adv* **31**: 1754–1767.

Dutta, K., Sen, S., and Veeranki, V.D. (2009) Production, characterization and applications of microbial cutinases. *Process Biochem* **44**: 127–134.

Eberl, A., Heumann, S., Brückner, T., Araujo, R., Cavaco-Paulo, A., Kaufmann, F., *et al.* (2009) Enzymatic surface hydrolysis of poly(ethylene terephthalate) and bis(benzoyloxyethyl) terephthalate by lipase and cutinase in the presence of surface active molecules. *J Biotechnol* **143**: 207–212.

Faber, M.D. (1979) Microbial degradation of recalcitrant compounds and synthetic aromatic polymers. *Enzyme Microb Technol* **1**: 226–232.

Feng, J., Hwang, R., Hwang, S.-F., Gaudet, D., and Strelkov, S.E. (2011) Molecular characterization of a *Stagonospora nodorum* lipase gene *LIP1*. *Plant Pathol* **60**: 698–708.

Fiers, M., Edel-Hermann, V., Chatot, C., Le Hingrat, Y., Alabouvette, C., and Steinberg, C. (2012) Potato soil-borne diseases. A review. *Agron Sustainable Dev* **32**: 93–132.

Hill, J., and Lazarovits, G. (2005) A mail survey of growers to estimate potato common scab prevalence and economic loss in Canada. *Can J Plant Pathol* **27**: 46–52.

Khatri, B.B., Tegg, R.S., Brown, P.H., and Wilson, C.R. (2011) Temporal association of potato tuber development with susceptibility to common scab and *Streptomyces scabiei*-induced responses in the potato periderm. *Plant Pathol* **60**: 776–786.

Kolattukudy, P.E., and Agrawal, V.P. (1974) Structure and composition of aliphatic constituents of potato tuber skin (suberin). *Lipids* **9**: 682–691.

Kolattukudy, P., Purdy, R., and Maiti, I. (1981) Cutinases from fungi and pollen. *Methods Enzymol* **71**: 652–664.

Komeil, D., Simao-Beaunoir, A.-M., and Beaulieu, C. (2013) Detection of potential suberinase-encoding genes in *Streptomyces scabiei* strains and other actinobacteria. *Can J Microbiol* **59**: 294–303.

Komeil, D., Padilla-Reynaud, R., Lerat, S., Simao-Beaunoir, A.-M., and Beaulieu, C. (2014) Comparative secretome analysis of *Streptomyces scabiei* during growth in the presence or absence of potato suberin. *Proteome Sci* **12**: 35.

Kontkanen, H., Westerholm-Parvinen, A., Saloheimo, M., Bailey, M., Rättö, M., Mattila, I., *et al.* (2009) Novel *Coprinopsis cinerea* polyesterase that hydrolyzes cutin and suberin. *Appl Environ Microbiol* **75**: 2148–2157.

Lacombe-Harvey, M.-È., Brzezinski, R., and Beaulieu, C. (2018) Chitinolytic functions in actinobacteria : ecology, enzymes, and evolution. *Appl Microbiol Biotechnol* **102**: 7219–7230.

Lauzier, A., Simao-Beaunoir, A.-M., Bourassa, S., Poirier, G.G., Talbot, B., and Beaulieu, C. (2008) Effect of potato suberin on *Streptomyces scabies* proteome. *Mol Plant Pathol* **9**: 753–762.

Liu, Z., Gosser, Y., Baker, P.J., Ravee, Y., Lu, Z., Alemu, G., *et al.* (2009) Structural and functional studies of *Aspergillus oryzae* cutinase: enhanced thermostability and hydrolytic activity of synthetic ester and polyester degradation. *J Am Chem Soc* **131**: 15711–15716.

Loria, R., Coombs, J., Yoshida, M., Kers, J.A., and Bukhalid, R.A. (2003) A paucity of bacterial root diseases : *Streptomyces* succeeds where others fail. *Physiol Mol Plant Pathol* **62**: 65–72.

Martinez, C., Nicolas, A., van Tilbeurgh, H., Egloff, M.P., Cudrey, C., Verger, R., and Cambillau, C. (1994) Cutinase, a lipolytic enzyme with a preformed oxyanion hole. *Biochemistry* **33**: 83–89.

McQueen, D.A.R., and Schottel, J.L. (1987) Purification and characterization of a novel extracellular esterase from pathogenic *Streptomyces scabies* that is inducible by zinc. *J Bacteriol* **169**: 1967–1971.

Monu, and Meena, L.S. (2016) Roles of triolein and lipolytic protein in the pathogenesis and survival of *Mycobacterium tuberculosis*: a novel therapeutic approach. *Appl Biochem Biotechnol* **178**: 1377–1389.

Murphy, C.A., Cameron, J.A., Huang, S.J., and Vinopal, R.T. (1996) *Fusarium* polycaprolactone depolymerase is cutinase. *Appl Environ Microbiol* **62**: 456–460.

Nimchua, T., Eveleigh, D.E., Sangwatanaroj, U., and Punnapayak, H. (2008) Screening of tropical fungi producing polyethylene terephthalate-hydrolyzing enzyme for fabric modification. *J Ind Microbiol Biotechnol* **35**: 843–850.

Purdy, R.E., and Kolattukudy, P.E. (1973) Depolymerization of a hydroxy fatty acid biopolymer, cutin, by an extracellular enzyme from *Fusarium solani* f. *pisi*: isolation and some properties of the enzyme. *Arch Biochem Biophys* **159**: 61–69.

Ribitsch, D., Acero, E.H., Przylucka, A., Zitzenbacher, S., Marold, A., Gamerith, C., *et al.* (2015) Enhanced cutinase-catalyzed hydrolysis of polyethylene terephthalate by covalent fusion to hydrophobins. *Appl Environ Microbiol* **81**: 3586–3592.

Sambrook, J.F., and Russell, D.W. (2001) *Molecular Cloning: A Laboratory Manual*, 3rd edn. Cold Spring Harbor, NY: Cold Spring Harbor Laboratory Press.

Schué, M., Maurin, D., Dhouib, R., Bakala N'Goma, J.-C., Delorme, V., Lambeau, G., *et al.* (2010) Two cutinase-like proteins secreted by *Mycobacterium tuberculosis* show very different lipolytic activities reflecting their physiological function. *FASEB J* **24**: 1631–2136.

Su, L., Woodard, R.W., Chen, J., and Wu, J. (2013) Extracellular location of *Thermobifida fusca* cutinase expressed in *Escherichia coli* BL21(DE3) without mediation of a signal peptide. *Appl Environ Microbiol* **79**: 4192–4198.

Tyner, D.N., Hocart, M.J., Lennard, J.H., and Graham, D.C. (1997) Periderm and lenticel characterization in relation to potato cultivar, soil moisture and tuber maturity. *Potato Res* **40**: 181–190.

van der Vlugt-Bergmans, C.J., Wagemakers, C.A., and van Kan, J.A. (1997) Cloning and expression of the cutinase A gene of *Botrytis cinerea*. *Mol Plant Microbe Interact* **10**: 21–29.

Vertommen, M.A.M.E., Nierstrasz, V.A., van der Veer, M., and Warmoeskerken, M.M.C.G. (2005) Enzymatic surface modification of poly(ethylene terephthalate). *J Biotechnol* **120**: 376–386.

Walton, T.J., and Kolattukudy, P.E. (1972) Determination of the structures of cutin monomers by a novel depolymerization procedure and combined gas chromatography and mass spectrometry. *Biochemistry* **11**: 1885–1897.

Wang, Y., Chen, J., Li, D.W., Zheng, L., and Huang, J. (2017) *CglCUT1* gene required for cutinase activity and pathogenicity of *Colletotrichum gloeosporioides* causing anthracnose of *Camellia oleifera*. *Eur J Plant Pathol* **147**: 103–114.

Wösten, H.A.B., and Willey, J.M. (2000) Surface-active proteins enable microbial aerial hyphae to grow into the air. *Microbiology* **146**: 767–773.

Yoshida, S., Hiraga, K., Takehana, T., Taniguchi, I., Yamaji, H., Maeda, Y., *et al.* (2016) A bacterium that degrades and assimilates poly(ethylene terephthalate). *Science* **351**: 1196–1199.

Microbes Environ. Vol. 29, No. 4, 427-430, 2014
https://www.jstage.jst.go.jp/browse/jsme2 doi:10.1264/jsme2.ME14054

Short Communication

Intestinal Colonization by a *Lachnospiraceae* Bacterium Contributes to the Development of Diabetes in Obese Mice

Keishi Kameyama[1]*, and Kikuji Itoh[2]

[1]*Institute for Innovation, Ajinomoto Co., Inc., Kawasaki 210–8681, Japan; and* [2]*Department of Veterinary Public Health, Graduate School of Agricultural and Life Sciences, The University of Tokyo, Tokyo 113–8657, Japan*

(Received April 4, 2014—Accepted July 17, 2014—Published online October 4, 2014)

The aim of the present study was to identify bacteria that may contribute to the onset of metabolic dysfunctions. We isolated and identified a candidate bacterium belonging to *Lachnospiraceae* (strain AJ110941) in the feces of hyperglycemic obese mice. The colonization of germ-free *ob/ob* mice by AJ110941 induced significant increases in fasting blood glucose levels as well as liver and mesenteric adipose tissue weights, and decreases in plasma insulin levels and HOMA-β values. These results indicated that the specific gut commensal bacterium AJ110941 influenced the development of obesity and diabetes in *ob/ob* mice with genetic susceptibility for obesity.

Key words: gut microbiota, diabetes, T-RFLP, gnotobiotic mouse, *Lachnospiraceae*

The gut microbiota has been shown to influence host energy homeostasis, metabolism, and inflammation; thus, microbial communities within the gut are now recognized as an important environmental factor in the onset of obesity and type 2 diabetes (T2D) (5, 7, 12, 14, 23). As a consequence, interest in the development of methods to target gut microbiota as a therapy for T2D is increasing (2, 12, 18, 21).

Several studies have conducted metagenomic analyses in an attempt to identify members of the gut microbial community that contribute most significantly to the progression of T2D. Qin *et al.* performed a metagenomic analysis on fecal samples obtained from 345 Chinese men and women with or without T2D (19). Karlsson *et al.* also conducted a metagenomic analysis to compare microbial communities in fecal samples collected from 145 European women who had either T2D, impaired glucose metabolism, or were healthy (13). Both of these studies reported that butyrate-producing *Roseburia* species and *Faecalibacterium prauznitzii* were rarer in subjects with T2D; however, the identified bacteria that existed in high population in T2D subjects differed between these studies (8). Cani *et al.* proposed that lipopolysaccharide (LPS), a cell wall component of almost all Gram-negative bacteria, may be a key substance responsible for metabolic endotoxemia, low-grade systemic inflammation, and insulin resistance in mouse models (1, 3). In support of this, a previous study reported that experimental endotoxemia induced adipose inflammation and insulin resistance in human subjects (17).

We herein searched for the specific gut commensal bacterium related to metabolic syndrome using the terminal restriction fragment length polymorphism (T-RFLP) analysis of fecal samples from a mouse model of T2D. In this study, a comparison of homozygous *db/db* (diabetic) with heterozygous *db/+* (non-diabetic) mice revealed that a specific fragment of the T-RFLP analysis was present at significantly higher levels in *db/db* mice than in *db/+* mice. Even though *ob/ob* obese mice gain weight rapidly and show the symptoms of insulin resistance, most of the obese mice do not develop severe hyperglycemia compared with *db/db* mice (22). However, one of the *ob/ob* mice in the present study showed an abnormally high fasting blood glucose (FBG) level similar to *db/db* mice. The specific fragment observed in *db/db* mice was also the most prominent in the abnormally hyperglycemic *ob/ob* mouse. We hypothesized that the specific bacterium harboring the fragment may have contributed to the progression of T2D; therefore, we isolated and cultured the bacterium (strain AJ110941). We then determined that colonization by the isolate with the LPS producer *E. coli* induced hyperglycemia and the accumulation of adipose tissue in the gnotobiotic *ob/ob* mouse model.

All experimental procedures were reviewed and approved by the Animal Care Committee of Ajinomoto Co., Inc. Male 5-week-old homozygous BKS.Cg-Dock7^{m} +/+Lepr^{db}/J (*db/db*, diabetic) mice, heterozygous control (*db/+*, non-diabetic) mice, and homozygous B6.V-Lep^{ob}/J (*ob/ob*, obese) mice were obtained from Charles River Japan (Yokohama, Japan). Male 5-week-old germ-free *ob/ob* mice were obtained from Sankyo Lab Service (Tokyo, Japan). These mice were housed in a controlled environment (on a 12-h light/dark cycle with lights turning off at 19:00) with free access to standard chow CRF-1 (Oriental Yeast, Tokyo, Japan) and water and kept in specific pathogen-free (SPF) or germ-free/gnotobiotic conditions throughout the experimental period. Fresh feces and blood were collected from 5- and 11-week-old mice after fasting for 16 h.

Blood glucose (FBG) levels were determined using DRI-CHEM 7000V (Fujifilm, Tokyo, Japan). Plasma insulin levels were determined using an ultrasensitive mouse insulin kit (Morinaga Institute of Biological Science, Yokohama, Japan). Plasma glucagon levels were determined using the

* Corresponding author. E-mail: keishi_kameyama@ajinomoto.com

Glucagon ELISA Kit Wako (Wako Pure Chemical Industries, Osaka, Japan). Insulin resistance (HOMA-IR) and β-cell function (HOMA-β) were both calculated on the basis of the fasting levels of plasma glucose and insulin according to the homeostasis model assessment (HOMA) method (16).

Fresh fecal samples were collected from mice, added to 99% ethanol, and stored at −30°C. Bacterial DNA was extracted from the fecal samples using the FastDNA spin kit for soil (MP Biomedicals, Santa Ana, CA) using the FastPrep instrument (MP Biomedicals). T-RFLP analyses of the mouse gut microbiota were performed as previously described (10). Two universal primers, 27F labeled with 6-carboxyfluorescein (FAM): 5'-FAM-AGAGTTTGATCCTGGCTCAG-3' and 1492R: 5'-GGTTACCTTGTTACGACTT-3' were used in PCR to amplify the 16S rRNA gene coding region. Purified PCR products of the 16S rRNA gene were digested with *Msp*I (Takara Bio, Otsu, Japan).

To isolate and culture the bacterium, fresh feces were collected and immediately weighed and transferred to an anaerobic chamber. The feces were homogenized with a 50-fold volume (v/w) of an anaerobic diluent, serially diluted, and then plated on Eggerth-Gagnon (EG) agar plates (11). The agar plates were incubated at 37°C for 4 d in the anaerobic chamber. All of the colonies were identified by their fragment size, and a target colony with a fragment size of 282 bp was then selected. The colony was passaged onto new EG agar plates, and the bacterial purity of the isolate was ensured by re-streaking and microscopic observations. The 16S rRNA gene sequence of the isolated bacterium was determined as previously described (15). The sequence was assembled using GENETYX version 7 (GENETYX, Tokyo, Japan). The identification and phylogenic tree analysis of the 16S rRNA gene sequence were carried out using the Ribosomal Database Project (RDP) (6).

When the mice were 8 weeks old, germ-free *ob/ob* mice were separated into 3 groups for the germ-free/gnotobiotic experiment: Group-1 (*n*=4), germ-free; Group-2 (*n*=4), colonization by the non-pathogenic *Escherichia coli* strain E-17, which had been isolated from SPF mice; Group-3 (*n*=4), colonization by AJ110941 with *E. coli* E-17. Groups-2 and -3 were then orally inoculated with *E. coli* E-17 or AJ110941 with *E. coli* E-17 (approximately 1×10^8 cells suspended in anaerobic PBS, respectively). Group-1 was orally administered PBS only. These mice were maintained under the germ-free or gnotobiotic conditions for 8 weeks.

We compared differences in gut microbiota patterns between *db/+* and *db/db* mice. Hyperglycemia was observed in 11-week-old, but not in 5-week-old mice (Fig. S1). The 282 bp fragment was significantly higher in *db/db* than *db/+* mice at both 5 and 11 weeks old (Fig. S2). We then evaluated the presence of the 282 bp fragment in another metabolic syndrome model, the *ob/ob* mouse. The highest FBG level observed among all *ob/ob* mice was in Mouse Number 4 (Fig. S3). The 282 bp fragment was also more prominent in hyperglycemic Mouse Number 4 than in the normal glycemic *ob/ob* mouse at both 5 and 11 weeks old (Fig. S4). Based on these *db/db* and *ob/ob* mice results, we focused on this 282 bp fragment bacteria.

We isolated a colony harboring the 282 bp fragment and established an axenic strain (strain AJ110941). The isolate was determined to be closely related to the genus *Anaerostipes* in the family *Lachnospiraceae* (Fig. 1).

We then generated gnotobiotic *ob/ob* mice colonized by AJ110941 with *E. coli*. Eight weeks after the inoculation, the cecum, liver, adipose tissue, and blood were collected after a 16-h fast. The gut microbiota of the cecal contents from the three groups was determined by T-RFLP analysis. No PCR amplicon was detected in Group-1. Only a single fragment (488 bp) that corresponded to *E. coli* was detected in Group-2. Only two fragments (282 bp and 488 bp) were detected in Group-3. These results clearly indicated that germ-free or gnotobiotic conditions were maintained during the experimental period. The weights of the liver and mesenteric adipose tissue significantly increased in Group-3, whereas no significant difference was observed in body weights between the three groups. FBG and plasma glucagon levels were significantly higher in Group-3, while plasma insulin levels were significantly lower. On the other hand, no significant differences were observed in these parameters between Groups-1 and -2. The homeostasis model assessment was calculated from FBG and plasma insulin levels as an index of insulin resistance (HOMA-IR) and pancreatic β cell function (HOMA-β). HOMA-β was significantly lower in Group-3, whereas no significant differences were noted in HOMA-IR between the three groups (Table 1). These results suggested that colonization by AJ110941 may have promoted the dysfunction of pancreatic β-cells.

Therefore, AJ110941 should be regarded as one of the important causative gut bacteria for the induction of T2D. A previous study reported that the relative abundance of the

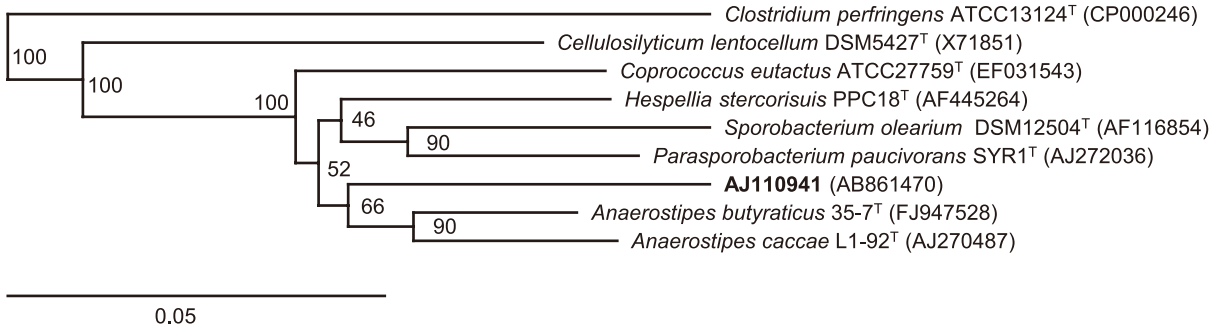

Fig. 1. Phylogenetic tree based on the 16S rRNA gene constructed by Weighbor, the weighted neighbor-joining tree building algorithm, showing AJ110941 and other strains of the family *Lachnospiraceae*. *Clostridium perfringens* ATCC13124^T was used as an outgroup. The numbers close to the nodes represent bootstrap values (*n*=100 replicates). The scale bar represents 0.05 substitutions per nucleotide position.

Table 1. Phenotypes of germ-free and gnotobiotic *ob/ob* mice

	Group-1	Group-2	Group-3
Body weight without the caecum (g)	58.10 ± 5.98^{a}	61.75 ± 4.29^{a}	63.48 ± 10.37^{a}
Cecum (% of body weight)	11.63 ± 4.89^{a}	12.88 ± 1.94^{a}	4.47 ± 0.93^{b}
Liver (% of body weight without the cecum)	6.91 ± 0.66^{a}	7.29 ± 1.83^{a}	9.70 ± 0.46^{b}
Mesenteric adipose tissue (% of body weight without the cecum)	1.64 ± 0.46^{a}	1.81 ± 0.39^{a}	2.63 ± 0.30^{b}
Fasting blood glucose (mg dL^{-1})	216.5 ± 113.6^{a}	286.5 ± 54.1^{ab}	433.25 ± 65.4^{b}
Fasting plasma insulin (μU mL^{-1})	339.7 ± 46.44^{a}	299.8 ± 105.0^{a}	159.4 ± 50.9^{b}
Fasting plasma glucagon (pg mL^{-1})	179.9 ± 43.0^{a}	324.2 ± 42.4^{a}	529.0 ± 18.3^{b}
HOMA-IR	132.5 ± 23.3^{a}	187.5 ± 70.6^{a}	184.4 ± 64.1^{a}
HOMA-β	1350.4 ± 468.9^{a}	638.5 ± 411.9^{ab}	141.7 ± 40.7^{b}

Group-1: germ-free, Group-2: colonization by *E. coli*, Group-3: colonization by AJ110941 with *E. coli*. Data are expressed as means±SD. Values not sharing a common letter are significantly different at $p<0.05$ by the Tukey–Kramer multiple comparisons test ($n=4$ per group) using the JMP 10.0.0 statistical software package (SAS Institute, Cary, NC).

taxonomic family *Lachnospiraceae* was increased by early-life subtherapeutic antibiotic treatments in an obese mouse model (4). Additionally, a metagenomic study indicated that the taxonomic family *Lachnospiraceae* may be associated with T2D (19). However, it remains unclear whether bacteria belonging to the family *Lachnospiraceae* actually affect obesity and FBG levels *in vivo*. Therefore, we generated gnotobiotic *ob/ob* mice colonized by AJ110941 with *E. coli* to reveal a possible causal relationship. In a preliminary examination, we microscopically observed that AJ110941 did not singly colonize the intestinal tract of *ob/ob* germ-free mice. *E. coli*, which is a facultative anaerobe, may be needed to maintain an oxygen-free environment in the intestinal tract because AJ110941 needs strict anaerobic conditions for growth. In our study, a mono-association with the LPS producer *E. coli* induced neither hyperglycemia nor the accumulation of adipose tissues. In contrast, LPS derived from Gram-negative bacteria in the gastrointestinal tract was previously identified as one of the most important factors inducing the development of T2D (1, 3). Our results indicated that the presence of LPS in the intestinal tract was necessary, but not sufficient for the pathogenesis of diabetes. We speculated that AJ110941 may have assisted with the translocation of LPS into the blood from the intestinal tract. We are currently investigating the effects of AJ110941 on LPS translocation in *in vitro*/*vivo* models.

Regarding the particular gut bacterium involved in metabolic syndrome, *Methanobrevibacter smithii* and *Bacteroides thetaiotaomicron* were previously shown to enhance host energy storage in di-associated mice (20). Furthermore, Fei and Zhao reported that the strain *Enterobacter cloacae* B29, which was isolated from an obese human subject, induced obesity and insulin resistance accompanied by serum endotoxemia in mono-associated mice (9).

This is the first study to have successfully identified a specific *Lachnospiraceae* bacterium involved in metabolic disorders. Future studies are needed to elucidate the molecular mechanisms underlying the adverse effects of AJ110941 on glucose and lipid metabolism in mouse models. It remains unclear whether AJ110941 or its closely-related species inhabits the human intestinal tract. We intend to perform a preliminary epidemiological study on obese and diabetic subjects to address this question.

The 16S rRNA gene sequence of the isolated bacterium (strain AJ110941) is available in the DDBJ/EMBL/GenBank databases under the accession number AB861470.

Acknowledgements

We thank Ranko Nishi and Mizuki Kobayashi for their research assistance.

References

1. Cani, P.D., J. Amar, M.A. Iglesias, *et al.* 2007. Metabolic endotoxemia initiates obesity and insulin resistance. Diabetes 56:1761–1772.
2. Cani, P.D., and N.M. Delzenne. 2012. The gut microbiome as therapeutic target. Pharmacol. Ther. 130:202–212.
3. Cani, P.D., S. Possemiers, T. Van de Wiele, *et al.* 2009. Changes in gut microbiota control inflammation in obese mice through a mechanism involving GLP-2-driven improvement of gut permeability. Gut 58:1091–1103.
4. Cho, I., S. Yamanishi, L. Cox, *et al.* 2012. Antibiotics in early life alter the murine colonic microbiome and adiposity. Nature 488:621–626.
5. Clemente, J.C., L.K. Ursell, L.W. Parfrey, and R. Knight. 2012. The impact of the gut microbiota on human health: an integrative view. Cell 148:1258–1270.
6. Cole, J.R., Q. Wang, J.A. Fish, *et al.* 2014. Ribosomal Database Project: data and tools for high throughput rRNA analysis. Nucleic Acids Res. 42:D633–642.
7. Cox, L.M., and M.J. Blaser. 2013. Pathways in microbe-induced obesity. Cell Metab. 17:883–894.
8. de Vos, W.M., and M. Nieuwdorp. 2013. Genomics: A gut prediction. Nature 498:48–49.
9. Fei, N., and L. Zhao. 2013. An opportunistic pathogen isolated from the gut of an obese human causes obesity in germfree mice. ISME J. 7:880–884.
10. Hayashi, H., M. Sakamoto, M. Kitahara, and Y. Benno. 2003. Molecular analysis of fecal microbiota in elderly individuals using 16S rDNA library and T-RFLP. Microbiol. Immunol. 47:557–570.
11. Itoh, K., and T. Mitsuoka. 1985. Characterization of clostridia isolated from faeces of limited flora mice and their effect on caecal size when associated with germ-free mice. Lab. Anim. 19:111–118.
12. Johnson, A.M., and J.M. Olefsky. 2013. The origins and drivers of insulin resistance. Cell 152:673–684.
13. Karlsson, F.H., V. Tremaroli, I. Nookaew, G. Bergström, C.J. Behre, B. Fagerberg, J. Nielsen, and F. Bäckhed. 2013. Gut metagenome in European women with normal, impaired and diabetic glucose control. Nature 498:99–103.
14. Le Chatelier, E., T. Nielsen, J. Qin, *et al.* 2013. Richness of human gut microbiome correlates with metabolic markers. Nature 500:541–546.
15. Liu, W.T., T.L. Marsh, H. Cheng, and L.J. Forney. 1997. Characterization of microbial diversity by determining terminal restriction fragment length polymorphisms of genes encoding 16S rRNA. Appl. Environ. Microbiol. 63:4516–4522.
16. Matthews, D.R., J.P. Hosker, A.S. Rudenski, B.A. Naylor, D.F. Treacher, and R.C. Turner. 1985. Homeostasis model assessment: insulin resistance and beta-cell function from fasting plasma glucose and insulin concentrations in man. Diabetologia 28:412–419.
17. Mehta, N.N., F.C. McGillicuddy, P.D. Anderson, *et al.* 2010. Experimental endotoxemia induces adipose inflammation and insulin resistance in humans. Diabetes 59:172–181.

18. Panwar, H., H.M. Rashmi, V.K. Batish, and S. Grover. 2013. Probiotics as potential biotherapeutics in the management of type 2 diabetes—prospects and perspectives. Diabetes Metab. Res. Rev. 29:103–112.
19. Qin, J., Y. Li, Z. Cai, *et al.* 2012. A metagenome-wide association study of gut microbiota in type 2 diabetes. Nature 490:55–60.
20. Samuel, B.S., and J.I. Gordon. 2006. A humanized gnotobiotic mouse model of host-archaeal-bacterial mutualism. Proc. Natl. Acad. Sci. U.S.A. 103:10011–10016.
21. Sanz, Y., A. Santacruz, and P. Gauffin. 2010. Gut microbiota in obesity and metabolic disorders. Proc. Nutr. Soc. 69:434–441.
22. Shafrir, E., E. Ziv, and L. Mosthaf. 1999. Nutritionally induced insulin resistance and receptor defect leading to beta-cell failure in animal models. Ann. N. Y. Acad. Sci. 892:223–246.
23. Tremaroli, V., and F. Bäckhed. 2012. Functional interactions between the gut microbiota and host metabolism. Nature 489:242–249.

Microbes Environ. 35(2), 2020
https://www.jstage.jst.go.jp/browse/jsme2 doi:10.1264/jsme2.ME20025

Minireview

Size Matters: Ultra-small and Filterable Microorganisms in the Environment

Ryosuke Nakai[1]*†

[1]*Applied Molecular Microbiology Research Group, Bioproduction Research Institute, National Institute of Advanced Industrial Science and Technology (AIST), 2–17–2–1, Tsukisamu-Higashi, Sapporo, 062–8517, Japan*

(Received February 29, 2020—Accepted April 17, 2020—Published online June 3, 2020)

Ultra-small microorganisms are ubiquitous in Earth's environments. Ultramicrobacteria, which are defined as having a cell volume of <0.1 μm^3, are often numerically dominant in aqueous environments. Cultivated representatives among these bacteria, such as members of the marine SAR11 clade (*e.g.*, "*Candidatus* Pelagibacter ubique") and freshwater *Actinobacteria* and *Betaproteobacteria*, possess highly streamlined, small genomes and unique ecophysiological traits. Many ultramicrobacteria may pass through a 0.2-μm-pore-sized filter, which is commonly used for filter sterilization in various fields and processes. Cultivation efforts focusing on filterable small microorganisms revealed that filtered fractions contained not only ultramicrocells (*i.e.*, miniaturized cells because of external factors) and ultramicrobacteria, but also slender filamentous bacteria sometimes with pleomorphic cells, including a special reference to members of *Oligoflexia*, the eighth class of the phylum *Proteobacteria*. Furthermore, the advent of culture-independent "omics" approaches to filterable microorganisms yielded the existence of candidate phyla radiation (CPR) bacteria (also referred to as "*Ca.* Patescibacteria") and ultra-small members of DPANN (an acronym of the names of the first phyla included in this superphyla) archaea. Notably, certain groups in CPR and DPANN are predicted to have minimal or few biosynthetic capacities, as reflected by their extremely small genome sizes, or possess no known function. Therefore, filtered fractions contain a greater variety and complexity of microorganisms than previously expected. This review summarizes the broad diversity of overlooked filterable agents remaining in "sterile" (<0.2-μm filtered) environmental samples.

Key words: filterable microorganisms, ultramicrocells, ultramicrobacteria, candidate phyla radiation, minimal cell

How small may actual organisms be? This question has long fascinated scientists in various fields. Prokaryotic microorganisms (*Archaea* and *Bacteria*) constitute the smallest life forms. Bacterial cells range in volume from ultramicrobacteria (UMB; <0.1 μm^3; Duda *et al.*, 2012) to the typical bacterium *Escherichia coli* (1.6 μm^3; Moore, 1999) and the giant bacterium *Epulopiscium fishelsoni* (3.0×10^6 μm^3; Schulz and Jørgensen, 2001; note that the cells of *Thiomargarita namibiensis* are larger [2.2×10^8 μm^3], but are occupied by a liquid vacuole, that is, they do not have large cytoplasmic bodies; Schulz *et al.*, 1999). Thus, bacteria exhibit cell-size plasticity by varying cell volume by more than seven orders of magnitude in different species. UMB may pass through membrane filters down to 0.2-μm-pore-size, which is commonly used for filter sterilization in research laboratories as well as in medical, food, and industrial processes (Levy and Jornitz, 2006). In fact, efforts to culture microorganisms remaining in the 0.2-μm filtrate (hereafter called filterable microorganisms) of environmental samples have yielded diverse UMB members. The several isolates were affiliated with unique lineages, such as cosmopolitan freshwater *Actinobacteria* and *Betaproteobacteria* (Hahn, 2003; Hahn *et al.*, 2003) as well as the candidate phylum termite group 1 (TG1) described as *Elusimicrobia* (Geissinger *et al.*, 2009). The existence of UMB has expanded our knowledge of microbial life at the lower size limit.

In the last five years, filterable microorganisms have been attracting increasing interest with the discovery of other ultra-small members: the candidate phyla radiation (CPR) bacteria, also referred to as "*Candidatus* Patescibacteria" (hereafter described as CPR/Patescibacteria; Rinke *et al.*, 2013; Brown *et al.*, 2015), and some members of DPANN (an acronym of the names of the first phyla included in this superphyla, "*Ca.* Diapherotrites", "*Ca.* Parvarchaeota", "*Ca.* Aenigmarchaeota", *Nanoarchaeota*, and "*Ca.* Nanohalorchaeota"; Rinke *et al.*, 2013; Dombrowski *et al.*, 2019). Several CPR members have an extremely small cell volume (approximately 0.01 μm^3) that was unveiled by cryo-transmission electron microscopy imaging (Luef *et al.*, 2015). Moreover, the emergence of these ultra-small prokaryotes has re-opened debate on the tree of life (Hug *et al.*, 2016; Parks *et al.*, 2018; Zhu *et al.*, 2019). These members are ubiquitous in the environment and recent studies have provided insights into their contribution to the material cycle (*e.g.*, carbon and nitrogen cycles; Danczak *et al.*, 2017; Lannes *et al.*, 2019). This review focuses on the phylogenetic diversity and complexity of filterable microorganisms in natural systems, with specific references to UMB and pleomorphic bacteria. Other reviews presented aspects of ultra-small microorganisms including CPR/Patescibacteria and DPANN members (*e.g.*, terminology, biogeography,

* Corresponding author. E-mail: nakai-ryosuke@aist.go.jp;
Tel: +81–11–857–8408; Fax: +81–11–857–8980.
† Present address: Microbial Ecology and Technology Research Group, Bioproduction Research Institute, National Institute of Advanced Industrial Science and Technology (AIST), 2–17–2–1, Tsukisamu-Higashi, Sapporo, 062–8517, Japan.

Citation: Nakai, R. (2020) Size Matters: Ultra-small and Filterable Microorganisms in the Environment. *Microbes Environ* **35:** ME20025. https://doi.org/10.1264/jsme2.ME20025

genomic diversity, and metabolic variety; Duda *et al.*, 2012; Castelle *et al.*, 2018; Ghuneim *et al.*, 2018; Dombrowski *et al.*, 2019). In this review, archaea with a cell volume of <0.1 μm^3 are specifically referred to as ultramicroarchaea (UMA) to distinguish them from UMB.

Filterable microorganisms

To date, many studies have reported the presence of filterable microorganisms in various environments (mainly aqueous environments) including seawater (Haller *et al.*, 2000; Elsaied *et al.*, 2001; Lannes *et al.*, 2019; Obayashi and Suzuki, 2019), lake water (Hahn, 2003; Hahn *et al.*, 2003; Watanabe *et al.*, 2009; Fedotova *et al.*, 2012; Maejima *et al.*, 2018; Vigneron *et al.*, 2019), terrestrial aquifers (Miyoshi *et al.*, 2005; Luef *et al.*, 2015), glacier ice and the ice cover of lakes (Miteva and Brenchley, 2005; Kuhn *et al.*, 2014), deep-sea hydrothermal fluids (Naganuma *et al.*, 2007; Nakai *et al.*, 2011), and soil and sand (Nakai *et al.*, 2013). However, the use of membrane filters with a small pore size (approximately 0.2 μm) was traditionally recommended for the retention of bacteria in the field of marine microbial ecology in the 1960s (*e.g.*, Anderson and Heffernan, 1965) and is still widely practiced today in various fields. The existence of very small microorganisms has been well recognized since the 1980s. The term "ultramicrobacteria" was first used by Torrella and Morita (1981) to describe very small coccoid cell forms of <0.3 μm in diameter from seawater. MacDonell and Hood (1982) subsequently isolated and characterized viable filterable microorganisms potentially belonging to the genera *Vibrio*, *Aeromonas*, *Pseudomonas*, and *Alcaligenes* from estuarine waters. They concluded that these filterable microorganisms represented a state of dormancy for adaptation to low nutrient conditions and were not completely novel bacteria. Other studies also reported that external factors reduced cell sizes, such as *Staphylococcus aureus* and *Pseudomonas syringae* (~50% reduction in size as described in Table 1; Watson *et al.*, 1998; Monier and Lindow, 2003). Therefore, the cells of miniaturized microorganisms need to be distinguished from true UMB and are described in this review as "ultramicrocells", which has the synonyms dwarf cells and midget cells, according to Duda *et al.* (2012). Schut *et al.* (1997) and Duda *et al.* (2012) subsequently defined a cell volume index of <0.1 μm^3 as being characteristic of true UMB.

Based on previous studies, filterable microorganisms have been classified into five groups (Fig. 1): (I) ultramicrocells that are miniaturized microorganisms because of external factors (*e.g.*, environmental stress) as described above; (II) obligate UMB that maintain small cell volumes (<0.1 μm^3) regardless of their growth conditions; (III) facultative UMB that contain a small proportion of larger cells with a cell volume >0.1 μm^3 (note that the definitions of the terms "obligate" and "facultative" UMB follow those of Duda *et al.* [2012]); (IV) slender filamentous bacteria; and (V) ultra-small members among CPR/Patescibacteria bacteria and DPANN archaea. In contrast to UMB strains, the cell shapes and morphological characteristics of members in group V are largely unknown under different environmental or culture conditions because all of the members of CPR and DPANN are uncultivated, with a few exceptions of members belonging to the phyla "*Ca.* Saccharibacteria" (former TM7) and *Nanoarchaeota* (*e.g.*, Huber *et al.*, 2002; He *et al.*, 2015). Incidentally, the groups presented in this review do not include filterable cell-wall-less mycoplasmas as well as "nanobacteria" or "nannobacteria" as microfossils, which are often referred to in geological literature (Folk, 1999), or as calcium carbonate nanoparticles in the human body, as reported in medical literature (Martel and Young, 2008). Representative cases of groups II to V are described below and Table 1 shows a summarized list.

Obligate UMB

Obligate UMB are often reported from aqueous environments. One of the most prominent representatives is "*Candidatus* Pelagibacter ubique" HTCC1062, which is a SAR11 clade bacterium that is ubiquitous in marine environments. Previous studies found that SAR11 members consistently dominated ribosomal RNA gene clone libraries derived from seawater DNA and estimated their global population size as 2.4×10^{28} cells—approximately 25% of all prokaryotic cells—in oceans (Giovannoni *et al.*, 1990; Morris *et al.*, 2002). Despite their ubiquitous and abundant presence, it was not possible to isolate them. However, the first cultivated strain HTCC1062 was established in 2002 using a high-throughput dilution-to-extinction culturing (HTC) technique (Rappé *et al.*, 2002). This HTC technique involves cultivation with serial dilutions of natural seawater samples into very low nutrient media (Connon and Giovannoni, 2002). The cell volume (approximately 0.01 μm^3) of "*Ca.* P. ubique" was reported as one of the smallest free-living cells known. Subsequent studies characterized the SAR11 clade with the small, streamlined genomes (<1.5 Mbp) described below, an unusual mode of glycine auxotrophy, a light-dependent proton pump known as proteorhodopsin, and the ability to utilize various one-carbon compounds (reviewed in Tripp, 2013; Giovannoni, 2017). The SAR11 clade is highly divergent with multiple ecotypes and has freshwater members known as LD12 classified in SAR11 subclade IIIb (Grote *et al.*, 2012). An LD12 cultivated representative, "*Ca.* Fonsibacter ubiquis" strain LSUCC0530, was subsequently established (Henson *et al.*, 2018), and its genomic characteristics promoted the hypothesis that gene losses for osmolyte uptake were related to the evolutionary transition, or metabolic tuning, of freshwater SAR11 (LD12) from a salt to freshwater habitat.

Another marine ultramicrobacterium, *Sphingopyxis alaskensis* (formerly known as *Sphingomonas alaskensis*) RB2256 was intensively investigated before the study of the SAR11 clade (*e.g.*, Eguchi *et al.*, 1996; Schut *et al.*, 1997). This strain was also characterized as an obligate UMB (Duda *et al.*, 2012). When the cultivation of this strain transitioned from low-carbon to highly-enriched media, the cell volume of *S. alaskensis* remained at <0.1 μm^3 in most media; however, larger elongated cells, not UMB cells, were observed in trypticase soy agar medium (Vancanneyt *et al.*, 2001). Furthermore, this strain possesses a larger genome of 3.3 Mb (DDBJ/ENA/GenBank accession no. CP000356) than other UMB (Table 1).

Table 1. An overview of ultra-small and filterable microorganisms in the environment

Taxa	Phylum (and class for *Proteobacteria*)	Isolation source	Cell shape	Cell size (length×width and/or volume)	Genome size (Mbp)	Physiological and ecological trait(s) or its potential	Reference
Ultramicrocells							
Staphylococcus aureus 8325-4	*Firmicutes*	derivative of *S. aureus* NCTC8325 (patient's strain)	cocci	cell size reduction from 0.69±0.08 to 0.41±0.08 μm	n.d.	host cell invasion, starvation-associated cell size reduction	Watson *et al.* (1998)
Pseudomonas syringae pv. *syringae* B728a	*Proteobacteria* (*γ-proteobacteria*)	snap bean leaflet	rods	cell length reduction from ~2.5 to ~1.2 μm	6.09	host cell invasion, leaf environment-induced cell size reduction	Monier and Lindow (2003); Feil *et al.* (2005)
Obligate ultramicrobacteria and related candidates							
"*Candidatus* Pelagibacter ubique" HTCC1062	*Proteobacteria* (*α-proteobacteria*)	coastal sea	curved rods	0.01 μm^3	1.31	glycine auxotrophy, rhodopsin-based photometabolism, utilization of one-carbon compounds	Rappé *et al.* (2002); Tripp (2013); Giovannoni (2017)
"*Candidatus* Fonsibacter ubiquis" LSUCC0530	*Proteobacteria* (*α-proteobacteria*)	coastal lagoon	curved rods	1.0×0.1 μm	1.16	glycine auxotrophy, rhodopsin-based photometabolism, tetrahydrafolate metabolism**	Henson *et al.* (2018)
Sphingopyxis alaskensis RB2256	*Proteobacteria* (*α-proteobacteria*)	fjord estuary	short rods	0.05–0.09 μm^3	3.35	utilization of various amino acids, resistance to heat shock, H_2O_2, and ethanol	Eguchi *et al.* (1996); Schut *et al.* (1997)
Aurantimicrobium minutum KNC^T	*Actinobacteria*	freshwater river	curved rods	0.7–0.8×0.3 μm; 0.04–0.05 μm^3	1.62	rhodopsin-based photometabolism**	Nakai *et al.* (2015, 2016b)
Rhodoluna lacicola MWH-Ta8^T	*Actinobacteria*	freshwater lake	curved rods	0.85×0.30 μm; 0.053 μm^3	1.43	rhodopsin-based photometabolism	Hahn *et al.* (2014); Keffer *et al.* (2015)
Rhodoluna limnophila 27D-LEPI^T	*Actinobacteria*	freshwater pond	short rods	0.49×0.28 μm	1.40	nitrate uptake and nitrite excretion system**	Pitt *et al.* (2019)
"*Candidatus* Planktophila rubra" IMCC25003	*Actinobacteria*	freshwater lake	curved rods	0.041 μm^3	1.35	catalase-dependent growth	Kim *et al.* (2019)
"*Candidatus* Planktophila aquatilis" IMCC26103	*Actinobacteria*	freshwater lake	curved rods	0.061 μm^3	1.46	catalase-dependent growth	Kim *et al.* (2019)
Polynucleobacter necessarius subsp. *asymbioticus* QLW-P1DMWA-1^T	*Proteobacteria* (*β-proteobacteria*)	freshwater pond	straight rods	0.7–1.2×0.4–0.5 μm	2.16	utilization of low-molecular-weight substrates	Hahn *et al.* (2012); Meincke *et al.* (2012)
Opitutus sp. VeCb1	*Verrucomicrobia*	rice paddy soil	ellipsoids	0.49×0.33 μm; 0.030 μm^3	n.d.	utilization of sugars and sugar polymers, strict fermentative metabolism, oxygen tolerance	Janssen *et al.* (1997); Chin *et al.* (2001)
Facultative ultramicrobacteria							
Endomicrobium proavitum Rsa215	*Elusimicrobia*	gut homogenate of *Reticulitermes santonensis*	cocci, rods showing budding cell division	0.3–0.5 μm (for cocci); 0.5–3.5×0.15–0.30 μm (for rods)	1.59	nitrogen fixation	Zheng and Brune (2015); Zheng *et al.* (2016)
Chryseobacterium solincola NF4	*Bacteroidetes*	lake sediment	cocci, rods showing budding cell division or cell septation	0.004–0.04 μm^3 (for cocci); 0.1–0.3 μm^3 (for rods)	~1.7	ectoparasite of *Bacillus subtilis*	Suzina *et al.* (2011); Duda *et al.* (2012)
Slender filamentous bacteria							
Hylemonella gracilis CB	*Proteobacteria* (*β-proteobacteria*)	freshwater	spirals	0.12 μm^3 (smallest width=0.2 μm)	n.d.	n.d.	Wang *et al.* (2007, 2008)
Oligoflexus tunisiensis Shr3^T	*Proteobacteria* (*Oligoflexia*)*	desert sand	pleomorphic (rods, filaments, spirals, and spherical [or curled] cells)	various lengths×0.4–0.8 μm (for filaments)	7.57	multidrug resistance, incomplete denitrification**	Nakai *et al.* (2014, 2016a)
Silvanigrella aquatica MWH-Nonnen-W8red^T	*Proteobacteria* (*Oligoflexia*)*	freshwater lake	pleomorphic (rods, filaments, and spirals)	3.6×0.6 μm (for rods)	3.51	antimicrobial peptides, plasmid-encoded type IV secretion systems**	Hahn *et al.* (2017)
Silvanigrella paludirubra SP-Ram-0.45-NSY-1^T	*Proteobacteria* (*Oligoflexia*)*	freshwater pond	pleomorphic (rods and filaments)	various lengths	3.94	utilization of limited substrates	Pitt *et al.* (2020)
Fluviispira multicolorata 33A1-SZDP^T	*Proteobacteria* (*Oligoflexia*)*	freshwater creek	pleomorphic (rods and filaments)	various lengths	3.39	violacein-like production	Pitt *et al.* (2020)
CPR/Patescibacteria bacteria							
WWE3-OP11-OD1 bacteria	candidate division WWE3, "*Candidatus* Microgenomates" (OP11), "*Candidatus* Parcubacteria" (OD1)	deep aquifer	cocci or oval-shaped	0.009±0.002 μm^3	0.69–1.05	potential interaction with other bacterial cells via pili-like structures	Luef *et al.* (2015)
"*Candidatus* Sonnebornia yantaiensis"	"*Candidatus* Parcubacteria" (OD1)	ciliated protist *Paramecium bursaria*	straight rods	1.6–1.9×0.5–0.6 μm	n.d.	endoplasmic symbiont of the ciliate *P. bursaria*	Gong *et al.* (2014)
TM7x bacterium	"*Candidatus* Saccharibacteria" (TM7)	human oral cavity	cocci	0.2–0.3 μm	0.71	ectosymbiont of *Actinomyces odontolyticus*	He *et al.* (2015)
DPANN archaea							
Nanoarchaeum equitans	*Nanoarchaeota*	submarine hot vent	cocci	0.4 μm	~0.5	ectosymbiont of *Ignicoccus hospitalis*	Huber *et al.* (2002)
"*Candidatus* Nanopusillus acidilobi"	*Nanoarchaeota*	hot spring	cocci	0.1–0.3 μm	0.61	ectosymbiont of *Acidilobus* species	Wurch *et al.* (2016)
"*Candidatus* Nanoclepta minutus" Ncl-1	*Nanoarchaeota*	hot spring	flagellated cocci	~0.2 μm	0.58	ectosymbiont of *Zestosphaera tikiterensis*	John *et al.* (2019)
"*Candidatus* Nanosalina" sp. J07AB43	"*Candidatus* Nanohaloarchaeota"	hypersaline lake	cocci-like	0.6 μm	1.23	possible free-living lifestyle	Narasingarao *et al.* (2012)
"*Candidatus* Nanosalinarum" sp. J07AB56	"*Candidatus* Nanohaloarchaeota"	hypersaline lake	cocci-like	0.6 μm	1.22	possible free-living lifestyle	Narasingarao *et al.* (2012)
ARMAN-2, -4, and -5	"*Candidatus* Micrarchaeota"	acid mine drainage	cocci	~0.5 μm	~1.0	potential interaction with *Thermoplasmatales* cells via pili-like structures	Baker *et al.* (2010)
"*Candidatus* Mancarchaeum acidiphilum" Mia14	"*Candidatus* Micrarchaeota"	acid mine drainage	n.d.	n.d.	0.95	ectoparasite of *Cuniculiplasma divulgatum*	Golyshina *et al.* (2017)

n.d.: no data.
* The proteobacterial class *Oligoflexia* is classified in the candidate phylum "Bdellovibrionota" in the Genome Taxonomy Database (GTDB).
** Putative physiological traits are inferred from their genomic and plasmid annotation.

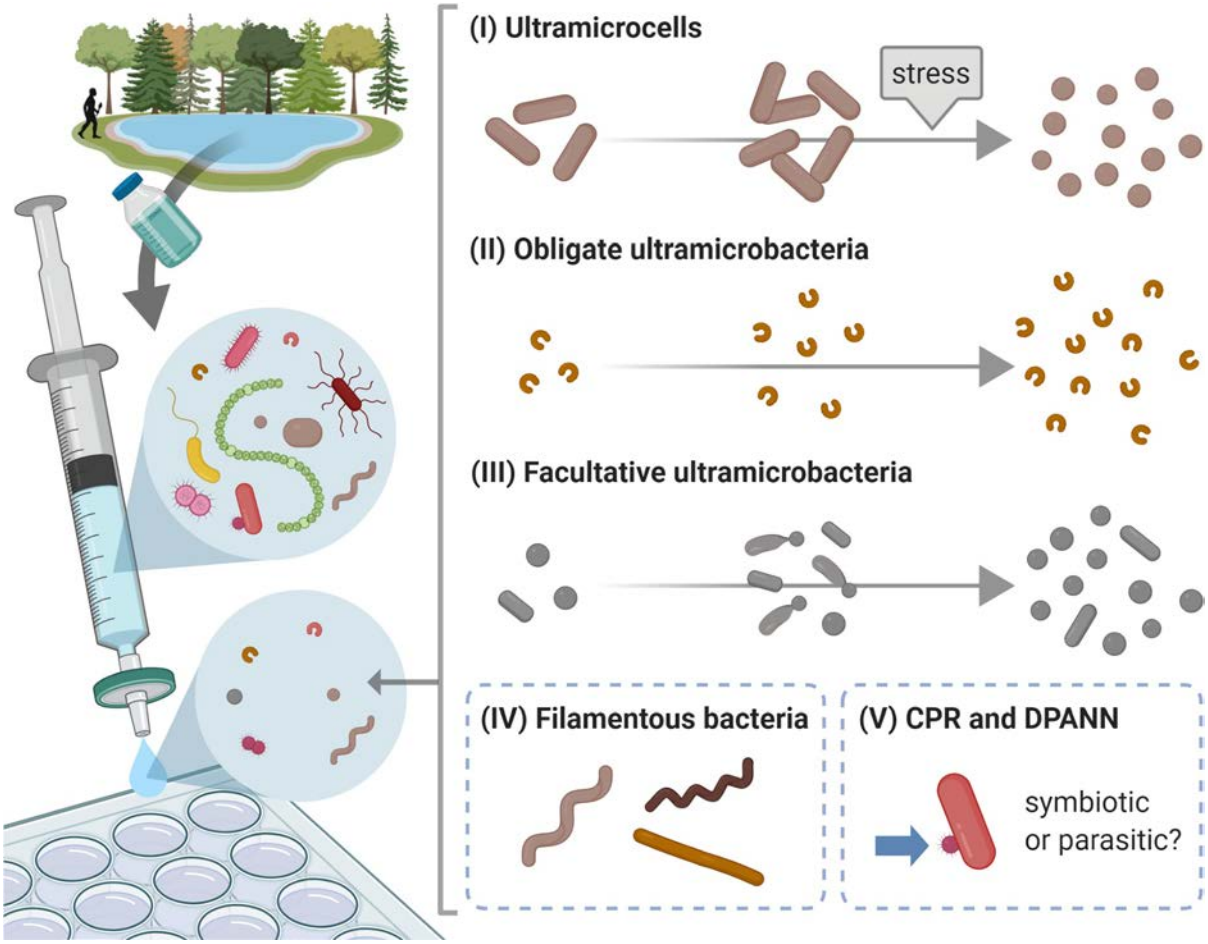

Fig. 1. Diagram showing filterable microorganisms in the environment. (I) ultramicrocells; (II) obligate ultramicrobacteria; (III) facultative ultramicrobacteria; (IV) slender filamentous bacteria; (V) ultra-small members of CPR bacteria (also referred to as "*Candidatus* Patescibacteria") and DPANN archaea indicated by the arrow in this Figure. See details in the text. This figure was created with BioRender (https://biorender.com/).

Other prominent representatives of obligate UMB are freshwater actinobacterial strains. Typically, actinobacteria are among the numerically dominant groups in freshwater and their cells are found in smaller size fractions (Glöckner *et al.*, 2000; Sekar *et al.*, 2003). Hahn *et al.* (2003) first isolated nine filterable UMB of the class *Actinobacteria* from freshwater habitats and newly described a novel phylogenetic cluster (Luna cluster). This isolation was achieved by the "filtration-acclimatization" method of filter separation combined with an acclimatization procedure, which is a stepwise transition from low substrate conditions to artificial culture conditions. The important features of Luna cluster strains are their wide distribution in freshwater systems (Hahn and Pöckl, 2005) and their small cell sizes are stable and maintained in nutrient-rich media (Hahn *et al.*, 2003). Our group also isolated an ultamicrosize actinobacterium related to Luna strains from river water in Japan and named it *Aurantimicrobium minutum* KNC^{T} (Fig. 2; Nakai *et al.*, 2015). This strain showed high 16S rRNA gene sequence similarity (>99%) to strains isolated from freshwater systems in other places in Japan as well as in Austria, Australia, China, Nicaragua, and Uganda (accession nos. AB278121, AB599783, AJ507461, AJ507467, AJ565412, AJ565413, and AJ630367), suggesting its cosmopolitan distribution in freshwater.

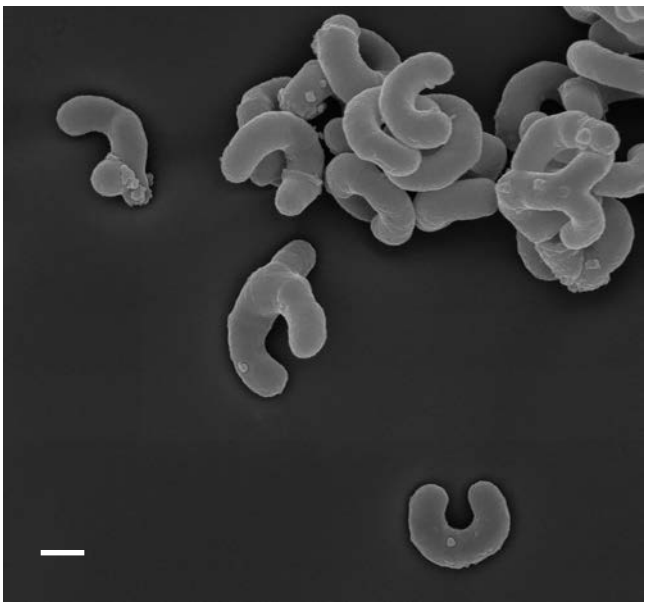

Fig. 2. Scanning electron micrograph of c-shaped cells of *Aurantimicrobium minutum* KNC^{T}. Cells were cultured in organic NSY (nutrient broth, soytone, and yeast extract; Hahn *et al.*, 2004) medium for two weeks. Scale bar: 200 nm. This micrograph is an unpublished figure from the author; other micrographs of this species are shown in Nakai *et al.* (2013, 2015).

The other freshwater bacterium belonging to the Luna cluster, *Rhodoluna lacicola* MWH-Ta8^T, was also described as an obligate UMB (Hahn *et al.*, 2014); an additional three *Rhodoluna* strains smaller than *R. lacicola* were subsequently reported (Pitt *et al.*, 2019). From an ecophysiological point of view, the genomes of freshwater actinobacteria possess rhodopsin photosystems (Neuenschwander *et al.*, 2018), while *R. lacicola* has an unconventional proton-pumping rhodopsin that requires external supplementation with the cofactor retinal (Keffer *et al.*, 2015). The underlying cause is considered to be an inability to biosynthesize the cofactor (Neuenschwander *et al.*, 2018), suggesting that *R. lacicola* obtains retinal from the surrounding environment. One potential source in freshwater appears to be retinoids produced and released by cyanobacteria (Ruch *et al.*, 2005; Wu *et al.*, 2013).

Freshwater actinobacteria, including UMB strains, were previously shown to be phylogenetically diverse and subsequent studies yielded nine lineages (acI, acTH1, acSTL, Luna1, acIII, Luna3, acTH2, acIV, and acV; Newton *et al.*, 2011). Among these lineages, acI containing multiple tribes is considered to be the most successful and ubiquitous group in the environment (Zwart *et al.*, 2002; Warnecke *et al.*, 2004; Kang *et al.*, 2017), although pure cultures had not been established despite various cultivation trials. However, Kim *et al.* (2019) recently reported the first two pure acI cultures with very small sizes (volume, 0.04–0.06 μm^3; Table 1), which are assumed to be obligate UMB. A key factor for their growth was the supplementation of a "helper" catalase, an enzyme that degrades hydrogen peroxide (H_2O_2), to the culture medium. Previous studies showed that H_2O_2 generated in medium affected the culture efficiency of microorganisms sensitive to oxidative stress (Kawasaki and Kamagata, 2017) and that the growth of the cyanobacterium *Prochlorococcus* was promoted by the presence of H_2O_2-scavenging microbes (Morris *et al.*, 2011). These findings demonstrated that a catalase-supplemented cultivation strategy may facilitate the successful isolation of previously uncultured freshwater UMB.

Freshwater habitats also harbor another obligate UMB belonging to the genus *Polynucleobacter* in the class *Betaproteobacteria*. Similar to some actinobacteria described earlier, UMB members of this genus also showed a cosmopolitan distribution in freshwater systems (Hahn, 2003). The relative abundance of the subspecies named PnecC was high, ranging between <1% and 67% (average 14.5%) of total bacterial numbers, in more than 130 lakes studied in Central Europe, as assessed by fluorescent *in situ* hybridization (Jezberová *et al.*, 2010). Culture experiments and genomic characterization suggested that PnecC bacteria in nature can utilize low-molecular-weight products derived from photooxidation and/or the direct enzymatic cleavage of high-molecular-weight substrates, such as humic substances (Watanabe *et al.*, 2009; Hahn *et al.*, 2012). Certain PnecC strains sharing ≥99% similarity in 16S rRNA gene sequences differed in their ecophysiological and genomic features (*e.g.*, the presence/absence of iron transporter genes), suggesting cryptic diversity among the abundant lineage not covered by 16S rRNA gene-based typing (Hahn *et al.*, 2016).

The obligate UMB inhabiting sea and freshwaters described above were characterized by minute cell sizes, but also small genome sizes (<2 Mbp) with a low genomic guanine-cytosine (GC) content: this genome "streamlining" is considered to reflect an adaptation to nutrient-limited conditions (*e.g.*, SAR11 members; 1.16–1.46 Mb; Giovannoni *et al.*, 2005; Grote *et al.*, 2012; Henson *et al.*, 2018) (Table 1). This phenomenon of a reduced genome size with gene loss also indicates metabolic dependencies on co-existing microorganisms in nature, as described by the "Black Queen Hypothesis" (Morris *et al.*, 2012). As another example, the reconstructed genomes of ultra-small and uncultivated marine actinobacteria ("*Candidatus* Actinomarinidae") were very small (<1 Mb) and had a very low GC content of 33% (Ghai *et al.*, 2013). In addition, known obligate UMB of different lineages, such as "*Ca.* P. ubique" (*Alphaproteobacteria*), *Polynucleobacter* strains (*Betaproteobacteria*), and *A. minutum* and *R. lacicola* (*Actinobacteria*), showed similar "c-shaped" (curved-rod) cells (Table 1; *A. minutum* for Fig. 2; Hahn, 2003). This unique shape may be advantageous for the efficient acquisition of substances because of their increased surface-to-volume ratio of cells or grazing resistance against bacteriovorus protists for planktonic life in waters.

In contrast to aquatic environments, limited information is currently available on UMB, including the obligate type, from soil habitats. Janssen *et al.* (1997) previously reported anaerobic obligate UMB with very small ellipsoid to nearly spherical shapes (*e.g.*, *Opitutus* sp. VeCb1 with a cell volume of 0.030 μm^3) belonging to the *Verrucomicrobiales* lineage from rice paddy soil using dilution culture techniques. Nakai *et al.* (2013) isolated and cultivated filterable strains from soil and sand suspensions; however, obligate UMB were not found among these strains. High-throughput sequencing of the 16S rRNA gene revealed that the smaller size fractions in soils were more likely to harbor rare or poorly characterized bacterial and archaeal taxa, such as *Acidobacteria*, *Gemmatimonadetes*, *Elusimicrobia*, *Verrucomicrobia*, and *Crenarchaeota* (Portillo *et al.*, 2013). However, further studies are needed to clarify whether the members detected in the small fractions contain UMB.

Facultative UMB

Facultative UMB that contain a small proportion of larger cells with a cell volume >0.1 μm^3 have not yet been characterized in detail (Table 1) because morphological changes throughout the growth cycle have only been examined in a limited number of UMB. *Endomicrobium proavitum* Rsa215 (now deposited as DSM29378^T=JCM32103^T) belonging to the phylum *Elusimicrobia* appears to be a well-studied example of facultative UMB. The phylum *Elusimicrobia* (former termite group 1 candidate phylum) was initially established with the cultivated ultramicrobacterium of *Elusimicrobium minutum* strain Pei191^T from the 0.2 μm-filtered filtrate—originally prepared as a growth promoting supplement for gut bacteria—of the gut homogenates of a scarab beetle larva (Geissinger *et al.*, 2009; Herlemann *et al.*, 2009). *E. proavitum* Rsa215 was isolated from the filtrate of the gut homogenate and was identified as a free-

living bacterium of a novel class-level lineage in *Elusimicrobia* (Zheng *et al.*, 2016). *E. proavitum* has an unusual cell cycle that involves different cell forms, *i.e.*, cocci, rods, and budding-like cells, during the cell cycle. Under laboratory cultivation conditions, before growth commences, the cell population is comprised of a large population of UMB coccoid cells with a few rod-shaped cells (~3.5 μm in length); small cocci are formed from a bud-like swelling at one pole of the rod-shaped cells during growth. Although its morphological variation in the host gut currently remains unclear, cell characteristics as observed in the laboratory result in the classification of facultative UMB. Another important trait for *E. proavitum* is the ability to fix nitrogen gas with a group IV nitrogenase, which was considered to harbor functions other than nitrogen fixation (Dos Santos *et al.*, 2012).

Slender filamentous bacteria

In addition to ultramicrocells and UMB, slender filamentous bacteria have frequently been found in 0.2 μm-filtered fractions of environmental samples. Slender spirillum-shaped *Hylemonella gracilis* was isolated from filtrates of freshwater samples (*e.g.*, Hahn *et al.*, 2004; Nakai *et al.*, 2013) and passes through membrane filters with small pore sizes of not only 0.22–0.45 μm, but also 0.1 μm (Wang *et al.*, 2007). The smallest widths of *H. gracilis* cells are approximately 0.2 μm and close to filter pore sizes, which may allow its slender cells to "squeeze" through these pores. Regarding the quality control and assessment of filter sterilization, Wang *et al.* (2008) proposed that filterable slender bacteria, such as *H. gracilis* with small cell widths, may be used for the microbiological validation of membrane filters instead of *Brevundimonas diminuta*, which is the current standard strain tested.

During a screening of UMB, our group isolated a slender filamentous bacterium from the filtrate of a suspension of desert sands collected in Tunisia, and described *Oligoflexus tunisiensis* Shr3^T, which represents the eighth novel class named *Oligoflexia* within the phylum *Proteobacteria* (Nakai *et al.*, 2014; 2016a). The cell shape of this species is mainly slender, filamentous, and of variable lengths, but shows a pleomorphism with other shapes, such as a spiral, spherical (or curled), or curved rod morphology (Fig. 3; Nakai and Naganuma, 2015). This polymorphic flexibility of cells with small widths down to 0.4 μm appears to be related to their ability to pass through membrane filters; however, it has not yet been clarified whether each morphological shape is associated with a resting state or other states. Regarding filamentous formation, this shape may be related to resistance to protozoan grazing, as reported in previous studies (*e.g.*, Jürgens *et al.*, 1999; Suzuki *et al.*, 2017a). The environmental sequences closely related (>97%) to the 16S rRNA gene sequence of *O. tunisiensis* were recovered from paddy soil, cyanobacterial bloom in lake water, bioreactors, and human skin using culture-independent approaches; however, their detection frequency was low, with at most ~0.6% (Nakai and Naganuma, 2015). Thus, *O. tunisiensis* and its relatives appear to be rare species, and their ecological roles are currently unclear; one possible role for *O. tunisiensis* may be incomplete denitrification to nitrous oxide, as inferred from its genome sequence (Nakai *et al.*, 2016a).

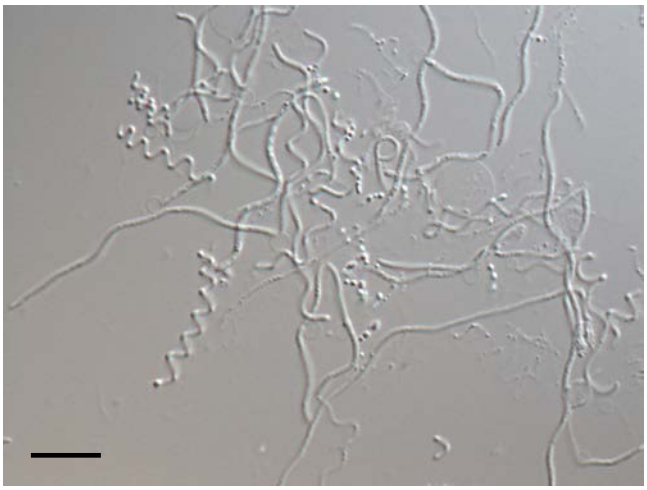

Fig. 3. Micrograph of pleomorphic cells of *Oligoflexus tunisiensis* Shr3^T. Cells were cultured in R2A medium for more than two weeks. This micrograph is slightly modified from the figure originally published in Nakai and Naganuma (2015). Scale bar: 10 μm.

Despite the potential rarity of its occurrence, the size filtration method led to the isolation of an additional slender filamentous strain, *Silvanigrella aquatica* MWH-Nonnen-W8red^T, with a pleomorphic morphology in the class (Hahn *et al.*, 2017). Hahn *et al.* (2017) reclassified the order *Bdellovibrionales*, including *Bdellovibrio* spp. known as small "bacteria-eating" bacteria (reviewed in Sockett, 2009), from the class *Deltaproteobacteria* to the class *Oligoflexia* based on in-depth phylogenetic analyses. Incidentally, 0.45-μm filtrates of environmental samples are frequently used for the enrichment culture of *Bdellovibrio* predatory bacteria. In the Genome Taxonomy Database (GTDB) based on genome phylogeny (https://gtdb.ecogenomic.org/; Parks *et al.*, 2018), the class *Oligoflexia* belongs to the candidate phylum "Bdellovibrionota", named after the genus *Bdellovibrio*, and not the phylum *Proteobacteria*; its taxonomic assignment will be discussed in future studies. *Oligoflexia* very recently gained two more species, *Fluviispira multicolorata* 33A1-SZDP^T and *Silvanigrella paludirubra* SP-Ram-0.45-NSY-1^T, from freshwater habitats (Pitt *et al.*, 2020). *Silvanigrella* spp. are phylogenetically closely aligned with "*Candidatus* Spirobacillus cienkowskii" (Pitt *et al.*, 2020), which is an uncultured pathogen of water fleas (*Daphnia* spp.) described morphologically almost 130 years ago (Metchnikoff, 1889). Since *Silvanigrella* spp. are isolated from the filtrates of micropore filtration, size fractionation may be an effective method for isolating the uncultivated pathogen as well as additionally overlooked agents in *Oligoflexia*. A detailed comparison within members of this class will also be important for pursuing the evolutionary acquisition and divergence of predatory and pathogenic behaviors.

Diverse ultra-small members and their potentials

Metagenomic investigations on microbial communities have generated genomes for an astounding diversity of bac-

teria and archaea; CPR/Patescibacteria inhabiting groundwater has attracted increasing attention in recent years. Traditionally, certain types of groundwater bacteria were known to pass through a micropore filter (*e.g.*, Shirey and Bissonnette, 1991). Additionally, Miyoshi *et al.* (2005) phylogenetically characterized filterable microorganisms captured by 0.1-μm-pore-sized filters from deep aquifers of the Tono uranium mine, Japan and then discovered candidate divisions OD1 and OP11 (now recognized as candidate phyla "*Ca.* Parcubacteria" and "*Ca.* Microgenomates", respectively) enriched by approximately 44% in 16S rRNA gene clones from the filtered fraction. The specific occurrence of "*Ca.* Parcubacteria" (OD1) in the 0.2-μm filtrate was also detected in deep-sea hydrothermal fluid (Naganuma *et al.*, 2007). It was previously unclear whether members of these candidate divisions were UMB. In subsequent studies using cryo-imaging, ultra-small cells (approximately 0.009±0.002 μm^3) were reported in the filtrate of an aquifer water near Colorado, USA, which were enriched with the candidate divisions WWE3, OD1, and OP11, all recently belonging to CPR/Patescibacteria (Luef *et al.*, 2015).

Metagenomics was then used to reconstruct the genomes of filterable members in the aquifer system, representing >35 candidate phyla named CPR (Brown *et al.*, 2015). This highly diversified group of uncultivated bacteria may subdivide the domain *Bacteria* (Hug *et al.*, 2016); however, this scenario remains controversial (*e.g.*, Parks *et al.*, 2018; Zhu *et al.*, 2019). Importantly, measurements of replication rates (Brown *et al.*, 2016; Suzuki *et al.*, 2017b) and cryo-transmission electron microscopy images showing a dividing cell (Luef *et al.*, 2015) indicated that the extremely small cells of CPR/Patescibacteria are metabolically active and not simply ultramicrocells during starvation. Moreover, CPR/Patescibacteria genomes have been recovered from other environments, such as highly alkaline groundwater (Suzuki *et al.*, 2017b; Sato *et al.*, 2019), lakes (Vigneron *et al.*, 2019), soil (Starr *et al.*, 2018), and marine sediment (Orsi *et al.*, 2018) as well as the human microbiome (He *et al.*, 2015) and dolphin mouse (Dudek *et al.*, 2017), suggesting a wide distribution across environments. Besides describing ultra-small life forms with high phylogenetic novelty, genomic analyses of CPR/Patescibacteria members have provided information on their small genomes, fermentative metabolism, and other unusual features (*e.g.*, self-splicing introns varying in length and proteins encoded within their 16S rRNA genes; Brown *et al.*, 2015; Castelle *et al.*, 2018). Divergent 16S rRNA gene sequences prevent many specific phyla (*e.g.*, ~50% of "*Ca.* Microgenomates" [OP11] and 60% of candidate division WWE3) from being detected by typical PCR surveys with the universal bacterial primer set 515F and 806R (Brown *et al.*, 2016). The small genome sizes observed (often <1 Mb) appear to be a reflection of a symbiotic lifestyle and/or high *in situ* selection pressure in a stable environment, rather than the genome streamlining of free-living obligate UMB, as described earlier, assuming streamlining characteristics (*e.g.*, highly conserved core genomes with few pseudogenes; Giovannoni *et al.*, 2014). Although the CPR/Patescibacteria genomes studied to date possess incomplete biosynthetic pathways for their cellular building blocks (*e.g.*, nucleotides and fatty acids; Castelle *et al.*, 2018), the possibility of their ability to *de novo* synthesize them by unknown pathways cannot be ruled out. Furthermore, their host-associated distribution was reported: "*Candidatus* Sonnebornia yantaiensis" of "*Ca.* Parcubacteria" (OD1) as an endoplasmic symbiont of the protist (Gong *et al.*, 2014) and TM7x bacterium of "*Ca.* Saccharibacteria" (TM7) attached to *Actinomyces odontolyticus* (He *et al.*, 2015), as shown in Table 1.

The features of small cell sizes and small genomes observed in CPR/Patescibacteria are shared by some members of the DPANN archaea, particularly *Nanoarchaeota* (Huber *et al.*, 2002), "*Ca.* Nanohalorchaeota" (Narasingarao *et al.*, 2012), and so-called ARMAN (archaeal Richmond Mine acidophilic nano-organisms; Baker *et al.*, 2010). DPANN including these UMA has been expanded by the addition of novel phylum-level groups, and, at the time of writing, encompasses at least ten different lineages (reviewed in Dombrowski *et al.*, 2019). In several cases, except for the members of "*Ca.* Nanohalorchaeota", as with CPR/Patescibacteria, DPANN-affiliated UMA showed an ectosymbiotic localization: *Nanoarchaeum equitans* attached to *Ignicoccus hospitalis* (Huber *et al.*, 2002), "*Ca.* Nanopusillus acidilobi" and its host *Acidilobus* species (Wurch *et al.*, 2016), and "*Ca.* Mancarchaeum acidiphilum" Mia14 (ARMAN-2-related organism) and its host *Cuniculiplasma divulgatum* (Golyshina *et al.*, 2017) (other data in Table 1). Additionally, DPANN organisms lack the ability to biosynthesize their building blocks (Castelle *et al.*, 2018). Although it is still unclear whether these symbiotic or parasitic lifestyles represent a way of life for the CPR/Patescibacteria and DPANN groups, the cases described above indicate that several members of these groups appear to be important in organism-organism interactions.

The characterization of ultra-small life forms may provide a new perspective for minimal cells and synthetic cells. In the field of synthetic biology, the top-down approach has been employed to reduce and simplify the genomes of microbial cells by genetic engineering, and then to identify essential genes for living systems; the bottom-up approach, which is the opposite of the top-down approach, has been used to examine what is sufficient for living systems by assembling non-living components, such as nucleic acids, proteins, and lipids (*e.g.*, Matsuura *et al.*, 2011; Xu *et al.*, 2016). In this context, DeWall and Cheng (2011) pointed out that the small genomes of microorganisms in nature may be models for the identification of a minimal genome. Since the ultra-small members described here as well as free-living obligate UMB already harbor small and sometimes streamlined genome structures (<2 Mb) through the loss of unnecessary components, the "middle-out" approach, referring to the metabolic pathway of these members (Fig. 4), which effectively combines traditional top-down and bottom-up approaches, will be useful for the rational design of artificial cells.

Conclusions

Numerous cultivation efforts have clearly shown that some previously uncultured members remain viable in

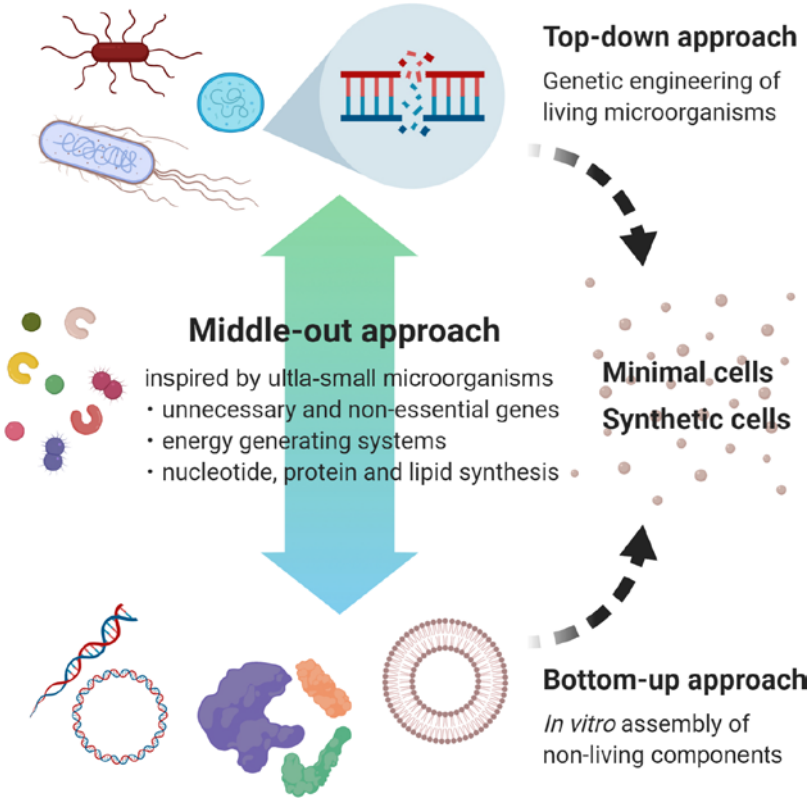

Fig. 4. A schematic diagram of the "middle-out" approach toward the development of minimal cells or synthetic cells. This approach, inspired by the unusual biology of ultra-small life forms, may provide a new perspective to traditional top-down or bottom-up approaches. This figure was created with BioRender (https://biorender.com/).

small-size fractions. Some obligate UMB are ubiquitous and dominant in water systems and may play important roles in natural microbiome functions. In parallel, the advent of high-throughput sequencing technology has greatly expanded our knowledge of ultra-small microbial diversity. Future studies are required to shed light on small microorganisms hidden in various environmental samples (*e.g.*, soils and sediments) other than aqueous environments, and on the ecophysiological traits and biogeochemical roles of these members, including CPR/Patescibacteria and DPANN. Further studies on "extreme" microorganisms at the lower size limit will undoubtedly lead to new conundrums about life on Earth.

Acknowledgement

I would like to thank Dr. K. Takai (JAMSTEC) and one anonymous reviewer for their helpful comments and suggestions on an earlier draft of this review.

References

Anderson, J.I.W., and Heffernan, W.P. (1965) Isolation and characterization of filterable marine bacteria1. *J Bacteriol* **90**: 1713–1718.

Baker, B.J., Comolli, L.R., Dick, G.J., Hauser, L.J., Hyatt, D., Dill, B.D., *et al.* (2010) Enigmatic, ultrasmall, uncultivated Archaea. *Proc Natl Acad Sci U S A* **107**: 8806–8811.

Brown, C.T., Hug, L.A., Thomas, B.C., Sharon, I., Castelle, C.J., Singh, A., *et al.* (2015) Unusual biology across a group comprising more than 15% of domain Bacteria. *Nature* **523**: 208–211.

Brown, C.T., Olm, M.R., Thomas, B.C., and Banfield, J.F. (2016) Measurement of bacterial replication rates in microbial communities. *Nat Biotechnol* **34**: 1256–1263.

Castelle, C.J., Brown, C.T., Anantharaman, K., Probst, A.J., Huang, R.H., and Banfield, J.F. (2018) Biosynthetic capacity, metabolic variety and unusual biology in the CPR and DPANN radiations. *Nat Rev Microbiol* **16**: 629–645.

Chin, K.J., Liesack, W., and Janssen, P.H. (2001) *Opitutus terrae* gen. nov., sp. nov., to accommodate novel strains of the division '*Verrucomicrobia*' isolated from rice paddy soil. *Int J Syst Evol Microbiol* **51**: 1965–1968.

Connon, S.A., and Giovannoni, S.J. (2002) High-throughput methods for culturing microorganisms in very-low-nutrient media yield diverse new marine isolates. *Appl Environ Microbiol* **68**: 3878.

Danczak, R.E., Johnston, M.D., Kenah, C., Slattery, M., Wrighton, K.C., and Wilkins, M.J. (2017) Members of the Candidate Phyla Radiation are functionally differentiated by carbon- and nitrogen-cycling capabilities. *Microbiome* **5**: 112.

DeWall, M.T., and Cheng, D.W. (2011) The minimal genome—a metabolic and environmental comparison. *Briefings Funct Genomics* **10**: 312–315.

Dombrowski, N., Lee, J.-H., Williams, T.A., Offre, P., and Spang, A. (2019) Genomic diversity, lifestyles and evolutionary origins of DPANN archaea. *FEMS Microbiol Lett* **366**: fnz008.

Dos Santos, P.C., Fang, Z., Mason, S.W., Setubal, J.C., and Dixon, R. (2012) Distribution of nitrogen fixation and nitrogenase-like sequences amongst microbial genomes. *BMC Genomics* **13**: 162.

Duda, V.I., Suzina, N.E., Polivtseva, V.N., and Boronin, A.M. (2012) Ultramicrobacteria: formation of the concept and contribution of ultramicrobacteria to biology. *Microbiology* **81**: 379–390.

Dudek, N.K., Sun, C.L., Burstein, D., Kantor, R.S., Aliaga Goltsman, D.S., Bik, E.M., *et al.* (2017) Novel microbial diversity and functional potential in the marine mammal oral microbiome. *Curr Biol* **27**: 3752–3762.e6.

Eguchi, M., Nishikawa, T., Macdonald, K., Cavicchioli, R., Gottschal, J.C., and Kjelleberg, S. (1996) Responses to stress and nutrient availability by the marine ultramicrobacterium *Sphingomonas* sp. strain RB2256. *Appl Environ Microbiol* **62**: 1287.

Elsaied, H.E., Sato, M., and Naganuma, T. (2001) Viable *Cytophaga*-like bacterium in the 0.2 μm-filtrate seawater. *Syst Appl Microbiol* **24**: 618–622.

Fedotova, A.V., Belova, S.E., Kulichevskaya, I.S., and Dedysh, S.N. (2012) Molecular identification of filterable bacteria and archaea in the water of acidic lakes of northern Russia. *Microbiology* **81**: 281–287.

Feil, H., Feil, W.S., Chain, P., Larimer, F., DiBartolo, G., Copeland, A., *et al.* (2005). Comparison of the complete genome sequences of *Pseudomonas syringae* pv. *syringae* B728a and pv. tomato DC3000. *Proc Natl Acad Sci U S A* **102**: 11064–11069.

Folk, R.L. (1999) Nannobacteria and the precipitation of carbonate in unusual environments. *Sediment Geol* **126**: 47–55.

Geissinger, O., Herlemann, D.P.R., Mörschel, E., Maier, U.G., and Brune, A. (2009) The ultramicrobacterium "*Elusimicrobium minutum*" gen. nov., sp. nov., the first cultivated representative of the termite group 1 phylum. *Appl Environ Microbiol* **75**: 2831.

Ghai, R., Mizuno, C.M., Picazo, A., Camacho, A., and Rodriguez-Valera, F. (2013) Metagenomics uncovers a new group of low GC and ultra-small marine Actinobacteria. *Sci Rep* **3**: 2471.

Ghuneim, L.-A.J., Jones, D.L., Golyshin, P.N., and Golyshina, O.V. (2018) Nano-sized and filterable bacteria and archaea: biodiversity and function. *Front Microbiol* **9**: 1971.

Giovannoni, S.J., Britschgi, T.B., Moyer, C.L., and Field, K.G. (1990) Genetic diversity in Sargasso Sea bacterioplankton. *Nature* **345**: 60–63.

Giovannoni, S.J., Tripp, H.J., Givan, S., Podar, M., Vergin, K.L., Baptista, D., *et al.* (2005) Genome streamlining in a cosmopolitan oceanic bacterium. *Science* **309**: 1242.

Giovannoni, S.J., Cameron Thrash, J., and Temperton, B. (2014) Implications of streamlining theory for microbial ecology. *ISME J* **8**: 1553–1565.

Giovannoni, S.J. (2017) SAR11 bacteria: the most abundant plankton in the oceans. *Ann Rev Mar Sci* **9**: 231–255.

Glöckner, F.O., Zaichikov, E., Belkova, N., Denissova, L., Pernthaler, J., Pernthaler, A., and Amann, R. (2000) Comparative 16S rRNA analysis of lake bacterioplankton reveals globally distributed phylogenetic clusters including an abundant group of actinobacteria. *Appl Environ Microbiol* **66**: 5053.

Golyshina, O.V., Toshchakov, S.V., Makarova, K.S., Gavrilov, S.N., Korzhenkov, A.A., La Cono, V., *et al.* (2017) 'ARMAN' archaea depend on association with euryarchaeal host in culture and in situ. *Nat Commun* **8**: 60.

Gong, J., Qing, Y., Guo, X., and Warren, A. (2014) "*Candidatus* Sonnebornia yantaiensis", a member of candidate division OD1, as intracellular bacteria of the ciliated protist *Paramecium bursaria* (Ciliophora, Oligohymenophorea). *Syst Appl Microbiol* **37**: 35–41.

Grote, J., Thrash, J.C., Huggett, M.J., Landry, Z.C., Carini, P., Giovannoni, S.J., and Rappé, M.S. (2012) Streamlining and core genome conservation among highly divergent members of the SAR11 clade. *mBio* **3**: e00252-12.

Hahn, M.W. (2003) Isolation of strains belonging to the cosmopolitan *Polynucleobacter necessarius* cluster from freshwater habitats located in three climatic zones. *Appl Environ Microbiol* **69**: 5248.

Hahn, M.W., Lünsdorf, H., Wu, Q., Schauer, M., Höfle, M.G., Boenigk, J., and Stadler, P. (2003) Isolation of novel ultramicrobacteria classified as actinobacteria from five freshwater habitats in Europe and Asia. *Appl Environ Microbiol* **69**: 1442.

Hahn, M.W., Stadler, P., Wu, Q.L., and Pöckl, M. (2004) The filtration–acclimatization method for isolation of an important fraction of the not readily cultivable bacteria. *J Microbiol Methods* **57**: 379–390.

Hahn, M.W., and Pöckl, M. (2005) Ecotypes of planktonic actinobacteria with identical 16S rRNA genes adapted to thermal niches in temperate, subtropical, and tropical freshwater habitats. *Appl Environ Microbiol* **71**: 766.

Hahn, M.W., Scheuerl, T., Jezberová, J., Koll, U., Jezbera, J., Šimek, K., *et al.* (2012) The passive yet successful way of planktonic life: genomic and experimental analysis of the ecology of a free-living polynucleobacter population. *PLoS One* **7**: e32772.

Hahn, M.W., Schmidt, J., Taipale, S.J., Doolittle, W.F., and Koll, U. (2014) *Rhodoluna lacicola* gen. nov., sp. nov., a planktonic freshwater bacterium with stream-lined genome. *Int J Syst Evol Microbiol* **64**: 3254–3263.

Hahn, M.W., Jezberová, J., Koll, U., Saueressig-Beck, T., and Schmidt, J. (2016) Complete ecological isolation and cryptic diversity in *Polynucleobacter* bacteria not resolved by 16S rRNA gene sequences. *ISME J* **10**: 1642–1655.

Hahn, M.W., Schmidt, J., Koll, U., Rohde, M., Verbarg, S., Pitt, A., *et al.* (2017) *Silvanigrella aquatica* gen. nov., sp. nov., isolated from a freshwater lake, description of *Silvanigrellaceae* fam. nov. and *Silvanigrellales* ord. nov., reclassification of the order *Bdellovibrionales* in the class *Oligoflexia*, reclassification of the families *Bacteriovoracaceae* and *Halobacteriovoraceae* in the new order *Bacteriovoracales* ord. nov., and reclassification of the family *Pseudobacteriovoracaceae* in the order *Oligoflexales*. *Int J Syst Evol Microbiol* **67**: 2555–2568.

Haller, C.M., Rölleke, S., Vybiral, D., Witte, A., and Velimirov, B. (2000) Investigation of 0.2 μm filterable bacteria from the Western Mediterranean Sea using a molecular approach: dominance of potential starvation forms. *FEMS Microbiol Ecol* **31**: 153–161.

He, X., McLean, J.S., Edlund, A., Yooseph, S., Hall, A.P., Liu, S.-Y., *et al.* (2015) Cultivation of a human-associated TM7 phylotype reveals a reduced genome and epibiotic parasitic lifestyle. *Proc Natl Acad Sci U S A* **112**: 244.

Henson, M.W., Lanclos, V.C., Faircloth, B.C., and Thrash, J.C. (2018) Cultivation and genomics of the first freshwater SAR11 (LD12) isolate. *ISME J* **12**: 1846–1860.

Herlemann, D.P.R., Geissinger, O., Ikeda-Ohtsubo, W., Kunin, V., Sun, H., Lapidus, A., *et al.* (2009) Genomic analysis of "*Elusimicrobium minutum*," the first cultivated representative of the phylum "*Elusimicrobia*" (formerly termite group 1). *Appl Environ Microbiol* **75**: 2841.

Huber, H., Hohn, M.J., Rachel, R., Fuchs, T., Wimmer, V.C., and Stetter, K.O. (2002) A new phylum of Archaea represented by a nanosized hyperthermophilic symbiont. *Nature* **417**: 63–67.

Hug, L.A., Baker, B.J., Anantharaman, K., Brown, C.T., Probst, A.J., Castelle, C.J., *et al.* (2016) A new view of the tree of life. *Nat Microbiol* **1**: 16048.

Janssen, P.H., Schuhmann, A., Mörschel, E., and Rainey, F.A. (1997) Novel anaerobic ultramicrobacteria belonging to the *Verrucomicrobiales* lineage of bacterial descent isolated by dilution culture from anoxic rice paddy soil. *Appl Environ Microbiol* **63**: 1382–1388.

Jezberová, J., Jezbera, J., Brandt, U., Lindström, E.S., Langenheder, S., and Hahn, M.W. (2010) Ubiquity of *Polynucleobacter necessarius* subsp. *asymbioticus* in lentic freshwater habitats of a heterogenous 2000 km^2 area. *Environ Microbiol* **12**: 658–669.

John, E.S., Liu, Y., Podar, M., Stott, M.B., Meneghin, J., Chen, Z., *et al.* (2019). A new symbiotic nanoarchaeote (*Candidatus* Nanoclepta minutus) and its host (*Zestosphaera tikiterensis* gen. nov., sp. nov.) from a New Zealand hot spring. *Syst Appl Microbiol* **42**: 94–106.

Jürgens, K., Pernthaler, J., Schalla, S., and Amann, R. (1999) Morphological and compositional changes in a planktonic bacterial community in response to enhanced protozoan grazing. *Appl Environ Microbiol* **65**: 1241–1250.

Kang, I., Kim, S., Islam, M.R., and Cho, J.C. (2017) The first complete genome sequences of the acI lineage, the most abundant freshwater *Actinobacteria*, obtained by whole-genome-amplification of dilution-to-extinction cultures. *Sci Rep* **7**: 42252.

Kawasaki, K., and Kamagata, Y. (2017) Phosphate-catalyzed hydrogen peroxide formation from agar, gellan, and κ-carrageenan and recovery of microbial cultivability via catalase and pyruvate. *Appl Environ Microbiol* **83**: e01366-17.

Keffer, J.L., Hahn, M.W., and Maresca, J.A. (2015) Characterization of an unconventional rhodopsin from the freshwater actinobacterium *Rhodoluna lacicola*. *J Bacteriol* **197**: 2704–2712.

Kim, S., Kang, I., Seo, J.-H., and Cho, J.-C. (2019) Culturing the ubiquitous freshwater actinobacterial acI lineage by supplying a biochemical 'helper' catalase. *ISME J* **13**: 2252–2263.

Kuhn, E., Ichimura, A.S., Peng, V., Fritsen, C.H., Trubl, G., Doran, P.T., and Murray, A.E. (2014) Brine assemblages of ultrasmall microbial cells within the ice cover of Lake Vida, Antarctica. *Appl Environ Microbiol* **80**: 3687.

Lannes, R., Olsson-Francis, K., Lopez, P., and Bapteste, E. (2019) Carbon fixation by marine ultrasmall prokaryotes. *Genome Biol Evol* **11**: 1166–1177.

Levy, R.V., and Jornitz, M.W. (2006) Types of filtration. In *Sterile Filtration*. Jornitz, M.W. (ed.) Berlin, Heidelberg: Springer, pp. 1–26.

Luef, B., Frischkorn, K.R., Wrighton, K.C., Holman, H.-Y.N., Birarda, G., Thomas, B.C., *et al.* (2015) Diverse uncultivated ultra-small bacterial cells in groundwater. *Nat Commun* **6**: 6372.

MacDonell, M.T., and Hood, M.A. (1982) Isolation and characterization of ultramicrobacteria from a Gulf Coast estuary. *Appl Environ Microbiol* **43**: 566.

Maejima, Y., Kushimoto, K., Muraguchi, Y., Fukuda, K., Miura, T., Yamazoe, A., *et al.* (2018) *Proteobacteria* and *Bacteroidetes* are major phyla of filterable bacteria passing through 0.22 μm pore size membrane filter, in Lake Sanaru, Hamamatsu, Japan. *Biosci Biotechnol Biochem* **82**: 1260–1263.

Martel, J., and Young, J.D.-E. (2008) Purported nanobacteria in human blood as calcium carbonate nanoparticles. *Proc Natl Acad Sci U S A* **105**: 5549.

Matsuura, T., Ichihashi, N., Sunami, T., Kita, H., Suzuki, H., and Yomo, T. (2011) Evolvability and self-replication of genetic information in liposomes. In *The Minimal Cell*. Luisi, P., and Stano, P. (eds). Dordrecht: Springer, pp. 275–287.

Meincke, L., Copeland, A., Lapidus, A., Lucas, S., Berry, K.W., Del Rio, T.G., *et al.* (2012) Complete genome sequence of *Polynucleobacter necessarius* subsp. *asymbioticus* type strain (QLW-P1DMWA-1^T). *Stand Genomic Sci* **6**: 74–83.

Metchnikoff, E. (1889) Contributions á l'etude du pleomorphisme des bacteriens. *Ann Inst Pasteur* **3**: 61–68.

Miteva, V.I., and Brenchley, J.E. (2005) Detection and isolation of ultrasmall microorganisms from a 120,000-year-old Greenland glacier ice core. *Appl Environ Microbiol* **71**: 7806.

Miyoshi, T., Iwatsuki, T., and Naganuma, T. (2005) Phylogenetic characterization of 16S rRNA gene clones from deep-groundwater microorganisms that pass through 0.2-micrometer-pore-size filters. *Appl Environ Microbiol* **71**: 1084.

Monier, J.-M., and Lindow, S.E. (2003) *Pseudomonas syringae* responds to the environment on leaves by cell size reduction. *Phytopathology* **93**: 1209–1216.

Moore, P.B. (1999) A biophysical chemist's thoughts on cell size. In *Size Limits of Very Small Microorganisms: Proceedings of a Workshop*. Washington, DC: National Academies Press, pp. 16–20.

Morris, J.J., Johnson, Z.I., Szul, M.J., Keller, M., and Zinser, E.R. (2011) Dependence of the cyanobacterium *Prochlorococcus* on hydrogen peroxide scavenging microbes for growth at the ocean's surface. *PLoS One* **6**: e16805.

Morris, J.J., Lenski, R.E., and Zinser, E.R. (2012) The Black Queen hypothesis: evolution of dependencies through adaptive gene loss. *mBio* **3**: e00036-12.

Morris, R.M., Rappé, M.S., Connon, S.A., Vergin, K.L., Siebold, W.A., Carlson, C.A., and Giovannoni, S.J. (2002) SAR11 clade dominates ocean surface bacterioplankton communities. *Nature* **420**: 806–810.

Naganuma, T., Miyoshi, T., and Kimura, H. (2007) Phylotype diversity of deep-sea hydrothermal vent prokaryotes trapped by 0.2- and 0.1-μm-pore-size filters. *Extremophiles* **11**: 637–646.

Nakai, R., Abe, T., Takeyama, H., and Naganuma, T. (2011) Metagenomic analysis of 0.2-μm-passable microorganisms in deep-sea hydrothermal fluid. *Mar Biotechnol* **13**: 900–908.

Nakai, R., Shibuya, E., Justel, A., Rico, E., Quesada, A., Kobayashi, F., *et al.* (2013) Phylogeographic analysis of filterable bacteria with special reference to *Rhizobiales* strains that occur in cryospheric habitats. *Antarct Sci* **25**: 219–228.

Nakai, R.*, Nishijima, M.*, Tazato, N., Handa, Y., Karray, F., Sayadi, S., *et al.* (*equal contribution) (2014) *Oligoflexus tunisiensis* gen. nov., sp. nov., a Gram-negative, aerobic, filamentous bacterium of a novel proteobacterial lineage, and description of *Oligoflexaceae* fam. nov., *Oligoflexales* ord. nov. and *Oligoflexia* classis nov. *Int J Syst Evol Microbiol* **64**: 3353–3359.

Nakai, R., Baba, T., Niki, H., Nishijima, M., and Naganuma, T. (2015) *Aurantimicrobium minutum* gen. nov., sp. nov., a novel ultramicrobacterium of the family *Microbacteriaceae*, isolated from river water. *Int J Syst Evol Microbiol* **65**: 4072–4079.

Nakai, R., and Naganuma, T. (2015) *Oligoflexia*, the newest class of the phylum *Proteobacteria*, consisting of only one cultured species and uncultured bacterial phylotypes from diverse habitats. *J Phylogenet Evol Biol* **3**: 141.

Nakai, R., Fujisawa, T., Nakamura, Y., Baba, T., Nishijima, M., Karray, F., *et al.* (2016a) Genome sequence and overview of *Oligoflexus tunisiensis* Shr3^T in the eighth class *Oligoflexia* of the phylum *Proteobacteria*. *Stand Genomic Sci* **11**: 90.

Nakai, R., Fujisawa, T., Nakamura, Y., Nishide, H., Uchiyama, I., Baba, T., *et al.* (2016b) Complete genome sequence of *Aurantimicrobium minutum* type Strain KNC^T, a planktonic ultramicrobacterium isolated from river water. *Genome Announc* **4**: e00616-16.

Narasingarao, P., Podell, S., Ugalde, J.A., Brochier-Armanet, C., Emerson, J.B., Brocks, J.J., *et al.* (2012) *De novo* metagenomic assembly reveals abundant novel major lineage of Archaea in hypersaline microbial communities. *ISME J* **6**: 81–93.

Neuenschwander, S.M., Ghai, R., Pernthaler, J., and Salcher, M.M. (2018) Microdiversification in genome-streamlined ubiquitous freshwater Actinobacteria. *ISME J* **12**: 185–198.

Newton, R.J., Jones, S.E., Eiler, A., McMahon, K.D., and Bertilsson, S. (2011) A guide to the natural history of freshwater lake bacteria. *Microbiol Mol Biol Rev* **75**: 14.

Obayashi, Y., and Suzuki, S. (2019) High growth potential of transiently 0.2-μm-filterable bacteria with extracellular protease activity in coastal seawater. *Plankton Benthos Res* **14**: 276–286.

Orsi, W.D., Richards, T.A., and Francis, W.R. (2018) Predicted microbial secretomes and their target substrates in marine sediment. *Nat Microbiol* **3**: 32–37.

Parks, D.H., Chuvochina, M., Waite, D.W., Rinke, C., Skarshewski, A., Chaumeil, P.-A., and Hugenholtz, P. (2018) A standardized bacterial taxonomy based on genome phylogeny substantially revises the tree of life. *Nat Biotechnol* **36**: 996–1004.

Pitt, A., Schmidt, J., Koll, U., and Hahn, M.W. (2019) *Rhodoluna limnophila* sp. nov., a bacterium with 1.4 Mbp genome size isolated from freshwater habitats located in Salzburg, Austria. *Int J Syst Evol Microbiol* **69**: 3946–3954.

Pitt, A., Koll, U., Schmidt, J., and Hahn, M.W. (2020) *Fluviispira multicolorata* gen. nov., sp. nov. and *Silvanigrella paludirubra* sp. nov., isolated from freshwater habitats. *Int J Syst Evol Microbiol* **70**: 1630–1638.

Portillo, M.C., Leff, J.W., Lauber, C.L., and Fierer, N. (2013) Cell size distributions of soil bacterial and archaeal taxa. *Appl Environ Microbiol* **79**: 7610.

Rappé, M.S., Connon, S.A., Vergin, K.L., and Giovannoni, S.J. (2002) Cultivation of the ubiquitous SAR11 marine bacterioplankton clade. *Nature* **418**: 630–633.

Rinke, C., Schwientek, P., Sczyrba, A., Ivanova, N.N., Anderson, I.J., Cheng, J.-F., *et al.* (2013) Insights into the phylogeny and coding potential of microbial dark matter. *Nature* **499**: 431–437.

Ruch, S., Beyer, P., Ernst, H., and Al-Babili, S. (2005) Retinal biosynthesis in Eubacteria: *in vitro* characterization of a novel carotenoid oxygenase from *Synechocystis* sp. PCC 6803. *Mol Microbiol* **55**: 1015–1024.

Sato, T., Yoshiya, K., and Maruyama, S. (2019) History of the Hadean "Living Microfossil" OD1 and ultra-reducing environments. *J Geogr (Tokyo, Japan)* **128**: 571–596.

Schulz, H.N., Brinkhoff, T., Ferdelman, T.G., Mariné, M.H., Teske, A., and Jørgensen, B.B. (1999) Dense populations of a giant sulfur bacterium in Namibian shelf sediments. *Science* **284**: 493.

Schulz, H.N., and Jørgensen, B.B. (2001) Big bacteria. *Annu Rev Microbiol* **55**: 105–137.

Schut, F., Gottschal, J.C., and Prins, R.A. (1997) Isolation and characterisation of the marine ultramicrobacterium *Sphingomonas* sp. strain RB2256. *FEMS Microbiol Rev* **20**: 363–369.

Sekar, R., Pernthaler, A., Pernthaler, J., Warnecke, F., Posch, T., and Amann, R. (2003) An improved protocol for quantification of freshwater *Actinobacteria* by fluorescence in situ hybridization. *Appl Environ Microbiol* **69**: 2928.

Shirey, J.J., and Bissonnette, G.K. (1991) Detection and identification of groundwater bacteria capable of escaping entrapment on 0.45-micron-pore-size membrane filters. *Appl Environ Microbiol* **57**: 2251.

Sockett, R.E. (2009) Predatory lifestyle of *Bdellovibrio bacteriovorus*. *Annu Rev Microbiol* **63**: 523–539.

Starr, E.P., Shi, S., Blazewicz, S.J., Probst, A.J., Herman, D.J., Firestone, M.K., and Banfield, J.F. (2018) Stable isotope informed genome-resolved metagenomics reveals that *Saccharibacteria* utilize microbially-processed plant-derived carbon. *Microbiome* **6**: 122.

Suzina, N.E., Duda, V.I., Esikova, T.Z., Shorokhova, A.P., Gafarov, A.B., Oleinikov, R.R., *et al.* (2011) Novel ultramicrobacteria, strains NF4 and NF5, of the genus *Chryseobacterium*: Facultative epibionts of *Bacillus subtilis*. *Microbiology* **80**: 535.

Suzuki, K., Yamauchi, Y., and Yoshida, T. (2017a) Interplay between microbial trait dynamics and population dynamics revealed by the combination of laboratory experiment and computational approaches. *J Theor Biol* **419**: 201–210.

Suzuki, S., Ishii, S., Hoshino, T., Rietze, A., Tenney, A., Morrill, P.L., *et al.* (2017b) Unusual metabolic diversity of hyperalkaliphilic microbial communities associated with subterranean serpentinization at The Cedars. *ISME J* **11**: 2584–2598.

Torrella, F., and Morita, M.Y. (1981) Microcultural study of bacterial size changes and microcolony and ultramicrocolony formation by heterotrophic bacteria in seawater. *Appl Environ Microbiol* **41**: 518.

Tripp, H.J. (2013) The unique metabolism of SAR11 aquatic bacteria. *J Microbiol* **51**: 147–153.

Vancanneyt, M., Schut, F., Snauwaert, C., Goris, J., Swings, J., and Gottschal, J.C. (2001) *Sphingomonas alaskensis* sp. nov., a dominant bacterium from a marine oligotrophic environment. *Int J Syst Evol Microbiol* **51**: 73–79.

Vigneron, A., Cruaud, P., Langlois, V., Lovejoy, C., Culley, A.I., and Vincent, W.F. (2019) Ultra-small and abundant: Candidate phyla radiation bacteria are potential catalysts of carbon transformation in a thermokarst lake ecosystem. *Limnol Oceanogr Lett* **5**:212–220.

Wang, Y., Hammes, F., Boon, N., and Egli, T. (2007) Quantification of the filterability of freshwater bacteria through 0.45, 0.22, and 0.1 µm pore size filters and shape-dependent enrichment of filterable bacterial communities. *Environ Sci Technol* **41**: 7080–7086.

Wang, Y., Hammes, F., Düggelin, M., and Egli, T. (2008) Influence of size, shape, and flexibility on bacterial passage through micropore membrane filters. *Environ Sci Technol* **42**: 6749–6754.

Warnecke, F., Amann, R., and Pernthaler, J. (2004) Actinobacterial 16S rRNA genes from freshwater habitats cluster in four distinct lineages. *Environ Microbiol* **6**: 242–253.

Watanabe, K., Komatsu, N., Ishii, Y., and Negishi, M. (2009) Effective isolation of bacterioplankton genus *Polynucleobacter* from freshwater environments grown on photochemically degraded dissolved organic matter. *FEMS Microbiol Ecol* **67**: 57–68.

Watson, S.P., Clements, M.O., and Foster, S.J. (1998) Characterization of the starvation-survival response of *Staphylococcus aureus*. *J Bacteriol* **180**: 1750–1758.

Wu, X., Jiang, J., and Hu, J. (2013) Determination and occurrence of retinoids in a eutrophic lake (Taihu Lake, China): cyanobacteria blooms produce teratogenic retinal. *Environ Sci Technol* **47**: 807–814.

Wurch, L., Giannone, R.J., Belisle, B.S., Swift, C., Utturkar, S., Hettich, R.L., *et al.* (2016) Genomics-informed isolation and characterization of a symbiotic Nanoarchaeota system from a terrestrial geothermal environment. *Nat Commun* **7**: 12115.

Xu, C., Hu, S., and Chen, X. (2016) Artificial cells: from basic science to applications. *Mater Today (Oxford, U K)* **19**: 516–532.

Zheng, H., and Brune, A. (2015). Complete genome sequence of *Endomicrobium proavitum*, a free-living relative of the intracellular symbionts of termite gut flagellates (phylum *Elusimicrobia*). *Genome Announc* **3**: e00679-15.

Zheng, H., Dietrich, C., Radek, R., and Brune, A. (2016) *Endomicrobium proavitum*, the first isolate of *Endomicrobia* class. nov. (phylum *Elusimicrobia*)—an ultramicrobacterium with an unusual cell cycle that fixes nitrogen with a Group IV nitrogenase. *Environ Microbiol* **18**: 191–204.

Zhu, Q., Mai, U., Pfeiffer, W., Janssen, S., Asnicar, F., Sanders, J.G., *et al.* (2019) Phylogenomics of 10,575 genomes reveals evolutionary proximity between domains Bacteria and Archaea. *Nat Commun* **10**: 5477.

Zwart, G., Crump, B.C., Kamst-van Agterveld, M.P., Hagen, F., and Han, S.-K. (2002) Typical freshwater bacteria: an analysis of available 16S rRNA gene sequences from plankton of lakes and rivers. *Aquat Microb Ecol* **28**: 141–155.

Microbes Environ. Vol. 32, No. 4, 300-313, 2017
https://www.jstage.jst.go.jp/browse/jsme2 doi:10.1264/jsme2.ME17017

Minireview

Microbial Ecology along the Gastrointestinal Tract

Ethan T. Hillman[1], Hang Lu[2], Tianming Yao[3], and Cindy H. Nakatsu[4]*

[1]*Department of Agricultural and Biological Engineering, Purdue University, West Lafayette, Indiana 47907, USA;* [2]*Department of Animal Science, Purdue University, West Lafayette, Indiana 47907, USA;* [3]*Department of Food Science, Purdue University, West Lafayette, Indiana 47907, USA; and* [4]*Department of Agronomy, Purdue University, West Lafayette, Indiana 47907, USA*

(Received January 31, 2017—Accepted August 19, 2017—Published online November 10, 2017)

The ecosystem of the human gastrointestinal (GI) tract traverses a number of environmental, chemical, and physical conditions because it runs from the oral cavity to the anus. These differences in conditions along with food or other ingested substrates affect the composition and density of the microbiota as well as their functional roles by selecting those that are the most suitable for that environment. Previous studies have mostly focused on *Bacteria*, with the number of studies conducted on *Archaea*, *Eukarya*, and *Viruses* being limited despite their important roles in this ecosystem. Furthermore, due to the challenges associated with collecting samples directly from the inside of humans, many studies are still exploratory, with a primary focus on the composition of microbiomes. Thus, mechanistic studies to investigate functions are conducted using animal models. However, differences in physiology and microbiomes need to be clarified in order to aid in the translation of animal model findings into the context of humans. This review will highlight *Bacteria*, *Archaea*, *Fungi*, and *Viruses*, discuss differences along the GI tract of healthy humans, and perform comparisons with three common animal models: rats, mice, and pigs.

Key words: Microbiome, mycobiome, virome, human gastrointestinal (GI) tract, animal models, diet

Researchers have been investigating the ecology of the intestinal microbiota for decades (120, 165) in order to identify, characterize, and count their numbers. These extensive efforts are due to the important roles the intestinal microbiota play in digestion, the production of essential vitamins, and protection of the gastrointestinal (GI) tract from pathogen colonization (141). In the past few decades, molecular techniques targeting the 16S rRNA gene and other genetic markers have been developed to characterize and analyze bacterial communities. These methods have been used to reveal the important roles played by microbes in the GI tract (23, 180, 183, 184, 189, 212). In healthy individuals, the microbiome (microbial community) and host have a mutualistic relationship in which both partners benefit; however, pathogens may invade and cause disease under certain conditions. The initial aim of most studies was to elucidate the role of the microbiome in disease. More recently, surveys have been performed on healthy individuals in order to assess the contribution of the microbiota to health, particularly in response to dietary changes/supplementation with probiotics and/or prebiotics.

The human GI tract is a complex system that starts from the oral cavity, continues through the stomach and intestines, and finally ends at the anus (Fig. 1). The density and composition of the microbiome change along the GI tract, with major populations being selected by the functions performed at the various locations. Bacteria along the GI tract have several possible functions, many of which are beneficial for health including vitamin production, the absorption of ions (Ca, Mg, and Fe), protection against pathogens, histological development, enhancement of the immune system, and the fermentation of "non-digestible foods" to short chain fatty acids (SCFA) and other metabolites (19, 58, 63, 77, 138). The roles of fungi and viruses have not been examined in as much detail; however, they are known to play important roles in microbiota dynamics and host physiology/immunity related to health and disease (45, 94, 133).

Food passes through the GI tract and the absorption rate of nutrients is largely dependent on the activities of various enzymes in the digestive system, such as amylase in saliva, pepsin in the stomach, and pancreatic enzymes in the small intestine. These mechanisms have been extensively examined (61, 62), particularly in the stomach. However, many food components cannot be digested in the upper GI tract and are passed into the lower intestinal tract, in which they are fermented by microbes. Functional studies commonly use animal models in order to obtain a better understanding of the processes in the GI tract that may lead to better health or decrease disease. However, information from animal models may not be directly translatable to humans. Therefore, researchers need to consider the limitations of the selected animal model when extrapolating findings to humans.

Although microbiome studies often include an ecological component, most of the research performed to date has focused on *Bacteria* and not all of the biota. This represents a logical approach because *Bacteria* comprise most of the microbiome. However, even biota representing a small proportion of the microbiome may play important roles in the ecosystem (133). Therefore, researchers need to start shifting their approach to include eukaryotic, prokaryotic, and viral (33, 133) interactions in efforts to elucidate the roles of all components of the microbiome.

In recent years, a number of reviews have summarized findings from the increasing number of studies being performed in this field (36, 73, 176, 188). While most studies have focused on disease, the microbiome is also important for maintaining

* Corresponding author. E-mail: cnakatsu@purdue.edu;
Tel: +1 (765) 496–2997; Fax: +1 (765) 496–2926.

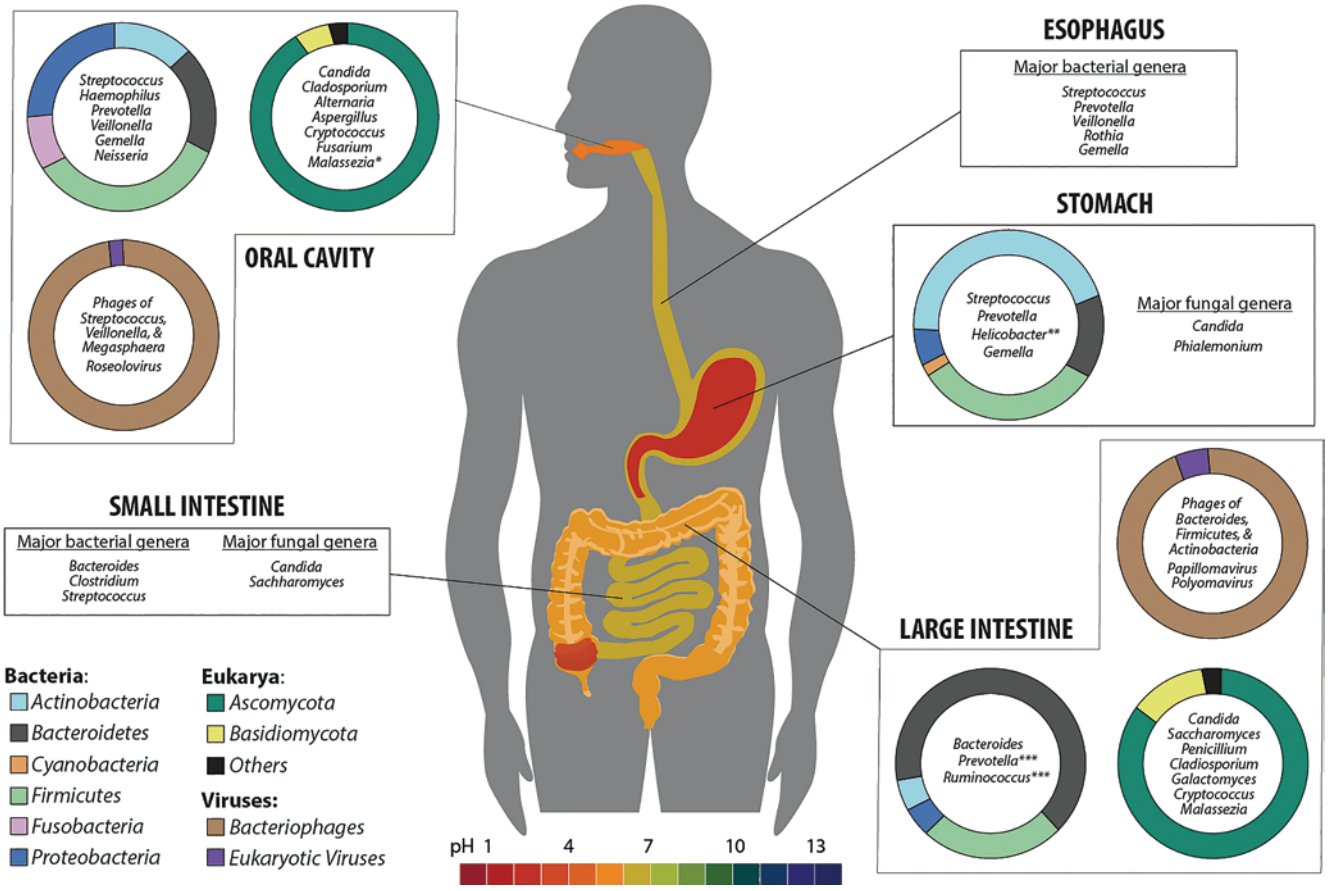

Fig. 1. Microbiome composition of *Bacteria* (1, 5, 20, 21, 43, 147, 156, 223), *Eukarya* (52, 85, 114, 126, 182, 197), and *Viruses* (45, 134, 151, 215) among the physiological niches of the human gastrointestinal (GI) tract. Phylum level compositional data are presented where available along with the most common genera in each GI tract location. The colors on the doughnut plots correspond to the legend in the lower left corner; the GI tract is colored according to the pH scale shown at the bottom of Fig. 1. (* *Malassezia* was very abundant in one study and was not detected in another study. ** The abundance of *Helicobacter* may vary greatly between individuals. *** Proportions of these and other colon genera vary with age, diet, & geographical location.)

health. We herein highlight differences in the microbiome (*Bacteria*, *Archaea*, *Fungi*, and *Viruses*) along the GI tract of healthy humans, and how it compares to those of typical animal models used in research. One finding that is consistent to most studies is that the microbiome of healthy individuals is unique; however, there are still some generalities that will be discussed in this review.

Microbiome diversity

Many factors contribute to the diversity of microbiomes, and most studies have demonstrated the individuality of microbiomes among subjects. Previous findings support microbial communities being more similar in subjects that are genetically related (191), of a similar age (135, 213), or with common diets (including the influences of ethnicity and geography) (63). Diseases will also have an impact on microbiome diversity, including autoimmune and neoplastic diseases, such as inflammatory bowel disease, diabetes, obesity, cardiovascular diseases, allergies, and cancer (37, 121). Treatments for diseases may also affect a patient's gut microbiota, and the consequences of antibiotic use have been intensively investigated (22, 95).

The host genotype has been shown to influence the development of the gut microbiota, and the immune system has been identified as a contributing factor (188). Crosstalk between the microbiome and human immune system occurs in response to a number of environmental factors, such as diet, xenobiotics, and pathogens. Microbial host interactions occur in the gut, mainly in the epithelial cell layer, myeloid cells, and innate lymphoid cells, in which crosstalk and feedback loops contribute to the microbiome composition, host physiology, and disease susceptibility. These interactions contribute not only to the bacterial community along the GI tract, but also to the other microbiota (*Fungi*, *Archaea*, and *Viruses*). Our understanding of the immunology associated with *Fungi* (150) and *Archaea* is currently limited. Transkingdom commensal relationships among microbiota (including *Viruses*) are considered to form from infancy (29, 30, 106, 200) and several co-occurring relationships have been identified (35, 75, 76, 85, 214).

Bacteria. A more complete picture of human-associated bacterial communities obtained using molecular techniques has revealed that their diversity is greater than initially considered through cultivation (9, 20, 56, 90, 113). Using almost full-length 16S rRNA gene sequences, predicted taxa numbers range from 100–300 (20, 56), while pyrosequencing suggests there are 1000s of phylotypes (38, 49). Most of the

gut bacteria identified by 16S rRNA gene sequencing belong to the five phyla originally identified by cultivation, namely, *Bacteroidetes*, *Firmicutes*, *Actinobacteria*, *Proteobacteria*, and *Verrucomicrobia* (90), and, at lower proportions, *Fusobacteria*, *Tenericutes*, *Spirochaetes*, *Cyanobacteria*, and TM7 (189). At lower levels of the taxonomic classification, microbiome compositions vary with each individual. Attempts have been made to identify a single core microbiome of *Bacteria* in the GI tract. Although this has not been possible in the lower GI tract (mainly using fecal samples) based on taxonomy, it appears there are core microbial functions (152, 189, 191). It is possible to identify some core microbiota in the oral cavity, esophagus, and stomach (148). Although extensive efforts have been made to cultivate representative gut microbiota in an attempt to gain a better understanding of the relationship between taxa and function (156), there are still many undescribed taxa with unknown functional roles in the gut.

As the price of sequencing decreases, it is becoming more common to use a metagenomic approach that provides information on all microbiota and potential functions (3, 70, 167, 189). This provides a means to go beyond *Bacteria* and obtain information on eukaryotic microbes (mainly fungi) and viruses. Although *Fungi*, *Archaea*, and *Viruses* in the microbiome are a part of the 'rare biosphere' (organisms that comprise <0.1% of the microbiome) (173), they still have a significant impact on host health.

Fungi

Fungi are considered to comprise approximately 0.03% of the fecal microbiome (143); making them approximately 3,300-fold less abundant than *Bacteria*. Fungal diversity in the human gut is also lower than that of *Bacteria* (143, 166), although more taxa are being found as the number of individuals being studied using next generation sequencing is increasing (44, 126, 166, 182). In 2015, a review of 36 fungal gut microbiome studies revealed that there have been at least 267 distinct fungi identified in the human gut (181), while another study reported 221 (72). Despite the number of taxa that have been reported, most fungi are highly variable among individuals, with few appearing to be common to all.

Cultivation-based analyses have typically identified *Candida* as the most common fungal genus (166), and it is also frequently identified using non-cultivation-based methods, whereas the other taxa identified have been variable, which may be because of the analytical method used and/or subject variability. For example, 66 genera of fungi were found using pyrosequencing when 98 individuals were examined, with the genera *Saccharomyces*, *Candida*, and *Cladosporium* being the most prevalent (85). *Mucor* was common in Spanish individuals (126) and the most common fungi in 16 vegetarians were *Fusarium*, *Malassezia*, *Penicillium*, and *Aspergillus* (182). These studies suggested that some taxa, *e.g.*, *Penicillium* and *Aspergillus*, are not resident in the gut and enter through environmental sources, such as food and water, in which they are commonly found. This may account for some of the variability in taxa reported in various studies and for the increasing number of fungi being identified as more studies are being performed, even those based on cultivation (71). Under certain conditions, some fungi may flourish and become pathogenic including *Candida*, *Aspergillus*, *Fusarium*, and *Cryptococcus* (44, 84, 140, 143). More information on fungal interactions and diseases is available in a review by Wang *et al.* (204).

Despite their low abundance, fungi appear to have developed in mammalian guts along with the rest of the body from infancy (106, 169). Although there is no consensus of a core mycobiome, *Candida*, *Saccharomyces*, and *Malassezia* have been commonly reported (72). Most of the fungal species detected appear to be either transient or environmental fungi that cannot colonize the gut and are often found in a single study and/or one host only. A previous study indicated that the fungal community is unstable; only 20% of the initially identified fungi were detected again 4 months later (78). More studies on the stability of the mycobiome are needed in order to establish the ecological roles of the components of the mycobiome. Many non-bacterial organisms have been found in numerous mammalian systems, which indicates that they play an important role that has been largely overlooked and may lead to important discoveries and understanding in the coming years.

Archaea

The most commonly reported genus of *Archaea* that has been found in the GI tract is *Methanobrevibacter* (51, 55, 66, 85, 109). Other genera that have also been detected are *Methanosphaera* (51), *Nitrososphaera*, *Thermogynomonas*, and *Thermoplasma* (85) and the new candidate species, *Methanomethylophilus alvus* (27, 131). Although *Archaea* comprise a very small proportion of the microbiota, *Methanobrevibacter* species are important contributors to methanogenesis (66). Differences in *Archaea* in microbiome samples may be due to the method used (51) and/or complex relationships with other microbiota. For example, *Methanobrevibacter* and *Nitrososphaera* were previously shown to be mutually exclusive and potentially related to carbohydrate intake (85). More studies are needed in order to clarify the interaction between *Archaea* and other microbiota groups, which may contribute to our understanding of their fitness and function (beyond methanogenesis) in the microbiome.

Viruses

Viruses in the human microbiome have also been understudied and available information is limited (161); the majority of data are related primarily to disease and do not address the commensal virome (34, 40). The majority of viral reads in studies that have been performed cannot be assigned to a known group; this has contributed to the difficulties associated with assessing their roles in the GI tract (124, 160). A number of teams have made extensive efforts in order to advance human virome studies (157, 161). In the last ten years, the number of identified polyomaviruses has increased from 4 to 13 species (some that cause disease and some that do not) (47), and the accuracy of identification techniques has been improved to identify taxa at the genus level (199) and use metagenomic information for viral taxonomy (172). Viral communities are mainly comprised of bacteria-infecting phage families (~90%), while eukaryotic viruses (~10%) are

in lower abundance (157, 161). Metagenomic analyses have suggested that the new bacteriophage, crAssphage associated with *Bacteroides*, is potentially common in humans (53). The greatest diversity of phages is considered to occur in infants and decreases with age, in contrast to increases in bacterial diversity (116, 117, 162). With the availability of methods to enrich viruses in samples (41), and with more metagenomic sequences and bioinformatics tools to identify viral sequences (53, 139), more information will be obtained on viral diversity and associated physiological factors in humans.

Similar to the microbiota, considerable variability appears to exist in the viral taxa found among subjects (133). Limited information is currently available on the functional roles of most viruses in the human GI tract. However, some possible functions are: to increase bacterial fitness as sources of genetic information (*e.g.*, the source of antibiotic resistance genes), to increase the immunity of bacteria or the human host, and to protect against pathogens (40, 64, 157). The general consensus is that the presence of bacteria is beneficial for viruses that are increasingly trying to evade the immune system. This relationship may also be beneficial to bacteria as viruses may be sources of potentially advantageous genes (resistance or tolerance to stress environments). Researchers are now examining the ecological and evolutionary influences of phages on bacterial ecosystems (102), and the findings obtained may provide insights into the important roles played by phages in the gut microbiome.

The GI tract

Many challenges are associated with studying the microbial ecology of the GI tract because it is composed of chemically and physically diverse microhabitats stretching from the esophagus to the rectum, providing a surface area of 150–200 m^2 for colonization or transient occupation by microbes (16). The adult GI tract was initially estimated to harbor 10^{14} bacteria, 10 times more cells than the human body (16, 120); however, a more recent calculation estimates there to be 10^{13} bacteria, which is equivalent to the number of human cells (170). Lower bacterial numbers (10^3 to 10^4 bacteria mL^{-1} of intestinal content) are found in the upper end of the GI tract, stomach, and small intestine, in which pH is low and the transit time is short (16). The highest biodiversity (richness and evenness) of bacteria (10^{10}–10^{11} bacteria g^{-1} of intestinal content) is in the colon, in which cell turnover rate is low, redox potential is low, and the transit time is long. This section highlights the different functions and associated microbiota along the human GI tract starting from the oral cavity, then the esophagus, stomach, and intestines (Fig. 1).

The oral cavity. Activity in the mouth may have a large impact on the further digestion of food in the lower GI tract. Food is mechanically ground into small particles, typically 0.1 mm, which increases the surface area. The oral microbiome is composed of transient and commensal populations that often form biofilms on soft and hard surfaces in the mouth (8). The most up-to-date information on taxa of the oral microbiome may be found in the Human Oral Microbiome Database (HOMD, http://www.homd.org/) (50). Information in this database is limited to *Bacteria* and one *Archaea*. Cultivation-independent analyses indicate that the most common genus is *Streptococcus*, while other genera include *Neisseria*, *Gemella*, *Granulicatella*, and *Veillonella*, but not in all individuals examined (1, 91, 92, 107). The taxa present appear to be dependent on interactions between microbes within the community. For example, using a graph theory-based algorithm of an organism's nutritional profile, the species *Streptococcus oralis* and *S. gordonii* have low metabolic complementarity and high metabolic competition, indicating they are antagonistic to each other (110). In contrast, *Porphyromonas gingivalis* was shown to have high metabolic complementarity, indicating its ability to grow symbiotically with diverse oral microbiota taxa. This computational method was tested and confirmed with growth assays, making it a viable means to assess the ability of species to inhabit the same environment. This has also been shown using an *in situ* spectral analysis of microbiota in biofilm plaques. Biofilms were shown to be composed of a number of taxa with *Corynebacterium* at the foundation (209). The other taxa are considered to play complementary roles driven by the environmental and chemical gradients formed in biofilms that control nutrient availability. These findings indicate that, despite the large number of taxa identified in oral microbiome studies, the core taxa of all microbiota may be identified in the future based on spatial locations and functional roles (10).

Similar to *Bacteria*, large variations have been noted in viruses found in the oral cavity among subjects (151). Most viruses are bacteriophages (approx. 99% of known sequences). Viral communities are reproducible across time points within a subject, suggesting that they are stable; however, the human and bacterial host significantly influence compositions (2, 151, 163). In addition to interactions among oral bacteria, many may associate with phages (57). Depending on the host range of the oral virome, this may make phages very common inhabitants of the oral cavity. Furthermore, in addition to survival within bacterial hosts, phages may also survive in the oral mucosa and contribute to host immunity (11). These are all new avenues of oral virome research that will likely be investigated in greater depth in the future.

In addition to the bacterial microbiome, two cultivation-independent studies have been conducted on oral fungi. Approximately 100 fungal species (20 genera) were detected in one study of the oral mycobiome of healthy individuals (68). Among the fungi detected, *Candida* species were the most common and abundant, while the other genera consisted of *Cladosporium*, *Aureobasidium*, *Saccharomycetales*, *Aspergillus*, *Fusarium*, and *Cryptococcus*. Most of these genera were also detected in a recent study on three subjects; however, *Malassezia*, a skin pathogen, accounted for the most sequence reads (52). Most of the other studies conducted on the oral mycobiome have focused on the role of fungi in disease (69, 136). Since the oral microbial community is directly exposed to the environment, the presence of a dynamic and transient community is expected, but warrants further study.

Esophagus. After swallowing, food is transported down the esophagus by peristalsis to the stomach. Limited information is available on microbes inhabiting the esophagus (5, 91, 147), and this may be due to the difficulties associated with obtaining samples because biopsies have typically been used. However, a less invasive method using an esophageal string has recently been demonstrated to be a feasible alternative

and yields similar findings to non-cultivation-based analyses of biopsies (60). Similar to the oral cavity, the most common genus found in the esophagus is *Streptococcus*; however, an overall comparison of the two communities has indicated that the number of taxa significantly differ between the two locations (15, 60). Among the few studies conducted on the viral and fungal microbiota of the esophagus, the focus has been on association with disease (204) and none of the pathogenic taxa inhabit healthy individuals.

Stomach. The stomach is the first digestive organ in the body (89). It holds food and mechanically mixes it with proteolytic enzymes and gastric acids that aid in the breakdown and subsequent absorption of nutrients. The growth of many common bacteria is inhibited by these acidic conditions (pH<4), making this a unique community with the lowest number of microbes, ranging between 10^1 and 10^3 CFU g^{-1}. In addition to digestion, the acidic conditions of the stomach are considered to have evolved as a means of protection from pathogens. This hypothesis is supported by the recent finding of a lower pH in the stomachs of scavengers and higher pH in herbivores, which are less likely to encounter pathogens in their food (13). Caution is needed when comparing the findings of various studies throughout the GI tract because gastric juice has a lower pH than the mucosal layer, resulting in differences in the microbiota present (89).

Despite the low pH, non-cultivation-based analyses on stomach biopsies revealed a more diverse microbiota than expected (5, 20, 115). Regardless of variations among subjects, there appears to be two major groups of individuals: those with and without *Helicobacter pylori* (20). There is a third subset in which *H. pylori* is present in lower proportions in some individuals that were negative using conventional testing. Microbiomes dominated by *H. pylori* had significantly greater proportions of the phylum *Proteobacteria*, of which it is a member, and lower alpha diversity (5, 20). Other common genera are *Streptococcus* and *Prevotella*, both of which are also found in the oral and esophageal communities; however, the communities at these locations appear to differ (5). Limited information is available on fungi analyzed in biopsy samples; although a cultivation study detected *Candida* species, this appeared to be associated more with disease (224). The major interaction currently studied in the stomach microbiota is with *Helicobacter* because of its association with gastritis, peptic ulcers, and gastric cancer. However, this taxon has been suggested to be beneficial for health, leading some to question whether the complete eradication of this microbe is the best option (67, 89).

In contrast, less information is available on the microbiome of stomach fluids; it appears to harbor fewer *Helicobacter* and an analysis of transcripts indicated that *Actinobacteria* are the most active phylum; however, the other major phyla, *Firmicutes*, *Bacteroidetes*, and *Proteobacteria*, are also present (197). In the same study, it also appeared to harbor novel fungi; 77.5% of the ITS reads were not identified at the phylum level or lower. *Candida* and *Phialemonium* were the only two identifiable fungal genera in all subjects tested, whereas an additional 66 genera were present in at least one of the nine subjects examined. Based on the infrequency and number of reads in this analysis, most of the taxa identified in stomach fluids appear to be transient, and those playing an active role are limited in this location.

Intestines. After mixing in the stomach, chime slowly passes through the pyloric sphincter and enters the intestines, in which the major digestion and absorption of nutrients begin (12). Humans have a small and large intestine. The small intestine, the main location in which food digestion and absorption occurs, is further divided into three parts, the duodenum, jejunum, and ileum. The duodenum, in which food chime enters from the stomach, is directly associated with digestion and is linked to the pancreas and gallbladder. Bile salts from the gallbladder and enzymes from the pancreas enter the duodenum and mix with stomach chime in order to start the digestion process. The epithelium in the jejunum and ileum is responsible for glucose absorption into the bloodstream via glucose transporters and sodium ions. The small intestine is followed by the large intestine (colon), which has a larger diameter, but shorter length and is divided into four sections: the ascending colon (cecum), transverse colon, descending colon, and sigmoid colon (123). Water and minerals are continuously absorbed along the colon before excretion. Furthermore, complex foods that cannot be digested by the host are used as growth substrates for the colonic microbiota (25, 178).

Spatial and temporal variabilities have been noted in the microbial composition among the different intestinal structures based on their functional roles and timing of food intake (18, 129, 186). Although spatial variability exists along the intestinal tract, the bacterial microbiome at the phylum level is considered to remain fairly stable over time (43, 155); however, many factors may affect its stability (119). Undigested food and most of the microbiota are found in the lumen, the central space surrounded by the mucosal layer of the tubular intestinal structure. The main absorption of growth substrates occurs through the epithelial cells of the mucosa, which also prevents the entry of the microbiota into host cells (174). A number of important host-microbe interactions occur within the mucosa. Energy from microbially produced metabolites, such as butyrate, contributes to epithelial metabolism (97). Most of the gut is anaerobic, but there is an oxygen gradient in the mucosa that provides a competitive advantage for facultative anaerobes (174). Recent studies have also shown the importance of metabolites produced by transkingdom microbiota to host physiology (185, 187, 188). Microbiota, such as *Akkermansia mucinophila*, are commonly found residing in the mucus layer and feed on mucin (39, 48). Therefore, the effects of host interactions with the gut microbiota, particularly those in the large intestine, have a prominent impact on overall human health, including energy reabsorption and immune system development.

Due to the difficulties associated with collecting multiple samples along a healthy human GI tract in order to capture the spatial heterogeneity of microbes in this environment, most studies use fecal samples as a surrogate. However, this limits the availability of regio-specific community information on the GI tract, resulting in portions, such as the small intestine, remaining poorly characterized. The few studies conducted on the small intestine have limited subject numbers because they used biopsy samples (4, 201, 203) or ileotomy patients (108, 195, 222). The bacterial genera most commonly found among these studies were *Clostridium*, *Streptococcus*, and *Bacteroides*. The number of studies that include fungi are

Table 1. Comparison of the anatomy of the intestinal tract in humans and animal models

	Human	Mouse	Rat	Pig
Stomach	Four regions: cardia, fundus, body, and pylorus	Three regions: forestomach, body, and pylorus	Three regions: forestomach, body, and pylorus	Four regions: esophagus, cardia, fundus, and pylorus
	pH 1.5 to 3.5	pH 3.0 to 4.0	pH 3.0 to 4.0	pH 1.5 to 2.5
Small intestine	5.5–6.4 m in length	350 mm in length	1,485 mm in length	1.2–2.1 m in length
	pH 6.4 to 7.3	pH 4.7 to 5.2	pH 5.0 to 6.1	pH 6.1 to 6.7
Cecum	Smaller than the colon	Larger than the colon	Larger than the colon	Smaller than the colon
	No fermentation	Main fermentation	Main fermentation	Some fermentation
	pH 5.7	pH 4.4 to 4.6	pH 5.9 to 6.6	pH 6.0 to 6.4
Appendix	Present	Absent	Absent	Absent
Colon	Divided into the ascending, transcending, and descending colon	Not divided	Not divided	Divided into the ascending, transcending, and descending colon
	Main fermentation	No fermentation	No fermentation	Main fermentation
	Thick mucosa	Thinner mucosa	Thinner mucosa	Thick mucosa
	pH 6.7	pH 4.4 to 5.0	pH 5.5 to 6.2	pH 6.1 to 6.6

Adapted from (59, 96, 128, 130, 137, 196)

even more limited, with the genera *Candida* and *Saccharomyces* being the most frequently detected (108, 114). Caution is also needed when extrapolating these findings to all individuals because the health of some subjects was compromised when samples were obtained.

Bacteria in the colon account for approximately 70% of all bacteria in the human body because it is the main site for the bacterial fermentation of non-digestible food components such as soluble fiber. The small number of studies that have examined microbial communities directly in the colon suggests that the bacterial composition is similar to that found in feces (86). However, fecal communities do not represent a single colonic environment, such as the mucosa (223), but a mixture of indigenous and transient microbes from the entire GI tract. In studies in which a global view of the GI tract microbial community is of interest, fecal material represents a good surrogate and is easily obtained, allowing for multiple samples to be obtained over short and long time periods from healthy individuals. The majority of microbiome reviews have extensively covered colonic communities using feces (74, 92, 121, 148, 189); therefore, we will not describe its composition in detail. However, later in this review, the impact of diet on the microbiome composition will be discussed. Furthermore, the above sections on fungi and viruses provide information on the taxa of these groups in the intestines.

Summary of the GI tract. The use of non-cultivation-based methods to investigate the microbiota in the GI tract has increased our knowledge of their diversity. One group that we neglected to mention in this review was *Protozoans*/*Protists*; however, recent reviews are available (79, 145). Despite representing a smaller biomass than fungi, they also appear to be important to the ecological structure of the gut microbiome. The predator-prey relationship they have with other microbiota (145) may, in some cases, lead to disease prevention (7). Difficulties are associated with elucidating the functional roles played by these various taxa at different points along the GI tract. Therefore, it is still important to obtain cultivated representatives to investigate their role and ecological significance along the GI tract. This consideration is important for all microbiota; however, it represents a larger issue for low diversity groups, such as fungi, which may not be numerically abundant, but still play a significant role (17).

Use of animal models

Animal models have been widely adopted in human gut microbiome research (28, 98, 220) to reduce confounding experimental factors such as genetics, age, and diet, which may be more easily controlled in laboratory animals. Additionally, animal models with modified genetic backgrounds are available for investigating potential mechanisms (137). Ideally, animal models with relatively similar genetic information (217), gut structures, metabolism (142), and diets and behavior patterns (202) to humans need to be selected. Comprehensive comparisons of mice (137) and pigs (217) to humans were recently conducted in order to aid in translating information from animal models to humans. In this section, we will highlight some of their findings and compare GI tract structures and microbial community compositions. Furthermore, some advantages and limitations associated with the use of animal models in human microbiome research will be discussed.

Similarities exist in the anatomy of the GI tract between humans and most animal models (Table 1). However, differences in anatomical structures and pH at different locations along the GI tract may contribute to differences in the microbiota found in humans versus animal models (26). The human colon also has a thicker mucosal layer than those of mice and rats (137), which may have an effect on the diversity of the microbiota colonizing the colon. Human gut bacteria are dominated by two phyla: *Firmicutes* and *Bacteroidetes* (189), which also dominate the GI tract of commonly used model animals (112). However, at lower taxonomic levels, some differences have been reported in microbiome compositions in the gut between humans and animal models (Table 2). The dominant taxa reported have varied as the number of comparisons performed has increased (137, 152); therefore, the findings shown in Table 2 need to be used cautiously.

A pig gut gene catalogue of metabolic function was recently developed and compared to catalogues available for humans and mice (217). They found that 96% of the KEGG orthologs in humans were also present in pigs, whereas the overlap at the gene level was markedly lower (9.46%). However, there was a greater overlap between humans and pigs than between humans and mice. Microbial activity also differs along the GI tract, with the most relevant being fermentation occurring in the ceca of most animal models, but

Table 2. Major taxa of the gut microbiota in humans and animal models

	Human	Mouse	Rat	Pig
Bacteria	*Firmicutes* *Bacteroidetes* *Actinobacteria* *Proteobacteria*	*Firmicutes* *Bacteroidetes*	*Firmicutes* *Bacteroidetes*	*Firmicutes* *Bacteroidetes*
Archaea	*Methanobrevibacter* *Nitrososphaera*	*Methanobrevibacter*	*Methanobrevibacter*	*Methanomicrobia*, *Methanosphaera*
Viruses	*Herpesviridae* *Papillomaviridae* *Polyomaviridae* *Adenoviridae*	Variable	Variable	*Picornaviridae* *Astroviridae* *Coronaviridae* *Caliciviridae*
Eukarya	*Candida* *Malassezia* *Saccharomyces* *Cladosporium*	*Ascomycota* *Basidiomycota* *Chytridiomycota* *Zygomycota*	*Ascomycota* *Basidiomycota* *Chytridiomycota* *Zygomycota*	*Kazachstania* *Candida* *Galactomyces* *Issatchenkia*

Adapted from (85, 103, 105, 112, 125, 137, 153, 154, 171, 179, 193, 194, 215, 216, 221)

not in humans (137). Strengths and weaknesses are associated with the major animal models being used, and these need to be taken into consideration when conducting translational research.

Rats. The use of rats as lab animals dates back to the 1850s. They were considered to be a good candidate for human microbiome research because the rat contains the same four dominant bacteria phyla in the GI tract (31), with *Firmicutes* (74%) and *Bacteroidetes* (23%) representing the largest proportions (221). The advantages of using rats in human microbiome research include quick reproduction, a fully sequenced genome, and easy handling and maintenance due to their relatively small size. The limitation of this model is that the diet used in rats differs from that for humans, and their behavior and living environment are also different, which will affect the gut microbiota. The diet used in rat studies is normal chow that is rich in fiber (205), and diet may rapidly alter gut microbiota diversity (46). Although most studies emphasize the impact of diet on the microbiota in the cecum and/or colon (feces), the oral cavity of rats has been used to clarify the impact of diet on the microbiome (93).

Mice. Many of the strengths and weaknesses associated with using rats are also applicable to mice. Similar to humans, the microbiota in the GI tract of mice is dominated by *Firmicutes* (74%) and *Bacteroidetes* (23%) at the phylum level (217). However, there are differences at the genus level, and this has led to the use of "humanized" mice. This is achieved by inoculating human gut microbiota into germ-free (GF) mice (192) or mice treated with antibiotics to eliminate their gut microbiome (83). The microbiome of these mice after fecal transplants may have a composition at the phyla level that is 100% similar to humans and 88% at the genus level (137). A recent study (175) used humanized mice to test microbiome diversity after feeding with poorly accessible carbohydrates, and found a similar reduction in OTU numbers to a human study (219). However, there are also some limitations to using these animals, including the diet and environmental living conditions. Furthermore, gnotobiotic mice may not reflect the human-microbe relationship due to their weaker immune system (6).

Approximately 10 years ago, Scupham (168) showed that all four major fungal phyla, *Ascomycota*, *Basidiomycota*, *Chytridiomycota*, and *Zygomycota*, were present in the murine gut. Additionally, many genera were identified, including *Acremonium*, *Monilinia*, *Fusarium*, *Cryptococcus*, *Filobasidium*, *Scleroderma*, *Catenomyces*, *Spizellomyces*, *Neocallimastix*, *Powellomyces*, *Entophlyctis*, *Mortierella*, and *Smittium*. When comparing these studies to the human gut, it is important to note that this study indicated a more diverse fungal community than those found in humans; the eukaryotic diversity of the human gut is low (143).

Pigs. Pigs have been used as surrogates for human microbiome research due to their highly similar genetics, physiological structures, behavior, metabolism, and immune functions to those of humans (81, 202). The greater similarities in the omnivorous diet and GI tract structure between pigs and humans are more advantageous than the murine model. The microbiome of pigs is dominated by two phyla: *Firmicutes* and *Bacteroidetes* (104); however, there are some notable differences at the genus level. The genus *Prevotella* was found to be common in two pig metagenomic studies (104, 118). Since the number of pigs used in most studies is less than humans, the pig core microbiome at the genus level may change as more pigs are studied. Another contributing factor to shaping the microbiome composition is diet. Most studies have found that the number of *Bifidobacteria* in pigs, even those on high fiber diets, is lower than that in humans (132, 218), while that of *Lactobacillus* is higher (149). In nutrition studies, humans and pigs are both dependent on the quality of the nutrient load; however, the pig cecum has a larger capacity to ferment indigestible compounds than the human cecum (54). The microbiota composition in pigs may differ from that in humans due in part to differences in diet (81). Similar to mice, humanized GF pigs have been developed and the microbiome after human fecal transplantation more closely resembles that of the donor than conventional pigs (144). However, the same disadvantages associated with using GF mice are also true for GF pigs.

The genome of pigs may be mutated to study human diseases; this is typically performed using miniature pigs such as those from the Ossabaw and Gottingen islands (146). Genetic mutations for metabolic syndrome and insulin resistance have successfully been performed using Ossabaw pigs to study human diseases such as type 2 diabetes (14, 177) and obesity (101). The ratio of *Firmicutes* to *Bacteroidetes* is higher in obese Ossabaw pigs than in lean pigs (146), similar to some

obese humans (111, 190). This finding suggests that Ossabaw pigs are a good model for researching the role of the microbiota in human obesity. However, disadvantages are associated with using miniature pigs, mainly the higher cost for maintenance and longer reproductive period than rodents (146).

Although more extensive efforts have been made to investigate fungi in pigs than in other animal models, many of these studies were cultivation-based or for use as probiotics. Fungi in pigs have been recently studied using a non-cultivation approach and up to 17 species of yeast (belonging to the genera *Kazachstania*, *Galactomyces*, *Candida*, *Issatchenkia*, *Pichia*, *Rhodotorula*, and *Trichosporon*) were common in the gut (194). The number of studies on viruses is limited, but the composition appears to be highly variable among samples (164, 171) and affected by disease (24). These groups need to be examined in more detail in order to establish whether pigs are good models for use in understanding fungi and viruses in humans.

Animal model summary. The convenience and cost of using animal models for human research are appealing. However, researchers need be very careful when selecting animal models appropriate for their objectives, particularly when the objective is to directly extrapolate findings from animals to humans, due to the significant differences in GI tract physiology and microbiome composition (65, 137, 217).

Diet in health

Many studies have found that diet is one of the main factors shaping the composition of gut microbial populations. Dietary approaches, such as the ingestion of non-digestible carbohydrates (prebiotics) and fermented food products containing live cultures (probiotics), have been suggested to confer health benefits by enhancing the growth of beneficial intestinal bacteria (100, 158). As described earlier, the microbiota may break down food components, such as non-digestible carbohydrates, which are indigestible by the host in order to aid in maximizing available nutrients (9) and produce metabolites that contribute to host health. Probiotics have been used as a means to replenish the gut with "beneficial" microbiota after antibiotic treatments or to treat diseases (82, 159). This section will highlight some studies that demonstrated the health benefits of prebiotics and probiotics and possible roles played by the microbiota.

Dietary prebiotics and probiotics. Non-digestible and fermentable food components are often consumed as prebiotics to selectively stimulate the growth and/or activity of endogenous colonic bacteria that may be beneficial to host health. The increased consumption of prebiotics often correlates with enhancements in certain bacterial genera (a common example is *Bifidobacterium* sp.); however, the reason they are beneficial remains unclear (208). Challenges are associated with elucidating the role being played by specific bacterial phylotypes because many of their processes are interactive (207). For example, SCFA produced by bacterial fermentation may lower intestinal pH, thereby increasing the solubility of essential minerals, such as calcium, iron, and magnesium, and consequently enhancing their absorption and improving health. Metabolites produced by microbes may also play an important role in cellular differentiation and proliferation in the colonic mucosa by inducing apoptosis and may confer protection against colitis and colorectal cancer by modulating oncogene expression. These functions do not appear to be performed by a single species; a number of different species may be acting independently or in combination. Research is leading to an understanding of microbial community structure and composition dynamics with respect to diet aids in establishing testable hypotheses for future research in health and beneficial microbes (32). Most research has been performed on the influence of beneficial intestinal bacteria such as *Bifidobacterium* spp. and *Lactobacillus* spp. on host health monitored using a cultivation approach. Cultivation-independent approaches have now become more popular, leading to the identification of new beneficial microbiota taxa and their potential functional roles in the gut as they relate to diet.

Dietary fibers and oligosaccharides are carbohydrate ingredients that vary in composition and structure, but are considered to be non-digestible because of the lack of appropriate intestinal enzymes to hydrolyze them or structural hindrances that prevent enzyme access in the gut. Although bacteria in the lower gut may ferment these carbohydrates, the rate and degree of fermentation vary with the polysaccharide (80). The range of fermentation in the colon for various fibers is broad, from approximately 5% for cellulose to nearly 100% for pectin (42). The resulting SCFA, including butyrate and propionate, are considered to reduce pH and solubilize minerals, thereby improving their absorption and subsequent utilization. Inulin, a long chain fructooligosaccharide (FOS) often obtained from chicory root, and FOS from other sources are the fibers that have been studied in the most detail (206). Several novel fibers have been tested in an *in vitro* large intestine model for their effects on the microbial stimulation and production of SCFA (122). All these novel fibers stimulated the growth of beneficial *Bifidobacteria* and some *Lactobacillus* species along with increases in SCFA production. Only a few studies have examined the effects of fibers and resistant starches on the human microbiome (87, 127, 198, 210, 211). A soluble corn fiber product has been demonstrated to increase Ca absorption in a number of different studies (210, 211). More benefits to human health may be attributed to the consumption of prebiotics and fermentation by the gut microbiome.

The number of studies that include diet effects on *Archaea*, *Fungi*, and/or *Viruses* are limited; however, some examples are included herein. Examinations of *Archaea*, *Fungi*, and *Bacteria* correlations in response to diet revealed a syntrophic model involving *Candida*, *Prevotella*, *Ruminococcus*, and *Methanobrevibacter* (85). *Candida* was considered to break down carbohydrates into metabolites used by *Prevotella* and *Ruminococcus* that produce CO_2 for *Methanobrevibacter* (85). However, shifts in carbon sources or breaking down starches via amylases from the human mouth may alter this relationship because *Prevotella* may no longer be dependent on *Candida*. This is a good example of how *Archaea*, which represent a very small portion of the microbiome, are a key contributor to methanogenesis and waste decomposition. The absence of *Archaea* may have severe effects on the surrounding community as hydrogen, glucose metabolites, and other carbon sources accumulate. Other organisms will eventually fill this niche, but may diminish or accumulate new metabolites that

ultimately shift the surrounding community based on their fitness for using these substrates.

A recent study investigated rapid changes in the microbiome composition when diets were either high in animal-based or plant-based fat and protein (46). The fungus *Candida* was found to increase in subjects placed on a plant-based diet, whereas *Penicillium* increased on animal-based diets. The most commonly found fungi in vegetarians were *Fusarium*, *Malassezia*, *Penicillium*, *Aspergillus*, and *Candida* (182). Caution is needed when interpreting findings because some of these fungi may be found on food prior to ingestion (46, 78, 182)

Phages assembled in the gut may also be modified by diet. A recent study examined changes in the fecal viral community over an 8-d period in six subjects supplied different diets (134). Shotgun sequencing of virus-like particles revealed that interpersonal differences in the virome were the largest source of variations in this study. However, the virome of subjects whose diets were changed differed more than in those who maintained their normal diet. Although this is only one study with a few human subjects, studies using a mouse model and different dietary fats support these findings (88, 99). Collectively, these findings indicate that diet plays a key role in shaping the gut virome, and further research is needed in order to investigate interactions between diet and the virome.

Summary

Advances have been made in the last decade in our understanding of the role of the GI tract microbiome in human health. This review has highlighted changes and differences in the microbiome along the GI tract that are due to changes in physical, chemical, and biological interactions. Although extensive research has been conducted on *Bacteria* in fecal samples, the main kingdom inhabiting the gut, our knowledge is still insufficient, particularly in other regions of the GI tract. Furthermore, other groups (*Archaea*, *Fungi*, and *Viruses*) have not yet been investigated in adequate detail, demonstrating a real void in knowledge. This highlights that the basic ecology of microbiomes is important for gaining a greater understanding to improve human health and decrease disease. In order to achieve this goal, it is important to include all microbiota in studies and remain cognizant of the limitations associated with understanding the entire GI tract of humans despite challenges in sampling and cultivation. Furthermore, the use of appropriate animal models in mechanistic studies requires careful consideration.

References

1. Aas, J.A., B.J. Paster, L.N. Stokes, I. Olsen, and F.E. Dewhirst. 2005. Defining the normal bacterial flora of the oral cavity. J. Clin. Microbiol. 43:5721–5732.
2. Abeles, S.R., R. Robles-Sikisaka, M. Ly, A.G. Lum, J. Salzman, T.K. Boehm, and D.T. Pride. 2014. Human oral viruses are personal, persistent and gender-consistent. ISME J. 8:1753–1767.
3. Abubucker, S., N. Segata, J. Goll, *et al.* 2012. Metabolic reconstruction for metagenomic data and Its application to the human microbiome. PLoS Comput. Biol. 8:e1002358.
4. Ahmed, S., G.T. Macfarlane, A. Fite, A.J. McBain, P. Gilbert, and S. Macfarlane. 2007. Mucosa-associated bacterial diversity in relation to human terminal ileum and colonic biopsy samples. Appl. Environ. Microbiol. 73:7435–7442.
5. Andersson, A.F., M. Lindberg, H. Jakobsson, F. Bäckhed, P. Nyrén, and L. Engstrand. 2008. Comparative analysis of human gut microbiota by barcoded pyrosequencing. PLoS One 3:e2836.
6. Atarashi, K., T. Tanoue, K. Oshima, *et al.* 2013. T-reg induction by a rationally selected mixture of Clostridia strains from the human microbiota. Nature 500:232–236.
7. Audebert, C., G. Even, A. Cian, A. Loywick, S. Merlin, E. Viscogliosi, and M. Chabe. 2016. Colonization with the enteric protozoa *Blastocystis* is associated with increased diversity of human gut bacterial microbiota. Sci. Rep. 6:25255.
8. Avila, M., D.M. Ojcius, and Ö. Yilmaz. 2009. The oral microbiota: Living with a permanent guest. DNA Cell Biol. 28:405–411.
9. Backhed, F., R.E. Ley, J.L. Sonnenburg, D.A. Peterson, and J.I. Gordon. 2005. Host-bacterial mutualism in the human intestine. Science 307:1915–1920.
10. Baker, J.L., B. Bor, M. Agnello, W.Y. Shi, and X.S. He. 2017. Ecology of the oral microbiome: Beyond bacteria. Trends Microbiol. 25:362–374.
11. Barr, J.J., R. Auro, M. Furlan, *et al.* 2013. Bacteriophage adhering to mucus provide a non-host-derived immunity. Proc. Natl. Acad. Sci. U.S.A. 110:10771–10776.
12. Barrett, K.E. 2014. Gastrointestinal Physiology, 2nd ed. Lange Medical Books/McGraw-Hill.
13. Beasley, D.E., A.M. Koltz, J.E. Lambert, N. Fierer, and R.R. Dunn. 2015. The evolution of stomach acidity and is relevance to the human microbiome. PLoS One 10:e.0134116.
14. Bellinger, D.A., E.P. Merricks, and T.C. Nichols. 2006. Swine models of type 2 diabetes mellitus: Insulin resistance, glucose tolerance, and cardiovascular complications. ILAR J. 47:243–258.
15. Benitez, A.J., C. Hoffmann, A.B. Muir, K.K. Dods, J.M. Spergel, F.D. Bushman, and M.-L. Wang. 2015. Inflammation-associated microbiota in pediatric eosinophilic esophagitis. Microbiome 3:23.
16. Berg, R.D. 1996. The indigenous gastrointestinal microflora. Trends Microbiol. 4:430–435.
17. Berrilli, F., D. Di Cave, S. Cavallero, and S. D'Amelio. 2012. Interactions between parasites and microbial communities in the human gut. Front. Cell. Infect. Microbiol. 2:141.
18. Biggs, M.B., G.L. Medlock, T.J. Moutinho, H.J. Lees, J.R. Swann, G.L. Kolling, and J.A. Papin. 2017. Systems-level metabolism of the altered Schaedler flora, a complete gut microbiota. ISME J. 11:426–438.
19. Bik, E.M. 2009. Composition and function of the human-associated microbiota. Nutr. Rev. 67:S164–S171.
20. Bik, E.M., P.B. Eckburg, S.R. Gill, K.E. Nelson, E.A. Purdom, F. Francois, G. Perez-Perez, M.J. Blaser, and D.A. Relman. 2006. Molecular analysis of the bacterial microbiota in the human stomach. Proc. Natl. Acad. Sci. U.S.A. 103:732–737.
21. Bik, E.M., C.D. Long, G.C. Armitage, *et al.* 2010. Bacterial diversity in the oral cavity of 10 healthy individuals. ISME J. 4:962–974.
22. Blaser, M.J. 2016. Antibiotic use and its consequences for the normal microbiome. Science 352:544–545.
23. Blaut, M., M.D. Collins, G.W. Welling, J. Dore, J. van Loo, and W. de Vos. 2002. Molecular biological methods for studying the gut microbiota: the EU human gut flora project. Brit. J. Nutr. 87:S203–S211.
24. Blomstrom, A.L., C. Fossum, P. Wallgren, and M. Berg. 2016. Viral metagenomic analysis displays the co-infection situation in healthy and PMWS affected pigs. PLoS One 11:e0166863.
25. Bolam, D.N., and J.L. Sonnenburg. 2011. Mechanistic insight into polysaccharide use within the intestinal microbiota. Gut microbes 2:86–90.
26. Booijink, C., E.G. Zoetendal, M. Kleerebezem, and W.M. de Vos. 2007. Microbial communities in the human small intestine: coupling diversity to metagenomics. Fut. Microbiol. 2:285–295.
27. Borrel, G., H.M. Harris, W. Tottey, *et al.* 2012. Genome sequence of "Candidatus *Methanomethylophilus alvus*" Mx1201, a methanogenic archaeon from the human gut belonging to a seventh order of methanogens. J. Bacteriol. 194:6944–6945.
28. Bowey, E., H. Adlercreutz, and I. Rowland. 2003. Metabolism of isoflavones and lignans by the gut microflora: a study in germ-free and human flora associated rats. Food Chem. Toxicol. 41:631–636.
29. Breitbart, M., I. Hewson, B. Felts, J.M. Mahaffy, J. Nulton, P. Salamon, and F. Rohwer. 2003. Metagenomic analyses of an uncultured viral community from human feces. J. Bacteriol. 185:6220–6223.

30. Breitbart, M., M. Haynes, S. Kelley, *et al.* 2008. Viral diversity and dynamics in an infant gut. Res. Microbiol. 159:367–373.
31. Brooks, S.P.J., M. McAllister, M. Sandoz, and M.L. Kalmokoff. 2003. Culture-independent phylogenetic analysis of the faecal flora of the rat. Can. J. Microbiol. 49:589–601.
32. Brownawell, A.M., W. Caers, G.R. Gibson, C.W.C. Kendall, K.D. Lewis, Y. Ringel, and J.L. Slavin. 2012. Prebiotics and the health benefits of fiber: Current regulatory status, future research, and goals. J. Nutr. 142:962–974.
33. Cadwell, K. 2015. Expanding the role of the virome: Commensalism in the gut. J. Virol. 89:1951–1953.
34. Cadwell, K. 2015. The virome in host health and disease. Immunity 42:805–813.
35. Cavalcanti, I.M.G., A.H. Nobbs, A.P. Ricomini, H.F. Jenkinson, and A.A.D. Cury. 2016. Interkingdom cooperation between *Candida albicans*, *Streptococcus oralis* and *Actinomyces oris* modulates early biofilm development on denture material. Pathog. Dis. 74:ftw002.
36. Charbonneau, M.R., L.V. Blanton, D.B. DiGiulio, D.A. Relman, C.B. Lebrilla, D.A. Mills, and J.I. Gordon. 2016. A microbial perspective of human developmental biology. Nature 535:48–55.
37. Cho, I., and M.J. Blaser. 2012. The human microbiome: at the interface of health and disease. Nat. Rev. Genet. 13.
38. Claesson, M.J., O. O'Sullivan, Q. Wang, J. Nikkilä, J.R. Marchesi, H. Smidt, W.M. de Vos, R.P. Ross, and P.W. O'Toole. 2009. Comparative analysis of pyrosequencing and a phylogenetic microarray for exploring microbial community structures in the human distal intestine. PLoS ONE 4:e6669.
39. Collado, M.C., M. Derrien, E. Isolauri, W.M. de Vos, and S. Salminen. 2007. Intestinal Integrity and *Akkermansia muciniphila*, a mucin-degrading member of the intestinal microbiota present in infants, adults, and the elderly. Appl. Environ. Microbiol. 73:7767–7770.
40. Columpsi, P., P. Sacchi, V. Zuccaro, S. Cima, C. Sarda, M. Mariani, A. Gori, and R. Bruno. 2016. Beyond the gut bacterial microbiota: The gut virome. J. Med. Virol. 88:1467–1472.
41. Conceição-Neto, N., M. Zeller, H. Lefrère, *et al.* 2015. Modular approach to customise sample preparation procedures for viral metagenomics: a reproducible protocol for virome analysis. Sci. Rep. 5:16532.
42. Cook, S.I., and J.H. Sellin. 1998. Review article: short chain fatty acids in health and disease. Ailment Pharmacol. Ther. 12:499–507.
43. Costello, E.K., C.L. Lauber, M. Hamady, N. Fierer, J.I. Gordon, and R. Knight. 2009. Bacterial community variation in human body habitats across space and time. Science 326:1694–1697.
44. Cui, L., A. Morris, and E. Ghedin. 2013. The human mycobiome in health and disease. Genome Med. 5:63.
45. Dalmasso, M., C. Hill, and R.P. Ross. 2014. Exploiting gut bacteriophages for human health. Trends Microbiol. 22:399–405.
46. David, L.A., C.F. Maurice, R.N. Carmody, *et al.* 2014. Diet rapidly and reproducibly alters the human gut microbiome. Nature 505:559–563.
47. DeCaprio, J.A., and R.L. Garcea. 2013. A cornucopia of human polyomaviruses. Nat. Rev. Microbiol. 11:264–276.
48. Derrien, M., E.E. Vaughan, C.M. Plugge, and W.M. de Vos. 2004. *Akkermansia muciniphila* gen. nov., sp nov., a human intestinal mucin-degrading bacterium. Internat. J. Syst. Evol. Microbiol. 54:1469–1476.
49. Dethlefsen, L., S. Huse, M.L. Sogin, and D.A. Relman. 2008. The pervasive effects of an antibiotic on the human gut microbiota, as revealed by deep 16S rRNA sequencing. PLoS Biol. 6:e280.
50. Dewhirst, F.E., T. Chen, J. Izard, B.J. Paster, A.C.R. Tanner, W.-H. Yu, A. Lakshmanan, and W.G. Wade. 2010. The human oral microbiome. J. Bacteriol. 192:5002–5017.
51. Dridi, B., D. Raoult, and M. Drancourt. 2011. Archaea as emerging organisms in complex human microbiomes. Anaerobe 17:56–63.
52. Dupuy, A.K., M.S. David, L. Li, T.N. Heider, J.D. Peterson, E.A. Montano, A. Dongari-Bagtzoglou, P.I. Diaz, and L.D. Strausbaugh. 2014. Redefining the human oral mycobiome with improved practices in amplicon-based taxonomy: Discovery of *Malassezia* as a prominent commensal. PLoS One 9:e90899.
53. Dutilh, B.E., C.W. Noriko, K. McNair, *et al.* 2014. A highly abundant bacteriophage discovered in the unknown sequences of human faecal metagenomes. Nat. Commun. 5:4498.
54. Eberhard, M., U. Hennig, S. Kuhla, R.M. Brunner, B. Kleessen, and C.C. Metges. 2007. Effect of inulin supplementation on selected gastric, duodenal, and caecal microbiota and short chain fatty acid pattern in growing piglets. Arch. Animal Nutr. 61:235–246.
55. Eckburg, P.B., P.W. Lepp, and D.A. Relman. 2003. Archaea and their potential role in human disease. Infect. Immun. 71:591–596.
56. Eckburg, P.B., E.M. Bik, C.N. Bernstein, E. Purdom, L. Dethlefsen, M. Sargent, S.R. Gill, K.E. Nelson, and D.A. Relman. 2005. Diversity of the human intestinal microbial flora. Science 308:1635–1638.
57. Edlund, A., T.M. Santiago-Rodriguez, T.K. Boehm, and D.T. Pride. 2015. Bacteriophage and their potential roles in the human oral cavity. J. Oral Microbiol. 7:27423.
58. Egert, M., A.A. de Graaf, H. Smidt, W.M. de Vos, and K. Venema. 2006. Beyond diversity: functional microbiomics of the human colon. Trends Microbiol. 14:86.
59. Fallingborg, J., L.A. Christensen, M. Ingeman-Nielsen, B.A. Jacobsen, K. Abildgaard, and H.H. Rasmussen. 1989. pH-profile and regional transit times of the normal gut measured by a radiotelemetry device. Aliment Pharmacol. Ther. 3:605–613.
60. Fillon, S.A., J.K. Harris, B.D. Wagner, *et al.* 2012. Novel device to sample the esophageal microbiome—The esophageal string test. PLoS One 7:e42938.
61. Fleet, J.C. 2006. Molecular regulation of calcium metabolism, p. 163–189. *In* C.M. Weaver and R.P. Heaney (ed.), Calcium in Human Health. Humana Press Inc., Totowa, NJ.
62. Fleet, J.C., and R.D. Schoch. 2010. Molecular mechanisms for regulation of intestinal calcium absorption by vitamin D and other factors. Crit. Rev. Clin.l Lab. Sci. 47:181–195.
63. Flint, H.J., S.H. Duncan, K.P. Scott, and P. Louis. 2007. Interactions and competition within the microbial community of the human colon: links between diet and health. Environ. Microbiol. 9:1101–1111.
64. Foca, A., M.C. Liberto, A. Quirino, N. Marascio, E. Zicca, and G. Pavia. 2015. Gut inflammation and immunity: What is the role of the human gut virome? Mediat. Inflamm. Article ID 326032.
65. Fritz, J.V., M.S. Desai, P. Shah, J.G. Schneider, and P. Wilmes. 2013. From meta-omics to causality: experimental models for human microbiome research. Microbiome 1:14.
66. Gaci, N., G. Borrel, W. Tottey, P.W. O'Toole, and J.-F. Brugère. 2014. Archaea and the human gut: New beginning of an old story. World J. Gastroenterol. 20:16062–16078.
67. Gagnaire, A., B. Nadel, D. Raoult, J. Neefjes, and J.-P. Gorvel. 2017. Collateral damage: insights into bacterial mechanisms that predispose host cells to cancer. Nat. Rev. Microbiol. 15:109–128.
68. Ghannoum, M.A., R.J. Jurevic, P.K. Mukherjee, F. Cui, M. Sikaroodi, A. Naqvi, and P.M. Gillevet. 2010. Characterization of the oral fungal microbiome (mycobiome) in healthy individuals. PLoS Pathog 6:e1000713.
69. Gholizadeh, P., H. Eslami, M. Yousefi, M. Asgharzadeh, M. Aghazadeh, and H.S. Kafil. 2016. Role of oral microbiome on oral cancers, a review. Biomed. Pharmacother. 84:552–558.
70. Gill, S.R., M. Pop, R.T. DeBoy, *et al.* 2006. Metagenomic analysis of the human distal gut microbiome. Science 312:1355–1359.
71. Gouba, N., D. Raoult, and M. Drancourt. 2014. Eukaryote culturomics of the gut reveals new species. PLoS One 9:e106994.
72. Gouba, N., and M. Drancourt. 2015. Digestive tract mycobiota: A source of infection. Med. Mal. Infect. 45:9–16.
73. Greenhalgh, K., K.M. Meyer, K.M. Aagaard, and P. Wilmes. 2016. The human gut microbiome in health: establishment and resilience of microbiota over a lifetime. Environ. Microbiol. 18:2103–2116.
74. Grice, E.A., and J.A. Segre. 2012. The human microbiome: Our second genome, p. 151–170. *In* A. Chakravarti and E. Green (ed.), Ann. Rev. Genom. Hum. Genet., vol. 13.
75. Grimaudo, N.J., W.E. Nesbitt, and W.B. Clark. 1996. Coaggregation of *Candida albicans* with oral Actinomyces species. Oral Microbiol. Immunol. 11:59–61.
76. Grimaudo, N.J., and W.E. Nesbitt. 1997. Coaggregation of *Candida albicans* with oral Fusobacterium species. Oral Microbiol. Immunol. 12:168–173.
77. Guarner, F., and J.-R. Malagelada. 2003. Gut flora in health and disease. The Lancet 361:512–519.
78. Hallen-Adams, H.E., S.D. Kachman, J. Kim, R.M. Legge, and I. Martínez. 2015. Fungi inhabiting the healthy human gastrointestinal tract: A diverse and dynamic community. Fung. Ecol. 15:9–17.

79. Hamad, I., D. Raoult, and F. Bittar. 2016. Repertory of eukaryotes (eukaryome) in the human gastrointestinal tract: Taxonomy and detection methods. Parasite Immunol. 38:12–36.
80. Hamaker, B.R., and Y.E. Tuncil. 2014. A perspective on the complexity of dietary fiber structures and their potential effect on the gut microbiota. J. Mol. Biol. 426:3838–3850.
81. Heinritz, S.N., R. Mosenthin, and E. Weiss. 2013. Use of pigs as a potential model for research into dietary modulation of the human gut microbiota. Nutr. Res. Rev. 26:191–209.
82. Hemarajata, P., and J. Versalovic. 2013. Effects of probiotics on gut microbiota: mechanisms of intestinal immunomodulation and neuromodulation. Therapeu. Adv. Gastroenterol. 6:39–51.
83. Hintze, K.J., J.E. Cox, G. Rompato, A.D. Benninghoff, R.E. Ward, J. Broadbent, and M. Lefevre. 2014. Broad scope method for creating humanized animal models for animal health and disease research through antibiotic treatment and human fecal transfer. Gut Microbes 5:183–191.
84. Hoarau, G., P.K. Mukherjee, C. Gower-Rousseau, *et al.* 2016. Bacteriome and mycobiome interactions underscore microbial dysbiosis in familial Crohn's disease. mBio 7:e01250-16.
85. Hoffmann, C., S. Dollive, S. Grunberg, J. Chen, H. Li, G.D. Wu, J.D. Lewis, and F.D. Bushman. 2013. Archaea and fungi of the human gut microbiome: Correlations with diet and bacterial residents. PLoS One 8:e66019.
86. Hold, G.L., S.E. Pryde, V.J. Russell, E. Furrie, and H.J. Flint. 2002. Assessment of microbial diversity in human colonic samples by 16S rDNA sequence analysis. FEMS Microbiol. Ecol. 39:33–39.
87. Hooda, S., B.M.V. Boler, M.C.R. Serao, J.M. Brulc, M.A. Staeger, T.W. Boileau, S.E. Dowd, G.C. Fahey, and K.S. Swanson. 2012. 454 Pyrosequencing reveals a shift in fecal microbiota of healthy adult men consuming polydextrose or soluble corn fiber. The J. Nutr. 142:1259–1265.
88. Howe, A., D.L. Ringus, R.J. Williams, Z.N. Choo, S.M. Greenwald, S.M. Owens, M.L. Coleman, F. Meyer, and E.B. Chang. 2016. Divergent responses of viral and bacterial communities in the gut microbiome to dietary disturbances in mice. ISME J. 10:1217–1227.
89. Hunt, R.H., M. Camilleri, S.E. Crowe, *et al.* 2015. The stomach in health and disease. Gut 64:1650–1668.
90. Huse, S.M., L. Dethlefsen, J.A. Huber, D. Mark Welch, D.A. Relman, and M.L. Sogin. 2008. Exploring microbial diversity and taxonomy using SSU rRNA hypervariable tag sequencing. PLoS Genet. 4:e1000255.
91. Huse, S.M., Y. Ye, Y. Zhou, and A.A. Fodor. 2012. A core human microbiome as viewed through 16S rRNA sequence clusters. PLoS ONE 7:e34242.
92. Huttenhower, C., D. Gevers, R. Knight, *et al.* 2012. Structure, function and diversity of the healthy human microbiome. Nature 486:207–214.
93. Hyde, E.R., B. Luk, S. Cron, *et al.* 2014. Characterization of the rat oral microbiome and the effects of dietary nitrate. Free Radic. Biol. Med. 77:249–257.
94. Iliev, I.D., V.A. Funari, K.D. Taylor, *et al.* 2012. Interactions between commensal fungi and the C-type lectin receptor dectin-1 Influence colitis. Science 336:1314–1317.
95. Jernberg, C., S. Lofmark, C. Edlund, and J.K. Jansson. 2010. Long-term impacts of antibiotic exposure on the human intestinal microbiota. Microbiol. 156:3216–3223.
96. Kararli, T.T. 1995. Comparison of the gastrointestinal anatomy, physiology, and biochemistry of humans and commonly used laboratory animals. Biopharm. Drug Dispos. 16:351–380.
97. Kelly, C.J., L. Zheng, E.L. Campbell, *et al.* 2015. Crosstalk between microbiota-derived short-chain fatty acids and intestinal epithelial HIF augments tissue barrier function. Cell Host Microbe 17:662–671.
98. Kibe, R., M. Sakamoto, H. Yokota, H. Ishikawa, Y. Aiba, Y. Koga, and Y. Benno. 2005. Movement and fixation of intestinal microbiota after administration of human feces to germfree mice. Appl. Environ. Microbiol. 71:3171–3178.
99. Kim, M.-S., and J.-W. Bae. 2016. Spatial disturbances in altered mucosal and luminal gut viromes of diet-induced obese mice. Environ. Microbiol. 18:1498–1510.
100. Kleerebezem, M., and E.E. Vaughan. 2009. Probiotic and gut Lactobacilli and Bifidobacteria: Molecular approaches to study diversity and activity. Ann. Rev. Microbiol. 63:269–290.
101. Koopmans, S.J., and T. Schuurman. 2015. Considerations on pig models for appetite, metabolic syndrome and obese type 2 diabetes: From food intake to metabolic disease. Eur. J. Pharmacol. 759:231–239.
102. Koskella, B., and M.A. Brockhurst. 2014. Bacteria–phage coevolution as a driver of ecological and evolutionary processes in microbial communities. FEMS Microbiol. Rev. 38:916–931.
103. Lam, V., J.D. Su, S. Koprowski, A.N. Hsu, J.S. Tweddell, P. Rafiee, G.J. Gross, N.H. Salzman, and J.E. Baker. 2012. Intestinal microbiota determine severity of myocardial infarction in rats. FASEB J. 26:1727–1735.
104. Lamendella, R., J.W.S. Domingo, S. Ghosh, J. Martinson, and D.B. Oerther. 2011. Comparative fecal metagenomics unveils unique functional capacity of the swine gut. BMC Microbiol. 11:103.
105. Lamendella, R., J.W. Santo Domingo, S. Ghosh, J. Martinson, and D.B. Oerther. 2011. Comparative fecal metagenomics unveils unique functional capacity of the swine gut. BMC Microbiol 11:103.
106. LaTuga, M.S., J.C. Ellis, C.M. Cotton, R.N. Goldberg, J.L. Wynn, R.B. Jackson, and P.C. Seed. 2011. Beyond bacteria: A study of the enteric microbial consortium in extremely low birth weight infants. PLoS ONE 6:e27858.
107. Lazarevic, V., K. Whiteson, S. Huse, D. Hernandez, L. Farinelli, M. Osteras, J. Schrenzel, and P. Francois. 2009. Metagenomic study of the oral microbiota by Illumina high-throughput sequencing. J. Microbiol. Meth. 79:266–271.
108. Leimena, M.M., J. Ramiro-Garcia, M. Davids, *et al.* 2013. A comprehensive metatranscriptome analysis pipeline and its validation using human small intestine microbiota datasets. BMC Genom. 14:530.
109. Lepp, P.W., M.M. Brinig, C.C. Ouverney, K. Palm, G.C. Armitage, and D.A. Relman. 2004. Methanogenic Archaea and human periodontal disease. Proc. Natl. Acad. Sci. U.S.A. 101:6176–6181.
110. Levy, R., and E. Borenstein. 2013. Metabolic modeling of species interaction in the human microbiome elucidates community-level assembly rules. Proc. Natl. Acad. Sci. U.S.A. 110:12804–12809.
111. Ley, R.E., P.J. Turnbaugh, S. Klein, and J.I. Gordon. 2006. Microbial ecology—Human gut microbes associated with obesity. Nature 444:1022–1023.
112. Ley, R.E., M. Hamady, C. Lozupone, *et al.* 2008. Evolution of mammals and their gut microbes. Science 320:1647–1651.
113. Li, M., B. Wang, M. Zhang, *et al.* 2008. Symbiotic gut microbes modulate human metabolic phenotypes. Proc. Natl. Acad. Sci. U.S.A. 105:2117–2122.
114. Li, Q., C. Wang, Q. Zhang, C. Tang, N. Li, B. Ruan, and J. Li. 2012. Use of 18S ribosomal DNA polymerase chain reaction–denaturing gradient gel electrophoresis to study composition of fungal community in 2 patients with intestinal transplants. Hum. Pathol. 43:1273–1281.
115. Li, X.-X., G.L.-H. Wong, K.-F. To, V.W.-S. Wong, L.H. Lai, D.K.-L. Chow, J.Y.-W. Lau, J.J.-Y. Sung, and C. Ding. 2009. Bacterial microbiota profiling in gastritis without *Helicobacter pylori* infection or non-steroidal anti-inflammatory drug use. PLoS One 4:e7985.
116. Lim, E.S., Y.J. Zhou, G.Y. Zhao, *et al.* 2015. Early life dynamics of the human gut virome and bacterial microbiome in infants. Nat. Med. 21:1228–1234.
117. Lim, E.S., D. Wang, and L.R. Holtz. 2016. The bacterial microbiome and virome milestones of infant development. Trends Microbiol. 24:801–810.
118. Looft, T., T.A. Johnson, H.K. Allen, *et al.* 2012. In-feed antibiotic effects on the swine intestinal microbiome. Proc. Natl. Acad. Sci. U.S.A. 109:1691–1696.
119. Lozupone, C.A., J.I. Stombaugh, J.I. Gordon, J.K. Jansson, and R. Knight. 2012. Diversity, stability and resilience of the human gut microbiota. Nature 489:220–230.
120. Luckey, T.D. 1972. Introduction to intestinal microecology Amer. J. Clin. Nutr. 25:1292–1294.
121. Lynch, S.V., and O. Pedersen. 2016. The human intestinal microbiome in health and disease. New Engl. J. Med. 375:2369–2379.
122. Maathuis, A., A. Hoffman, A. Evans, L. Sanders, and K. Venema. 2009. The effect of the undigested fraction of maize products on the activity and composition of the microbiota determined in a dynamic *in vitro* model of the human proximal large intestine. J. Am. Coll. Nutr. 28:657–666.

123. Macfarlane, G.T., and J.H. Cummings. 1991. The colonic flora, fermentation and large bowel digestive function. Raven Press, New York, N.Y.
124. Manrique, P., B. Bolduc, S.T. Walk, J. van der Oost, W.M. de Vos, and M.J. Young. 2016. Healthy human gut phageome. Proc. Natl. Acad. Sci. U.S.A. 113:10400–10405.
125. Mao, S.Y., C.F. Yang, and W.Y. Zhu. 2011. Phylogenetic analysis of methanogens in the pig feces. Curr. Microbiol. 62:1386–1389.
126. Mar Rodríguez, M., D. Pérez, F. Javier Chaves, *et al.* 2015. Obesity changes the human gut mycobiome. Sci. Rep. 5:14600.
127. Martinez, I., J. Kim, P.R. Duffy, V.L. Schlegel, and J. Walter. 2010. Resistant starches types 2 and 4 have differential effects on the composition of the fecal microbiota in human subjects. PLoS One 5:e15046.
128. McConnell, E.L., A.W. Basit, and S. Murdan. 2008. Measurements of rat and mouse gastrointestinal pH, fluid and lymphoid tissue, and implications for in-vivo experiments. J. Pharm. Pharmacol. 60:63–70.
129. McHardy, I.H., M. Goudarzi, M. Tong, *et al.* 2013. Integrative analysis of the microbiome and metabolome of the human intestinal mucosal surface reveals exquisite inter-relationships. Microbiome 1:17.
130. Merchant, H.A., E.L. McConnell, F. Liu, C. Ramaswamy, R.P. Kulkarni, A.W. Basit, and S. Murdan. 2011. Assessment of gastrointestinal pH, fluid and lymphoid tissue in the guinea pig, rabbit and pig, and implications for their use in drug development. Eur. J. Pharm. Sci. 42:3–10.
131. Mihajlovski, A., M. Alric, and J.-F. BrugËre. 2008. A putative new order of methanogenic Archaea inhabiting the human gut, as revealed by molecular analyses of the mcrA gene. Res. Microbiol. 159:516–521.
132. Mikkelsen, L.L., C. Bendixen, M. Jakobsen, and B.B. Jensen. 2003. Enumeration of bifidobacteria in gastrointestinal samples from piglets. Appl. Environ. Microbiol. 69:654–658.
133. Mills, S., F. Shanahan, C. Stanton, C. Hill, A. Coffey, and R.P. Ross. 2013. Movers and shakers: Influence of bacteriophages in shaping the mammalian gut microbiota. Gut Microbes 4:4–16.
134. Minot, S., R. Sinha, J. Chen, H.Z. Li, S.A. Keilbaugh, G.D. Wu, J.D. Lewis, and F.D. Bushman. 2011. The human gut virome: Inter-individual variation and dynamic response to diet. Genome Res. 21:1616–1625.
135. Mitsuoka, T. 1992. Intestinal flora and aging. Nutr. Rev. 50:438–446.
136. Mukherjee, P.K., J. Chandra, M. Retuerto, *et al.* 2014. Oral mycobiome analysis of HIV-infected patients: Identification of *Pichia* as an antagonist of opportunistic fungi. PLoS Pathog. 10:e1003996.
137. Nguyen, T.L.A., S. Vieira-Silva, A. Liston, and J. Raes. 2015. How informative is the mouse for human gut microbiota research? Dis. Mod. Mech. 8:1–16.
138. Nicholson, J.K., E. Holmes, and I.D. Wilson. 2005. Gut microorganisms, mammalian metabolism and personalized health care. Nat. Rev. Microbiol. 3:431–438.
139. Nielsen, H.B., M. Almeida, A.S. Juncker, *et al.* 2014. Identification and assembly of genomes and genetic elements in complex metagenomic samples without using reference genomes. Nat. Biotechnol. 32:822–828.
140. Noble, S.M., B.A. Gianetti, and J.N. Witchley. 2017. Candida albicans cell-type switching and functional plasticity in the mammalian host. Nat. Rev. Microbiol. 15:96–108.
141. O'Hara, A.M., and F. Shanahan. 2006. The gut flora as a forgotten organ. EMBO Rep. 7:688–693.
142. Odle, J., X. Lin, S.K. Jacobi, S.W. Kim, and C.H. Stahl. 2014. The suckling piglet as an agrimedical model for the study of pediatric nutrition and metabolism. Ann. Rev. Anim. Biosci. 2:419–444.
143. Ott, S.J., T. Kuhbacher, M. Musfeldt, *et al.* 2008. Fungi and inflammatory bowel diseases: Alterations of composition and diversity. Scand. J. Gastroenterol. 43:831–841.
144. Pang, X.Y., X.G. Hua, Q. Yang, D.H. Ding, C.Y. Che, L. Cui, W. Jia, P. Bucheli, and L.P. Zhao. 2007. Inter-species transplantation of gut microbiota from human to pigs. ISME J. 1:156–162.
145. Parfrey, L.W., W.A. Walters, and R. Knight. 2011. Microbial eukaryotes in the human microbiome: ecology, evolution, and future directions. Front. Microbiol. 2:153.
146. Pedersen, R., H.C. Ingerslev, M. Sturek, M. Alloosh, S. Cirera, B.O. Christoffersen, S.G. Moesgaard, N. Larsen, and M. Boye. 2013. Characterisation of gut microbiota in Ossabaw and Gottingen minipigs as models of obesity and metabolic syndrome. PLoS One 8:e 0056612.
147. Pei, Z.H., E.J. Bini, L.Y. Yang, M.S. Zhou, F. Francois, and M.J. Blaser. 2004. Bacterial biota in the human distal esophagus. Proc. Natl. Acad. Sci. U.S.A. 101:4250–4255.
148. Pflughoeft, K.J., and J. Versalovic. 2012. Human Microbiome in Health and Disease. Ann. Revi. Pathol. 7:99–122.
149. Pieper, R., P. Janczyk, A. Zeyner, H. Smidt, V. Guiard, and W.B. Souffrant. 2008. Ecophysiology of the developing total bacterial and *Lactobacillus* communities in the terminal small intestine of weaning piglets. Microb. Ecol. 56:474–483.
150. Pothoulakis, C. 2009. Review article: anti-inflammatory mechanisms of action of *Saccharomyces boulardii*. Alimen. Pharmacol. Therapeut. 30:826–833.
151. Pride, D.T., J. Salzman, M. Haynes, F. Rohwer, C. Davis-Long, R.A. White, III, P. Loomer, G.C. Armitage, and D.A. Relman. 2012. Evidence of a robust resident bacteriophage population revealed through analysis of the human salivary virome. ISME J. 6:915–926.
152. Qin, J., R. Li, J. Raes, *et al.* 2010. A human gut microbial gene catalogue established by metagenomic sequencing. Nature 464:59–65.
153. Qiu, X.Y., F. Zhang, X. Yang, N. Wu, W.W. Jiang, X. Li, X.X. Li, and Y.L. Liu. 2015. Changes in the composition of intestinal fungi and their role in mice with dextran sulfate sodium-induced colitis. Sci. Rep. 5:10416.
154. Queipo-Ortuno, M.I., L.M. Seoane, M. Murri, M. Pardo, J.M. Gomez-Zumaquero, F. Cardona, F. Casanueva, and F.J. Tinahones. 2013. Gut microbiota composition in male rat models under different nutritional status and physical activity and its association with serum leptin and ghrelin levels. PLoS One 8:e65465.
155. Rajilic-Stojanovic, M., H.G.H.J. Heilig, S. Tims, E.G. Zoetendal, and W.M. de Vos. 2013. Long-term monitoring of the human intestinal microbiota composition. Environ. Microbiol. 15:1146–1159.
156. Rajilic-Stojanovic, M., and W.M. de Vos. 2014. The first 1000 cultured species of the human gastrointestinal microbiota. FEMS Microbiol. Rev. 38:996–1047.
157. Rascovan, N., R. Duraisamy, and C. Desnues. 2016. Metagenomics and the human virome in asymptomatic individuals, p. 125–141. *In* S. Gottesman (ed.), Ann. Rev. Microbiol. 70:125–141.
158. Rastall, R.A., G.R. Gibson, H.S. Gill, F. Guarner, T.R. Klaenhammer, B. Pot, G. Reid, I.R. Rowland, and M.E. Sanders. 2005. Modulation of the microbial ecology of the human colon by probiotics, prebiotics and synbiotics to enhance human health: An overview of enabling science and potential applications. FEMS Microbiol. Ecol. 52:145.
159. Rauch, M., and S.V. Lynch. 2012. The potential for probiotic manipulation of the gastrointestinal microbiome. Curr. Opin. Biotechnol. 23:192–201.
160. Reyes, A., M. Haynes, N. Hanson, F.E. Angly, A.C. Heath, F. Rohwer, and J.I. Gordon. 2010. Viruses in the faecal microbiota of monozygotic twins and their mothers. Nature 466:334–338.
161. Reyes, A., N.P. Semenkovich, K. Whiteson, F. Rohwer, and J.I. Gordon. 2012. Going viral: next-generation sequencing applied to phage populations in the human gut. Nat. Rev. Microbiol. 10:607–617.
162. Reyes, A., L.V. Blanton, S. Cao, *et al.* 2015. Gut DNA viromes of Malawian twins discordant for severe acute malnutrition. Proc. Natl. Acad. Sci. U.S.A. 112:11941–11946.
163. Robles-Sikisaka, R., M. Ly, T. Boehm, M. Naidu, J. Salzman, and D.T. Pride. 2013. Association between living environment and human oral viral ecology. ISME J. 7:1710–1724.
164. Sachsenroder, J., S.O. Twardziok, M. Scheuch, and R. Johne. 2014. The general composition of the faecal virome of pigs depends on age, but not on feeding with a probiotic bacterium. PLoS One 9:e88888.
165. Savage, D.C. 1977. Microbial ecology of gastrointestinal-tract. Ann. Revi. Microbiol. 31:107–133.
166. Scanlan, P.D., F. Shanahan, C. O'Mahony, and J.R. Marchesi. 2006. Culture-independent analyses of temporal variation of the dominant fecal microbiota and targeted bacterial subgroups in Crohn's Disease. J. Clin. Microbiol. 44:3980–3988.
167. Schwartz, S., I. Friedberg, I.V. Ivanov, *et al.* 2012. A metagenomic study of diet-dependent interaction between gut microbiota and host in infants reveals differences in immune response. Genome Biol. 13:r32.
168. Scupham, A.J., L.L. Presley, B. Wei, *et al.* 2006. Abundant and diverse fungal microbiota in the murine intestine. Appl. Environ. Microbiol. 72:793–801.
169. Seed, P.C. 2015. The Human Mycobiome. Cold Spring Harbor Perspectives in Medicine 5.

170. Sender, R., S. Fuchs, and R. Milo. 2016. Revised estimates for the number of human and bacteria cells in the body. PLoS Biol. 14:e1002533.
171. Shan, T.L., L.L. Li, P. Simmonds, C.L. Wang, A. Moeser, and E. Delwart. 2011. The fecal virome of pigs on a high-density farm. J. Virol. 85:11697–11708.
172. Simmonds, P., M.J. Adams, M. Benko, *et al.* 2017. Virus taxonomy in the age of metagenomics. Nat. Rev. Microbiol. 15:161–168.
173. Sogin, M.L., H.G. Morrison, J.A. Huber, D.M. Welch, S.M. Huse, P.R. Neal, J.M. Arrieta, and G.J. Herndl. 2006. Microbial diversity in the deep sea and the underexplored "rare biosphere". Proc. Natl. Acad. Sci. U.S.A. 103:12115–12120.
174. Sommer, F., and F. Bäckhed. 2016. Know your neighbor: Microbiota and host epithelial cells interact locally to control intestinal function and physiology. BioEssays 38:455–464.
175. Sonnenburg, E.D., S.A. Smits, M. Tikhonov, S.K. Higginbottom, N.S. Wingreen, and J.L. Sonnenburg. 2016. Diet-induced extinctions in the gut microbiota compound over generations. Nature 529:212–215.
176. Sonnenburg, J.L., and F. Backhed. 2016. Diet-microbiota interactions as moderators of human metabolism. Nature 535:56–64.
177. Spurlock, M.E., and N.K. Gabler. 2008. The development of porcine models of obesity and the metabolic syndrome. J. Nutr. 138:397–402.
178. Stephen, A.M., and J.H. Cummings. 1980. Mechanism of action of dietary fibre in the human colon. Nature 284:283–284.
179. Su, Y., G.R. Bian, Z.G. Zhu, H. Smidt, and W.Y. Zhu. 2014. Early methanogenic colonisation in the faeces of Meishan and Yorkshire piglets as determined by pyrosequencing analysis. Archaea 2014:547908.
180. Suau, A., R. Bonnet, M. Sutren, J.J. Godon, G.R. Gibson, M.D. Collins, and J. Dore. 1999. Direct analysis of genes encoding 16S rRNA from complex communities reveals many novel molecular species within the human gut. Appl. Environ. Microbiol. 65:4799–4807.
181. Suhr, M.J., and H.E. Hallen-Adams. 2015. The human gut mycobiome: pitfalls and potentials—a mycologist's perspective. Mycologia 107:1057–1073.
182. Suhr, M.J., N. Banjara, and H.E. Hallen-Adams. 2016. Sequence-based methods for detecting and evaluating the human gut mycobiome. Lett. Appl. Microbiol. 62:209–215.
183. Tannock, G.W. 2002. Exploring the relationships between intestinal microflora and inflammatory conditions of the human bowel and spine. Anton. Leeuw. Int. J. G. 81:529–535.
184. Tannock, G.W. 2008. Molecular analysis of the intestinal microflora in IBD. Mucosal Immunol. 1:S15–S18.
185. Thaiss, C.A., D. Zeevi, M. Levy, *et al.* 2014. Transkingdom control of microbiota diurnal oscillations promotes metabolic homeostasis. Cell 159:514–529.
186. Thaiss, C.A., D. Zeevi, M. Levy, E. Segal, and E. Elinav. 2015. A day in the life of the meta-organism: diurnal rhythms of the intestinal microbiome and its host. Gut Microbes 6:137–142.
187. Thaiss, C.A., M. Levy, T. Korem, *et al.* 2016. Microbiota diurnal rhythmicity programs host transcriptome oscillations. Cell 167: 1495–1510.e12.
188. Thaiss, C.A., N. Zmora, M. Levy, and E. Elinav. 2016. The microbiome and innate immunity. Nature 535:65–74.
189. The Human Microbiome Project Consortium. 2012. Structure, function and diversity of the healthy human microbiome. Nature 486:207–214.
190. Turnbaugh, P., R. Ley, M.A. Mahowald, V. Magrini, E.R. Mardis, and J. Gordon. 2006. An obesity-associated gut microbiome with increased capacity for energy harvest. Nature 444:1027–1131.
191. Turnbaugh, P.J., and J.I. Gordon. 2009. The core gut microbiome, energy balance and obesity. J. Physiol. 587:4153–4158.
192. Turnbaugh, P.J., V.K. Ridaura, J.J. Faith, F.E. Rey, R. Knight, and J.I. Gordon. 2009. The effect of diet on the human gut microbiome: A metagenomic analysis in humanized gnotobiotic mice. Sci. Trans. Med. 1:6ra14–6ra14.
193. Underhill, D.M., and L.D. Lliev. 2014. The mycobiota: interactions between commensal fungi and the host immune system. Nat. Rev. Immunol. 14:405–416.
194. Urubschurov, V., P. Janczyk, W.B. Souffrant, G. Freyer, and A. Zeyner. 2011. Establishment of intestinal microbiota with focus on yeasts of unweaned and weaned piglets kept under different farm conditions. FEMS Microbiol. Ecol. 77:493–502.
195. van den Bogert, B., O. Erkus, J. Boekhorst, M. de Goffau, E.J. Smid, E.G. Zoetendal, and M. Kleerebezem. 2013. Diversity of human small intestinal *Streptococcus* and *Veillonella* populations. FEMS Microbiol. Ecol. 85:376–388.
196. Vdoviaková, K., E. Petrovová, M. Maloveská, L. Krešáková, J. Teleky, M.Z.J. Elias, and D. Petrášová. 2016. Surgical anatomy of the gastrointestinal tract and its vasculature in the laboratory rat. Gastroenterol. Res. Pract. 2016, Article ID 2632368.
197. von Rosenvinge, E.C., Y. Song, J.R. White, C. Maddox, T. Blanchard, and W.F. Fricke. 2013. Immune status, antibiotic medication and pH are associated with changes in the stomach fluid microbiota. ISME J. 7:1354–1366.
198. Walker, A.W., J. Ince, S.H. Duncan, *et al.* 2011. Dominant and diet-responsive groups of bacteria within the human colonic microbiota. ISME J. 5:220–230.
199. Waller, A.S., T. Yamada, D.M. Kristensen, J.R. Kultima, S. Sunagawa, E.V. Koonin, and P. Bork. 2014. Classification and quantification of bacteriophage taxa in human gut metagenomes. ISME J. 8:1391–1402.
200. Wampach, L., A. Heintz-Buschart, A. Hogan, *et al.* 2017. Colonization and succession within the human gut microbiome by Archaea, Bacteria, and Microeukaryotes during the first year of life. Front. Microbiol. 8:738.
201. Wang, M., S. Ahrn, B. Jeppsson, and G. Molin. 2005. Comparison of bacterial diversity along the human intestinal tract by direct cloning and sequencing of 16S rRNA genes. FEMS Microbiol. Ecol. 54:219.
202. Wang, M., and S.M. Donovan. 2015. Human microbiota-associated swine: Current progress and future opportunities. ILAR J. 56:63–73.
203. Wang, X., S.P. Heazlewood, D.O. Krause, and T.H.J. Florin. 2003. Molecular characterization of the microbial species that colonize human ileal and colonic mucosa by using 16S rDNA sequence analysis. J. Appl. Microbiol. 95:508–520.
204. Wang, Z.K., Y.S. Yang, A.T. Stefka, G. Sun, and L.H. Peng. 2014. Review article: fungal microbiota and digestive diseases. Alimen. Pharmacol. Therapeu. 39:751–766.
205. Warden, C.H., and J.S. Fisler. 2008. Comparisons of diets used in animal models of high fat feeding. Cell Metabol. 7:277.
206. Weaver, C.M., L.D. McCabe, G.M. McCabe, R. Novotny, M.D. Van Loan, S.B. Going, C. Boushey, D.A. Savaiano, and V. Matkovic. 2005. Bone mineral and predictors of whole body, total hip, and lumbar spine for 740 early pubertal white, Hispanic, and Asian girls. J. Bone Miner. Res. 20:S314–S314.
207. Weaver, C.M., B.R. Martin, J.A. Story, I. Hutchinson, and L. Sanders. 2010. Novel fibers Increase bone calcium content and strength beyond efficiency of large intestine fermentation. J. Ag. Food Chem. 58:8952–8957.
208. Weaver, C.M., B.R. Martin, C.H. Nakatsu, *et al.* 2011. Galactooligosaccharides improve mineral absorption and bone properties in growing rats through gut fermentation. J. Ag. Food Chem. 59:6501–6510.
209. Welch, J.L.M., B.J. Rossetti, C.W. Rieken, F.E. Dewhirst, and G.G. Borisy. 2016. Biogeography of a human oral microbiome at the micron scale. Proc. Natl. Acad. Sci. U.S.A. 113:E791–E800.
210. Whisner, C.M., B.R. Martin, C.H. Nakatsu, G.P. McCabe, L.D. McCabe, M. Peacock, and C.M. Weaver. 2014. Soluble maize fibre affects short-term calcium absorption in adolescent boys and girls: a randomised controlled trial using dual stable isotopic tracers. Brit. J. Nutr. 112:446–456.
211. Whisner, C.M., B.R. Martin, C.H. Nakatsu, J.A. Story, C.J. MacDonald-Clarke, L.D. McCabe, G.P. McCabe, and C.M. Weaver. 2016. Soluble corn fiber increases calcium absorption associated with shifts in the gut microbiome: A randomized dose-response trial in free-living pubertal girls. Nutr. J. 146:1298–1306
212. Wilson, K., and R. Blitchington. 1996. Human colonic biota studied by ribosomal DNA sequence analysis. Appl. Environ. Microbiol. 62:2273–2278.
213. Woodmansey, E.J. 2007. Intestinal bacteria and ageing. J. Appl. Microbiol. 102:1178–1186.
214. Wright, C.J., L.H. Burns, A.A. Jack, C.R. Back, L.C. Dutton, A.H. Nobbs, R.J. Lamont, and H.F. Jenkinson. 2013. Microbial interactions in building of communities. Mol. Oral Microbiol. 28:83–101.
215. Wylie, K.M., K.A. Mihindukulasuriya, Y. Zhou, E. Sodergren, G.A. Storch, and G.M. Weinstock. 2014. Metagenomic analysis of double-stranded DNA viruses in healthy adults. BMC Biol. 12:71.
216. Xiao, L., Q. Feng, S. Liang, *et al.* 2015. A catalog of the mouse gut metagenome. Nat Biotechnol. 33:1103–1108.

217. Xiao, L., J. Estellé, P. Kiilerich, *et al.* 2016. A reference gene catalogue of the pig gut microbiome. Nat. Microbiol. 1:16161.
218. Yan, H., R. Potu, H. Lu, *et al.* 2013. Dietary fat content and fiber type modulate hind gut microbial community and metabolic markers in the pig. PLoS One 8:e59581.
219. Yatsunenko, T., F.E. Rey, M.J. Manary, *et al.* 2012. Human gut microbiome viewed across age and geography. Nature 486:222–227.
220. Zhang, Q., G. Widmer, and S. Tzipori. 2013. A pig model of the human gastrointestinal tract. Gut Microbes 4:193–200.
221. Zhu, Y.Y., H. Li, X.L. Xu, C.B. Li, and G.H. Zhou. 2016. The gut microbiota in young and middle-aged rats showed different responses to chicken protein in their diet. BMC Microbiol. 16:281.
222. Zoetendal, E.G., A. von Wright, T. Vilpponen-Salmela, K. Ben-Amor, A.D.L. Akkermans, and W.M. de Vos. 2002. Mucosa-associated bacteria in the human gastrointestinal tract are uniformly distributed along the colon and differ from the community recovered from feces. Appl. Environ. Microbiol. 68:3401–3407.
223. Zoetendal, E.G., J. Raes, B. van den Bogert, *et al.* 2012. The human small intestinal microbiota is driven by rapid uptake and conversion of simple carbohydrates. ISME J. 6:1415–1426.
224. Zwolinska-Wcislo, M., A. Budak, D. Trojanowska, J. Bogdal, and J. Stachura. 1998. Fungal colonization of the stomach and its clinical relevance. Mycoses 41:327–334.

Microbes and Environments

EDITORIAL BOARD (2023)

This journal is partly subsidized by the Grant-in-Aid for Publication of Scientific Research Results from the Japan Society for the Promotion of Science (JSPS).

c/o Nakanishi Printing Co.
Shimodachiuri Ogawa Higashi Kamikyoku, Kyoto 602-8048, Japan TEL: +81–75–441–3155, FAX: +81–75–417–2050